USGS
science for a changing world

Prepared in cooperation with the U.S. Army Corps of Engineers Chicago District

Characterizing Variability in Vertical Profiles of Streamwise Velocity and Implications for Streamgaging Practices in the Chicago Sanitary and Ship Canal near Lemont, Illinois, January 2014 to July 2017

Scientific Investigations Report 2018–5128

U.S. Department of the Interior
U.S. Geological Survey

Front cover. The Canal Street Railroad Bridge on the south branch of the Chicago River. Image courtesy of J. Best, University of Illinois at Urbana-Champaign.

Back cover. Top: Instrumentation deployed in and around the upstream notch at the U.S. Geological Survey (USGS) streamgage on the Chicago Sanitary and Ship Canal near Lemont, Illinois (05536890). Image courtesy of C. Bosch, USGS. Center: A downstream-bound tow passing the USGS streamgage on the Chicago Sanitary and Ship Canal near Lemont, Illinois (05536890). Image courtesy of F. Engel, USGS. Bottom: The up-looking acoustic Doppler current profiler (in mount) deployed at the USGS streamgage on the Chicago Sanitary and Ship Canal near Lemont, Illinois (05536890). Image courtesy of C. Bosch, USGS.

Characterizing Variability in Vertical Profiles of Streamwise Velocity and Implications for Streamgaging Practices in the Chicago Sanitary and Ship Canal near Lemont, Illinois, January 2014 to July 2017

By P. Ryan Jackson

Prepared in cooperation with the U.S. Army Corps of Engineers Chicago District

Scientific Investigations Report 2018–5128

U.S. Department of the Interior
U.S. Geological Survey

U.S. Department of the Interior
RYAN K. ZINKE, Secretary

U.S. Geological Survey
James F. Reilly II, Director

U.S. Geological Survey, Reston, Virginia: 2018

For more information on the USGS—the Federal source for science about the Earth, its natural and living resources, natural hazards, and the environment—visit https://www.usgs.gov or call 1–888–ASK–USGS.

For an overview of USGS information products, including maps, imagery, and publications, visit https://store.usgs.gov.

Suggested citation:
Jackson, P.R., 2018, Characterizing variability in vertical profiles of streamwise velocity and implications for streamgaging practices in the Chicago Sanitary and Ship Canal near Lemont, Illinois, January 2014 to July 2017: U.S. Geological Survey Scientific Investigations Report 2018–5128, 73 p., https://doi.org/10.3133/sir20185128.

ISSN 2328-0328 (online)

Acknowledgments

The author acknowledges the Chicago District of the U.S. Army Corps of Engineers (USACE) for the funding to complete this study as part of Lake Michigan Diversion Accounting (LMDA). The author also acknowledges the Chicago Metropolitan Water Reclamation District of Greater Chicago and Kevin Johnson and technicians from the U.S. Geological Survey (USGS) Central Midwest Water Science Center for the work required to install and maintain the instrumentation in the Chicago Area Waterway System. Without their efforts, the data for this analysis would not exist. The author also gratefully acknowledges the help of students at the USGS Central Midwest Water Science Center for processing countless hours of barge-detection videos. Finally, the author thanks the USACE and USGS LMDA teams for their reviews of this study and tireless effort to ensure the best engineering practices and scientific knowledge are implemented in LMDA in accordance with the U.S. Supreme Court decree of 1967, as amended in 1980.

Contents

Figures

Tables

Appendix Tables

Conversion Factors

U.S. customary units to International System of Units

Multiply	By	To obtain
	Length	
foot (ft)	0.3048	meter (m)
mile (mi)	1.609	kilometer (km)
	Volume	
gallon (gal)	3.785	liter (L)
gallon (gal)	0.003785	cubic meter (m^3)
million gallons (Mgal)	3,785	cubic meter (m^3)
cubic foot (ft^3)	0.02832	cubic meter (m^3)
	Flow rate	
foot per second (ft/s)	0.3048	meter per second (m/s)
cubic foot per second (ft^3/s)	0.02832	cubic meter per second (m^3/s)
million gallons per day (Mgal/d)	0.04381	cubic meter per second (m^3/s)
	Density	
pound per cubic foot (lb/ft^3)	16.02	kilogram per cubic meter (kg/m^3)

International System of Units to U.S. customary units

Multiply	By	To obtain
	Length	
centimeter (cm)	0.3937	inch (in.)
	Density	
kilogram per cubic meter (kg/m^3)	0.06242	pound per cubic foot (lb/ft^3)

Temperature in degrees Celsius (°C) may be converted to degrees Fahrenheit (°F) as

$$°F=(1.8×°C)+32.$$

Temperature in degrees Fahrenheit (°F) may be converted to degrees Celsius (°C) as

$$°C=(°F–32)/1.8.$$

Datum

Vertical coordinate information is referenced to either the North American Vertical Datum of 1988 (NAVD 88) or the Chicago City Datum (CCD).

Supplemental Information

Specific conductance is given in microsiemens per centimeter at 25 degrees Celsius (µS/cm at 25 °C).

Abbreviations

ADCP	acoustic Doppler current profiler
ADVM	acoustic Doppler velocity meter
AVM	acoustic velocity meter
CAWS	Chicago Area Waterway System
CST	central standard time
DC	directly computed
GH	gage height
LMDA	Lake Michigan Diversion Accounting
MWRD	Metropolitan Water Reclamation District of Greater Chicago
OLS	ordinary least squares
RDI	RD Instruments
RSSI	receiver signal strength indicator
SA	stage-area
TRC	Technical Review Committee
USACE	U.S. Army Corps of Engineers
USGS	U.S. Geological Survey
WRP	Water Reclamation Plant

Characterizing Variability in Vertical Profiles of Streamwise Velocity and Implications for Streamgaging Practices in the Chicago Sanitary and Ship Canal near Lemont, Illinois, January 2014 to July 2017

By P. Ryan Jackson

Abstract

A critical component of the Lake Michigan Diversion Accounting program, which oversees the diversion of Great Lakes water by the State of Illinois, is the U.S. Geological Survey streamgage on the Chicago Sanitary and Ship Canal near Lemont, Illinois. The long-term application of an up-looking acoustic Doppler current profiler at this streamgage allows the flows at this study site to be examined from a new perspective: one that is not possible with the horizontally oriented instruments typically used at the site. This report presents results from more than 3.5 years of continuous monitoring data from the up-looking acoustic Doppler current profiler deployed at the study site, which allowed variability in the vertical profile of streamwise velocity to be characterized over a wide range of highly unsteady flows. These data revealed seasonal, density-driven underflows correlated with a combination of environmental variables. Two new methods for computing discharge were developed using this instrument and were determined to be of sufficient quality for Lake Michigan Diversion Accounting purposes. Finally, the up-looking acoustic Doppler current profiler and a barge-detection camera allowed the effect of commercial tows on streamgaging at the site to be evaluated. The addition of the up-looking acoustic Doppler current profiler to the U.S. Geological Survey streamgage on the Chicago Sanitary and Ship Canal near Lemont, Illinois, has ensured the best current engineering practices and scientific knowledge are implemented in the Lake Michigan Diversion Accounting program in accordance with the U.S. Supreme Court decree of 1967, as amended in 1980.

Introduction

One of the most highly scrutinized streamgages operated by the U.S. Geological Survey (USGS) in the United States is on the Chicago Sanitary and Ship Canal near Lemont, Illinois (streamgage 05536890; fig. 1). This streamgage is instrumental in monitoring the diversion of Great Lakes water from Lake Michigan into the man-made canal by the State of Illinois. The diversion of Great Lakes water through the canal is limited by the U.S. Supreme Court decree of 1967 to 3,200 cubic feet per second (ft^3/s), and the practice of computing and reporting the diversion, called Lake Michigan Diversion Accounting (LMDA), is overseen by the U.S. Army Corps of Engineers (USACE) Chicago District. In addition to internal USGS quality control (reviews) at the center and Bureau level, the streamgaging practices and records for this streamgage are independently reviewed by a panel of experts assembled by the USACE every 5 years for LMDA. The panel, also called the LMDA Technical Review Committee (TRC), is responsible for ensuring that the best current engineering practices and scientific knowledge are used at this streamgage and that the records for this streamgage are complete and accurate.

Discussions with the sixth (2008) and seventh (2013) LMDA TRCs focused, in part, on unsteadiness in the Chicago Sanitary and Ship Canal and the overall effect of the unsteadiness on the methods used to measure discharge in the canal near Lemont, Ill., as a part of LMDA. Those discussions identified a need to understand the vertical distribution of velocity in the canal near Lemont, Ill., and the evolution of the vertical velocity profile over time during high-flow events and transients created by operation of the lock at Lockport Lock and Dam and other sources in the system. The sixth LMDA TRC recommended that additional instrumentation (an up-looking acoustic Doppler current profiler [ADCP], for example) should be deployed at the site to qualify the effect of flow transients in the system (Espey and others, 2009). The seventh LMDA TRC recommended the USGS continue to use the up-looking ADCP to evaluate the vertical velocity distribution at the site and its effect on the uncertainty of diversion accounting (Espey and others, 2014). Additionally, questions were raised about the potential effects of commercial navigation on the flows measured at the streamgage, and the sixth LMDA TRC recommended "quantification of the barge transit effect" (Espey and others, 2009, p. 140). This study by the USGS,

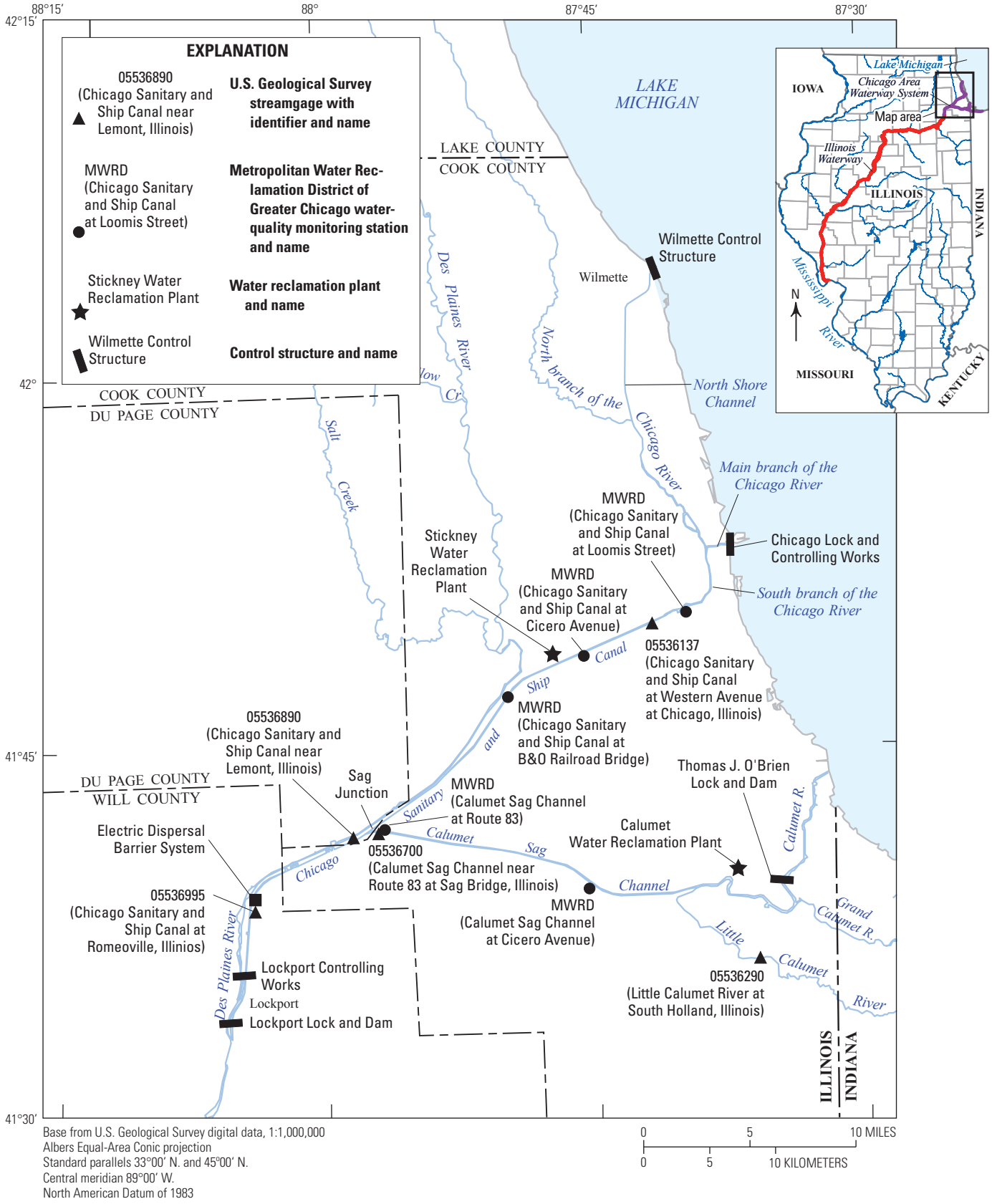

Figure 1. The Chicago Area Water System in and around Chicago, Illinois.

in cooperation with the USACE Chicago District, addresses these recommendations through the long-term deployment of an up-looking ADCP in the Chicago Sanitary and Ship Canal near Lemont, Ill. Analysis of more than 3.5 years of data from this instrument provides a detailed understanding of the evolution of the vertical velocity profile during highly unsteady flows in the canal and the response of the velocity field to passage of commercial tows. In addition, the data produced by this study have revealed additional complex hydraulics and stratified flows at this site and allowed two additional methods of computing discharge at this streamgage. The remainder of this report is dedicated to presenting the data collection methods, techniques for data analysis, and the results of this study, framed in the context of streamgaging practices in the Chicago Sanitary and Ship Canal near Lemont, Ill., as a part of the LMDA program.

The Chicago Area Waterway System

The Chicago Sanitary and Ship Canal was built in the late 1800s to keep Chicago's wastewater out of Lake Michigan, the primary source of potable water for the city. The canal connected the Chicago River, formerly a tributary to Lake Michigan before 1900, to the Des Plaines River, a tributary to the Illinois River (which is part of the Illinois Waterway), in the Mississippi River Basin (fig. 1). This man-made connection reversed the flow of the Chicago River and formed a diversion of Great Lakes water from the Great Lakes Basin to the Mississippi River Basin. The completion of the North Shore Channel in 1910 allowed the input of wastewater and diversion of lake water at Wilmette, Ill., on Chicago's north side into the Chicago Sanitary and Ship Canal; the completion of the Calumet Sag Channel in 1922 brought additional wastewater from south Chicago and flows from the Grand Calumet and Little Calumet Rivers to the canal, in addition to a diversion of lake water through the Thomas J. O'Brien Lock and Dam (fig. 1; also see Johnson and others, 2012). The complete 78-mile system of canals and channels, called the Chicago Area Waterway System (CAWS), is primarily made up of treated wastewater during dry periods and serves as the primary drainage system for the city of Chicago during wet periods.

Water quality is a major concern in the CAWS (Dorevitch, 2011) and is continuously monitored by the Metropolitan Water Reclamation District of Greater Chicago (MWRD) at about 30 locations in the system (MWRD, 2008). Discrete, periodic water-quality samples are collected at an additional 20 locations (MWRD, 2008). Discretionary diversion of Lake Michigan water into the CAWS typically occurs only during June to October and is used to dilute the wastewater effluent and improve water quality in the CAWS (primarily by increasing dissolved oxygen). During wet periods, combined sewer overflows are a regular occurrence in the CAWS, and backflows to Lake Michigan can occur at three locations (Wilmette Control Structure, Chicago Lock and Controlling Works, and Thomas J. O'Brien Lock and Dam; MWRD, 2008). There are numerous industrial water users and dischargers along the CAWS; consequently, thermal loading to the CAWS is substantial and keeps the system largely ice free during the winter (the Calumet Sag Channel may ice over during extended periods of subzero temperatures). Moreover, road-salt application is high in the greater Chicago area, and road-salt runoff can generate stratified flows including density-driven gravity currents in the main branch and north branch of the Chicago River (Jackson and others, 2008). Density-driven gravity currents have also been documented at the confluence of the Chicago Sanitary and Ship Canal and the Calumet Sag Channel (also called "Sag Junction") (Jackson, 2016) and studied through computational modeling (Wang and others, 2016).

A Brief History of Lake Michigan Diversion Accounting

The U.S. Supreme Court Decree of 1930 (30 years after the Chicago Sanitary and Ship Canal was completed) mandated that Illinois' diversion of Great Lakes water be based on the discharges reported at the control structures on the canal at Lockport, Ill. The mean daily and mean annual flows were computed from a combination of sluice gate and turbine settings at the powerhouse at Lockport Lock and Dam and the Lockport Controlling Works and the number of lockages per day at the Lockport Lock (fig. 1). The diversion computations were made by Metropolitan Sanitary District (precursor to the MWRD) engineers. A subsequent 1967 U.S. Supreme Court decree set the allowable mean annual diversion to 3,200 ft^3/s and transferred the flow-computation responsibility to the Illinois Department of Transportation-Division of Water Resources.

A 1980 amendment to the 1967 U.S. Supreme Court decree assigned the task of diversion accounting to the USACE and re-confirmed the State of Illinois diversion to a mean annual flow of 3,200 ft^3/s. Additional limits on the cumulative deviation of annual flows above or below the 3,200-ft^3/s limit also were added (see appendix 2 of Johnson and others, 2012). The decree directed the USACE to establish the diversion-accounting procedures, cooperate with the USGS to measure flows within the waterway, and convene a TRC every 5 years to review diversion accounting. A technical review of the LMDA program by a panel of independent experts ensures that best current engineering practices and scientific knowledge are being used in diversion accounting. Each TRC is appointed to comprehensively review current diversion-accounting procedures. The procedures include but are not limited to the following: (1) current accounting results; (2) diversion-related measurements and measurement techniques at USGS streamgages, control structures, precipitation gages, and other pertinent structures; (3) hydrologic and hydraulic modeling; (4) procedures used to calculate and verify flows that are not directly measured; and (5) the status of recommendations from previous TRCs.

Study Site

The primary streamgage currently used for LMDA and site of this study is USGS streamgage 05536890 on the Chicago Sanitary and Ship Canal near Lemont, Ill., about 0.7 mile (mi) downstream from Sag Junction (fig. 1). The canal at the study site is composed of a rectangular cross section about 162 feet (ft) wide and 25 ft deep (fig. 2) and is cut into the dolomite bedrock. Set block was placed atop the bedrock to build the upper part of the walls in areas where the bedrock did not extend to the land surface (Kay and others, 2016). A historical failure of the right wall of the canal created a sloughed bank downstream from the streamgage (fig. 2). The right or left wall is based on the perspective of looking downstream. The flows in the Chicago Sanitary and Ship Canal at this study site are highly unsteady, an artifact of controlling works and lock structures in the CAWS, industrial intakes and outfalls in the pool, wastewater outfalls, and heavy commercial navigation through this reach (Jackson and others, 2012). Stage variation at the study site is typically small (less than 4 ft) with a maximum range of about 6 ft over a historical discharge range of –3,159 to 21,420 ft^3/s (a negative discharge indicates upstream flow towards Lake Michigan).

Purpose and Scope

The purpose of this report is to present work related to characterizing the variation in the vertical profile of streamwise velocity in the Chicago Sanitary and Ship Canal near Lemont, Ill., over a wide range of unsteady flows. Specifically, the addition of an up-looking ADCP to the streamgage instrumentation allows the flows at the study site to be examined from a new perspective: one that is not possible with horizontally oriented instruments. This report presents results from more than 3.5 years of continuous monitoring data from an up-looking ADCP deployed in 2013 at the study site. In particular, this report examines the evolution of the vertical velocity profiles during high-flow events, assesses the potential for and effect of gravity currents on streamgaging practices at this site, evaluates the possibility of using the up-looking ADCP as a secondary index-velocity instrument, assesses the accuracy of direct discharge measurements made using data from the acoustic Doppler velocity meter (ADVM) and up-looking ADCP, and evaluates the effect of commercial tows on the velocity distribution and streamgaging at the site.

Methods

This section presents the data collection methods and data processing techniques used in this study. Although the data collection at this study site falls within the domain of the USGS streamgaging program and therefore adheres to USGS techniques and methods for index-velocity sites (Levesque and Oberg, 2012), the array of instrumentation at this site is unique to this site and atypical for the USGS. The array of instrumentation at this site has been chosen to provide redundancy, allow assessment of streamgaging practices, document and describe the unique and unsteady characteristics of flow in the Chicago Sanitary and Ship Canal (fig. 1), and provide accurate estimates of discharge in compliance with USGS standards and the LMDA directive to use the best current engineering practices and scientific knowledge.

Data Collection

This section describes the additional instrumentation installed in the CAWS as a part of this study. The additional instrumentation includes the up-looking ADCP, temperature and specific conductance sensors, and a barge-detection camera. Detailed descriptions of the instrumentation installed at the USGS streamgage on the Chicago Sanitary and Ship Canal near Lemont, Ill., prior to this study are in Jackson and others (2012). Except for the up-looking ADCP, the equipment and instrument configurations described in Jackson and others (2012) remained unchanged for this streamgage throughout the present study.

Up-Looking Acoustic Doppler Current Profiler

A 1,200-kilohertz Teledyne RD Instruments (RDI) Rio Grande ADCP was deployed in the Chicago Sanitary and Ship Canal about 170 ft upstream from the ADVM along the approximate centerline of the canal (fig. 2). The ADCP, oriented in an up-looking position, was mounted in a custom-built aluminum mount (fig. 3) and bolted to the bedrock at the bottom of the canal by divers on June 18, 2013. A direct connection between the streamgage house and the instrument was possible using a 300-ft armored power and communication cable. The trawl-resistant mount was designed to shed debris and placed the ADCP transducers 2.0 ft above the bed of the canal. The bed elevation at the deployment location at the time of deployment was measured to be 550.61 ft above the North American Vertical Datum of 1988 (NAVD 88). Divers were instructed to position the instrument such that beam 3 was oriented upstream (fig. 3).

An ADCP measures velocities from the head of the instrument to a specified distance from the head and divides this range into uniform segments called bins. A collection of bins yields a velocity profile. The up-looking ADCP is configured with thirty 0.98-ft bins and a 0.82-ft blanking distance (Teledyne RDI, 2007). The center of the first bin is 4.3 ft above the channel bed. The instrument was configured to use water mode 12 with 100 subpings per 1-minute (min) ensemble and a time between subpings of 0.55 seconds (s). Therefore, each 1-min ensemble represents an average over about 57 s of each minute. This configuration produces 1-min time-averaged velocity profiles with an estimated standard deviation of horizontal velocity of about 0.04 foot per second (ft/s) and an ambiguity velocity of 7.02 ft/s. Data from the

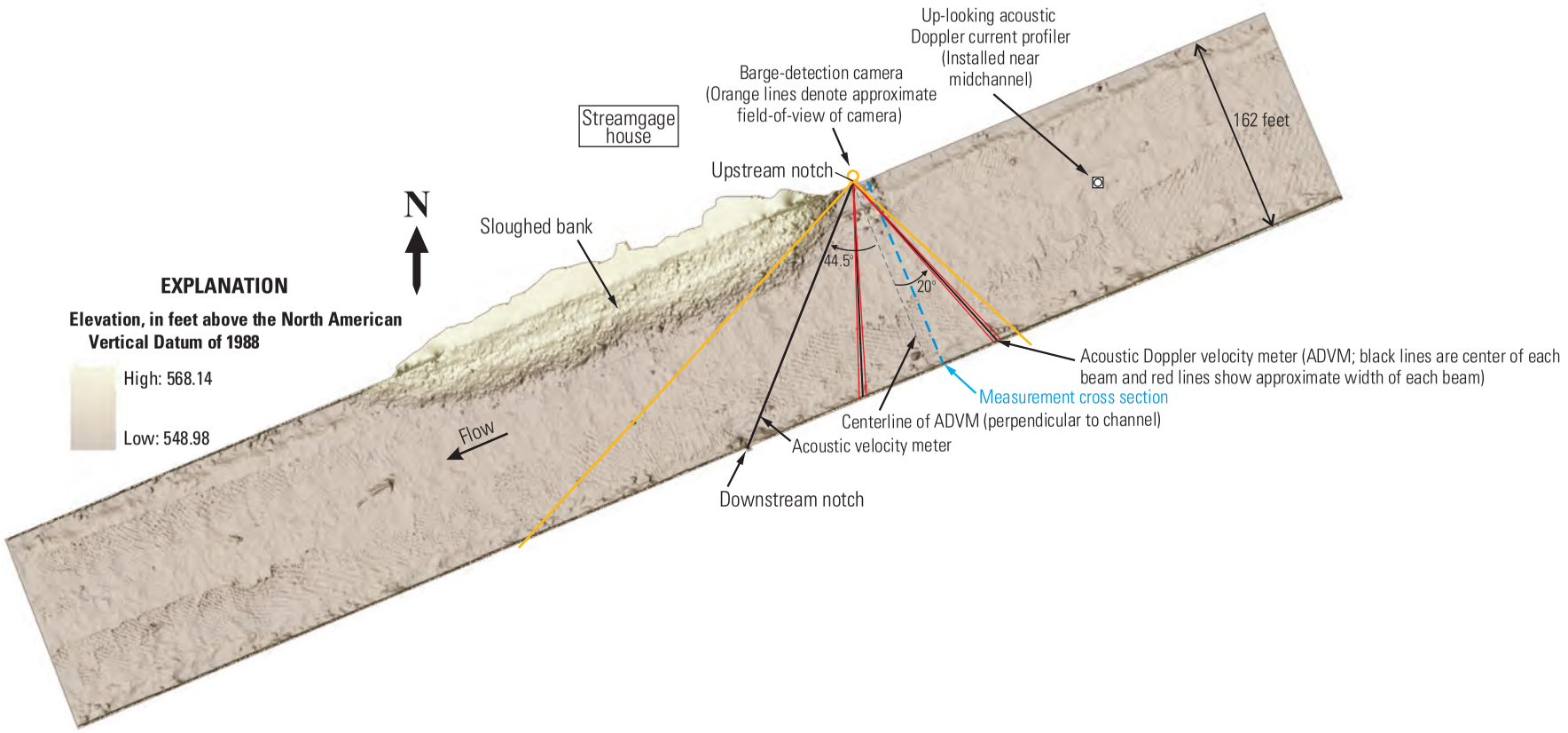

Figure 2. Instrument configurations superimposed on the channel bathymetry at the U.S. Geological Survey streamgage on the Chicago Sanitary and Ship Canal near Lemont, Illinois (05536890). Modified from Jackson and others (2012, fig. 2).

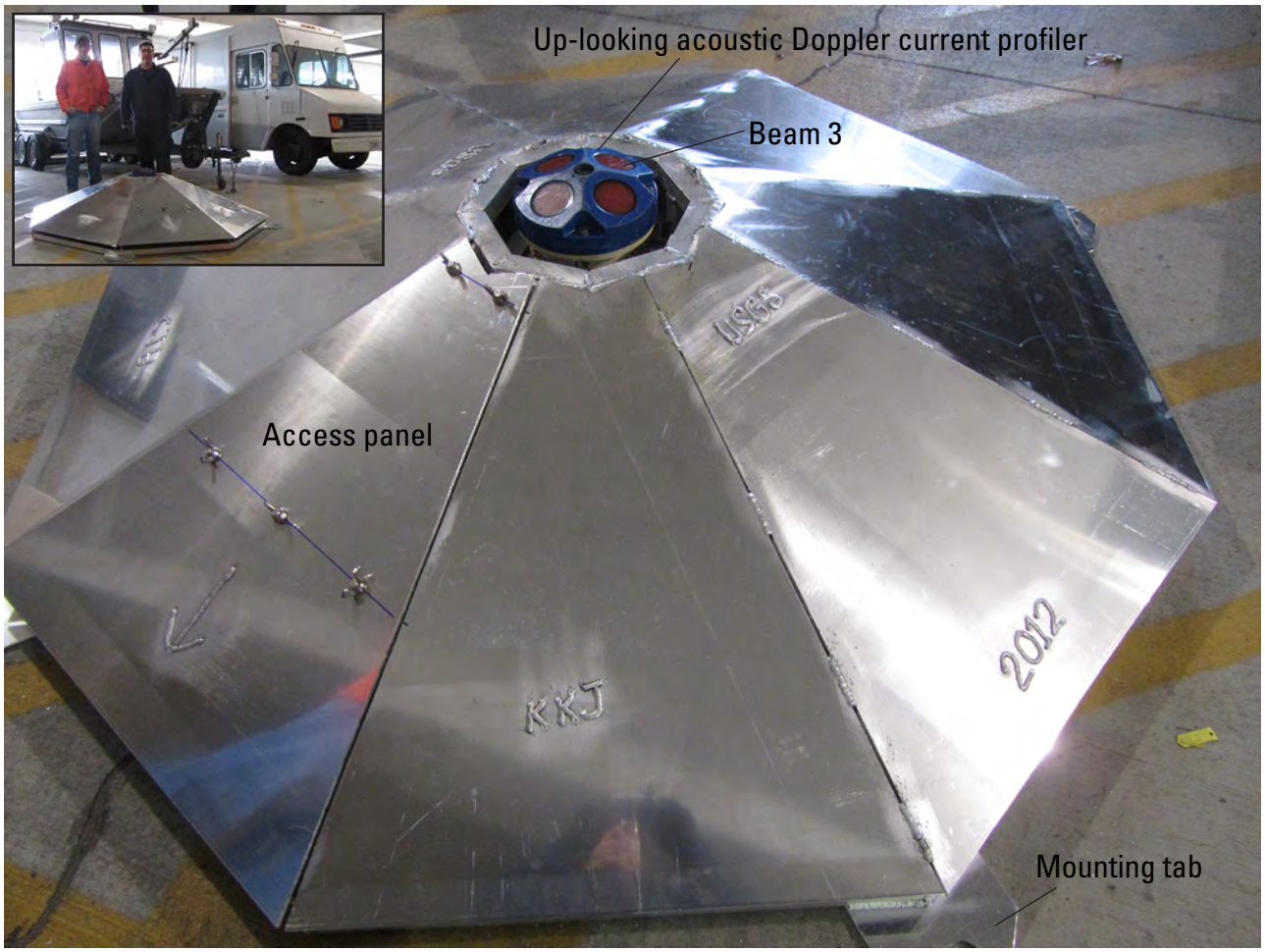

Image Credits: K. Johnson, U.S. Geological Survey

Figure 3. The up-looking acoustic Doppler current profiler mount installed on the channel bed approximately 170 feet upstream from the acoustic Doppler velocity meter at the U.S. Geological Survey streamgage on the Chicago Sanitary and Ship Canal near Lemont, Illinois (05536890). Inset photograph shown for scale.

instrument, including velocity components, receiver signal strength indictor (RSSI), correlation, pitch, roll, and water temperature at the transducer head, are logged using a Campbell Scientific CR1000 data logger. The 1-min time-averaged data are used by the data logger to compute the 15-min time-averaged data. Time stamps (in central standard time [CST]) are recorded at the end of the 1- and 15-min averaging intervals. After a period of instrument testing and configuration in 2013, the up-looking ADCP began delivering consistent data with no change in configuration since January 14, 2014. Periodic side-scan sonar surveys of the study site on the Chicago Sanitary and Ship Canal are used to ensure the mount is clear of debris, and no debris accumulation has been noted. The 1- and 15-min data from the up-looking ADCP data can be accessed through a USGS data release on ScienceBase (Jackson and Johnson, 2018).

Temperature and Specific Conductance

To continuously measure the variation in temperature, specific conductance, and density over the water column, the USGS installed a string of six Campbell Scientific temperature and specific conductance sensors in the notch along the right (northwest) bank of the Chicago Sanitary and Ship Canal near Lemont, Ill., in late 2014 (fig. 4). The sensors were installed at elevations of 554.76, 557.76, 560.76, 563.76, 566.76, and 569.76 ft (NAVD 88). The bed elevation below the sensors at the time of installation was about 551.5 ft (NAVD 88). Instantaneous readings from each sensor are recorded every 10 min. During routine streamgage visits, a YSI 6920 multiparameter sonde is used to independently measure the temperature and specific conductance at each elevation. Recalibration of a specific conductance sensor is completed when drift is detected. The sensors are cleaned and recalibrated (if necessary) each time the string is removed from the water.

Image Credit: C. Bosch, U.S. Geological Survey

Figure 4. Instrumentation deployed in and around the upstream notch at the U.S. Geological Survey streamgage on the Chicago Sanitary and Ship Canal near Lemont, Illinois (05536890).

To measure the temperature, specific conductance, and density of the water flowing from the Calumet Sag Channel into the Chicago Sanitary and Ship Canal, the USGS also installed a string of three Campbell Scientific temperature and specific conductance sensors on the left (southeast) bank of the Calumet Sag Channel at the USGS streamgage (05536700) about 0.4 mi upstream from Sag Junction (fig. 1). The elevations of the three sensor pairs are 568.76, 571.76, and 574.76 ft (NAVD 88). The bed elevation directly below the sensors at the time of installation was about 568.0 ft (NAVD 88). The sampling interval, maintenance and calibration checks, and recalibration procedures were the same as the Lemont streamgage.

The temperature and specific conductance in the Chicago Sanitary and Ship Canal also is monitored by the USGS at the USGS streamgage (05536137) at Western Avenue about 17 mi upstream from Sag Junction (fig. 1). A string of three Campbell Scientific temperature and specific conductance sensors were deployed on the left (southeast) bank of the canal at this streamgage. The elevations of the three sensor pairs are 569.70, 572.70, and 575.70 ft (NAVD 88). The bed elevation directly below the sensors at the time of installation was about 569.0 ft (NAVD 88). The sampling interval, maintenance and calibration checks, and recalibration procedures were the same as the Lemont streamgage.

Additional hourly temperature and specific conductance data were provided by the MWRD in the Chicago Sanitary and Ship Canal and Calumet Sag Channel. These data are collected as part of the MWRD Continuous Dissolved Oxygen Monitoring Program and were collected using YSI Inc. multiparameter sondes deployed about 3 ft below the water surface at several locations on the Chicago Sanitary and Ship Canal (Loomis Street, Cicero Avenue, and B&O Central Railroad Bridge) and on the Calumet Sag Channel (Cicero Avenue and Route 83 Bridge; fig. 1; MWRD, 2016). Additional information on MWRD's continuous monitoring program, including a full list of monitoring stations, can be found on the MWRD website (https://www.mwrd.org/irj/portal/anonymous/WQM).

Barge Detection Camera

In May 2016, a Hikvision DS–2CD2142FWD 4-megapixel dome camera with infrared night vision and motion detection was installed on the right bank of the Chicago Sanitary and Ship Canal at the Lemont streamgage to record and document the passage of commercial vessels through the reach. The barge-detection camera was mounted on a 12-ft mast near the upstream notch and oriented about 45 degrees downstream toward the downstream notch (figs. 2, 4, 5). The

Figure 5. A still image extracted from video from the barge-detection camera installed on the right bank at the U.S. Geological Survey streamgage on the Chicago Sanitary and Ship Canal near Lemont, Illinois (05536890).

camera was programmed to collect 30 s of video if a vessel passed by in either direction across the programmed motion detection line (fig. 5). Videos were recorded to an external hard drive that was retrieved and replaced with an empty drive at each streamgage visit.

Data Processing

This section is divided into subsections based on the data processing methods for each of the analyses in this study. Initial processing of the raw up-looking ADCP data leads this section because it is common to all analyses. Unless otherwise stated, Matlab R2015b (Mathworks, 2015) was used to process, analyze, and visualize these data using custom scripts.

Initial Processing of Up-Looking Acoustic Doppler Current Profiler Data

Extensive processing of the raw up-looking ADCP data were required to carry out the analyses in this report. Although data from the up-looking ADCP were processed in different manners depending on the analysis, some initial processing steps were common to all the analyses and were completed first to create the base datasets for each analysis. These steps were completed on the 1- and 15-min up-looking ADCP datasets, which consisted of DAT files from the CR1000 datalogger for January 14, 2014, to July 10, 2017 (Jackson and Johnson, 2018). The DAT files included 162 values for each 1- or 15-min averaging period (timestamp, record number, site identifier, water temperature at the face of the ADCP, pitch, roll, voltage, and 3 velocity components, 4-beam average RSSI, and correlation in each of the 30 bins, and an average of each over the 30 bins). The timestamp was assigned at the end of each averaging period. The 1-min dataset required a substantial amount of time to initially process because of its size (2.16 gigabytes), whereas the 15-min dataset was much more manageable (174 megabytes). A custom script was used to parse, process, and write these data files to a Matlab data file for use in further analyses.

The initial processing script read the DAT file, parsed the data, and created a Matlab data structure. For each bin, the height above bottom and elevation were computed using the configuration of the ADCP, the geometry of the mount, and the measured elevation of the bed at the deployment location of the ADCP (550.61 ft, NAVD 88). The RSSI profiles were then filtered to locate the water surface, apply a 6-percent sidelobe contamination region (Teledyne RDI, 2007), and invalidate data in all bins above the sidelobe. Initial analyses revealed some inconsistencies in the filter used to identify the water surface in the RSSI profiles and screen out data above the sidelobe. Therefore, an additional script was run that used stage records from the site to define the sidelobe cutoff and remove any remaining valid data above the stage-defined sidelobe. In addition, analysis of the velocity profiles over the period of record showed that the velocity in bins 1 and 2

(closest to the up-looking ADCP) were contaminated by flow disturbance from the up-looking ADCP mount. Therefore, data in these first two bins were considered invalid and were not used in any analysis in this study.

Mean values of the three velocity components (streamwise, transverse, and vertical) for each profile were then recomputed using the screened data. Difficulties in obtaining an accurate, in-situ ADCP compass calibration and blackwater diving conditions resulted in some ambiguity in the orientation of the instrument relative to the channel. Therefore, it was necessary to use the dataset and known channel orientation to compute the required rotational correction to align the measured primary flow direction with the channel orientation. The deviation from the streamwise direction (245.5 degrees from true north) was computed for every valid bin, the profile means, and the entire dataset. To correct for orientation of the ADCP relative to the channel, the mean value of the deviation of the primary flow direction from the streamwise direction for the entire dataset was used to apply a rotation correction to the velocity data. The magnitude and direction of the velocity in each bin (as well as the profile average) were then computed. The deviation from the streamwise direction was computed for each corrected velocity vector and used to compute the streamwise and transverse components of velocity for every bin at every time step. No rotations or corrections were applied to vertical velocity. Finally, water temperature data from the ADCP were plotted and edited to remove outliers. The processed data were written to a Matlab data structure and saved as a Matlab data file for use in further processing and analysis.

Evolution of Vertical Profiles of Velocity

The velocity data from the up-looking ADCP, the ADVM, and the acoustic velocity meter (AVM) were retrieved along with the stage and discharge data for the period of analysis (January 14, 2014, to July 10, 2017). To provide the best possible temporal resolution, the 1-min velocity data from the up-looking ADCP and ADVM are used for analysis. The stage, discharge, ADVM velocities, and AVM velocities were all interpolated to the same time steps as the 1-min up-looking ADCP data. The stage was converted to water-surface elevation using the defined gage datum (551.76 ft, NAVD 88), and elevations were assigned to the ADVM and AVM velocities based on Jackson and others (2012).

Of the possible 1,833,572 1-min velocity profiles between 12:06 (CST) January 14, 2014, and 19:38 (CST) July 10, 2017, 5.1 percent of the data were missing (equipment or power failure, corrupt data files) and 0.87 percent were invalid as determined by the internal thresholds of the instrument firmware, which resulted in 1,723,858 1-min time-averaged velocity profiles for analysis. This large dataset was divided into two datasets based on the time-rate-of-change of the discharge to identify data on the rising and falling limbs of a hydrograph. This was achieved by calculating a 5-point moving average of the 1-min discharge data from the ADVM and then computing the time-rate-of-change in discharge (dQ/dt), where Q is discharge and t is time. Rising limbs have a positive dQ/dt, whereas falling limbs have a negative dQ/dt. Events in the hydrograph that cause a change in discharge are due primarily to upstream-propagating negative surges (decreases in water level) induced by filling Lockport Lock, upstream-propagating positive surges (increases in water level) created by stoppage of flows at Lockport Lock and Dam (powerhouse shutdowns, closing of the lock-filling valves or sluice gates), downstream-propagating positive surges from lakefront locks, and more sustained high-flow events in the CAWS (both through natural runoff and operational changes) (Jackson and others, 2012). Further information about lock-induced surges is in USACE (1949) and Maeck and Lorke (2014).

Lockage surges from Lockport Lock were extracted from the dataset using a matched filter pattern-recognition algorithm for signal processing that relied on known characteristics of a typical lockage surge (Jackson and others, 2012) and manual review of the dataset. Before applying the matched filter, the 1-min ADVM discharge data were detrended by applying a 60-min moving average to the data and subtracting the averaged dataset from the original dataset (fig. 6). The detrended data were then smoothed using a 5-min moving average to remove noise in the data without removing the lockage surges. A typical lockage surge was identified in the dataset (using Jackson and others [2012] as guidance) and used as a template for the matched filter (fig. 6). The 1-min ADVM discharge dataset was then filtered forward and backward using the matched filter to identify the start and end of lockage surges that matched 50 percent of the template surge. The results were plotted on the hydrograph by identifying the filter-detected lockage surges in red and manually inspected for accuracy (fig. 7). Although the filter performed very well, it did not identify every lockage surge in the dataset. A total of 9,286 lockage surges were identified between October 2, 2013, and July 20, 2017. The results compared very well to manual identification of lockage surges for a subset of the data from October 2, 2013, to June 15, 2014. For this period, the filter identified 1,571 lockage surges and manual identification resulted in 1,639 surges (96-percent filter accuracy). Once the lockage surges were identified, the data subset was further subdivided into rising and falling limbs of the lockage surge based on dQ/dt.

To investigate the relation between discharge and the vertical profile of streamwise velocity, the datasets above were further subdivided based on the ADVM discharge. Discharge from −1,000 to 20,000 ft^3/s was divided into 1,000-ft^3/s ranges and used to sort the data into subsets. A median profile of velocity for each discharge range was computed. If the number of velocity observations used to compute a point in the median profile for any velocity bin was less than 30 percent of the median number of observations per bin for all the velocity bins, the data for that bin were deemed too sparse and that velocity bin was not included in the median velocity profile. To examine the relation between temperature and the vertical

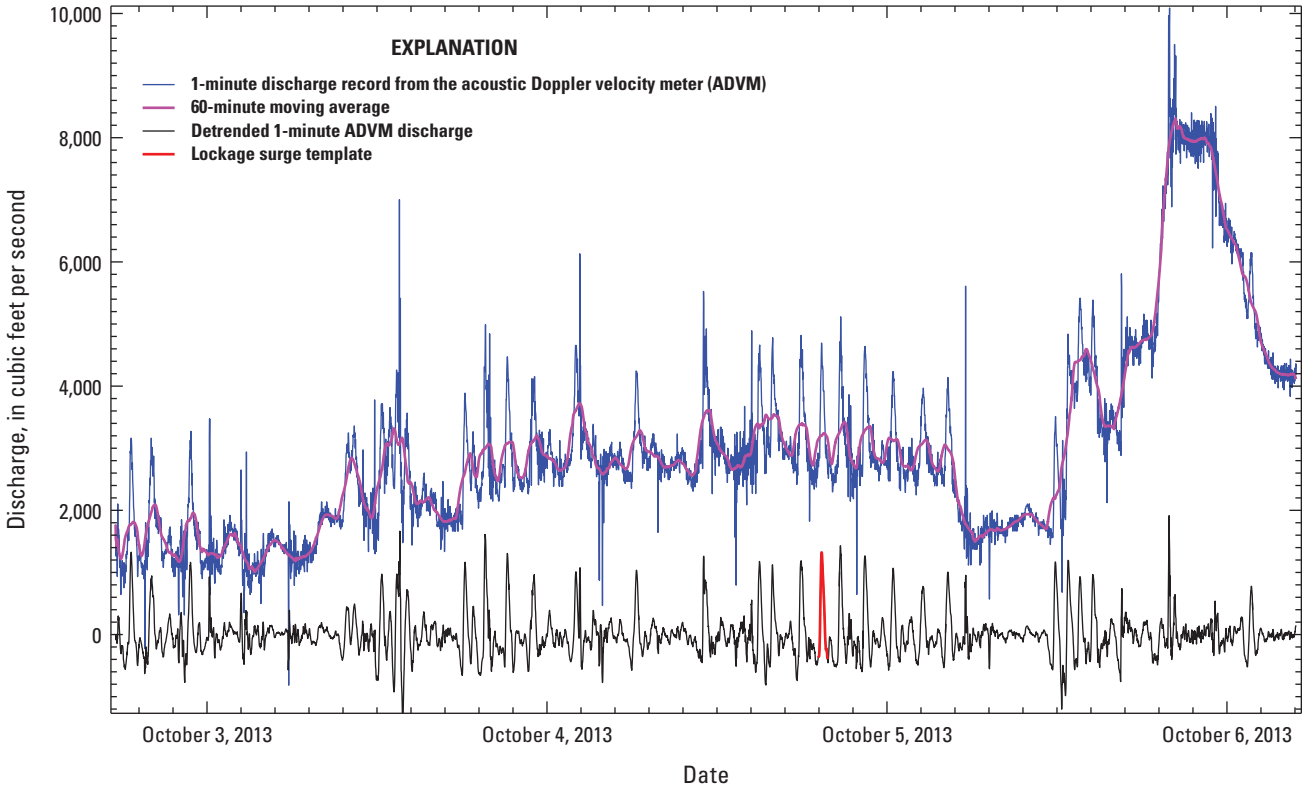

Figure 6. One-minute discharge data from the acoustic Doppler velocity meter at the U.S. Geological Survey streamgage on the Chicago Sanitary and Ship Canal near Lemont, Illinois (05536890) and the lockage surge template based on known characteristics of a typical lockage surge.

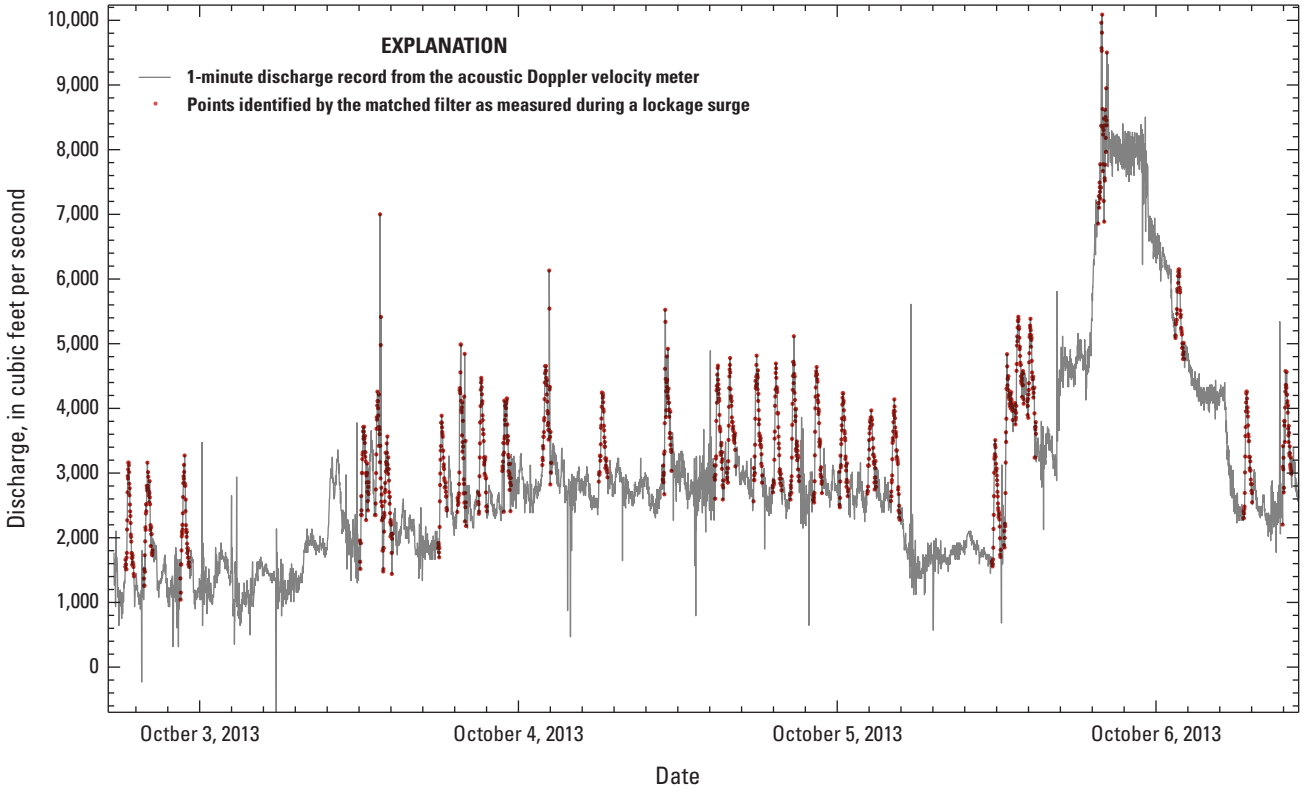

Figure 7. An example of lockage surges identified by a matched filter applied to 1-minute discharge data from the acoustic Doppler velocity meter at the U.S. Geological Survey streamgage on the Chicago Sanitary and Ship Canal near Lemont, Illinois (05536890).

profile of streamwise velocity, the data were sorted by temperature at the face of the up-looking ADCP (near-bottom water). The data were subdivided into 2-degree-Celsius ranges over the scale of 0 to 24 degrees Celsius, and median profiles were computed for each temperature range. The same threshold for defining and excluding bins with sparse data that was used in the discharge analysis was used in the temperature analysis.

Density-Driven Gravity Currents (Underflows)

Analysis of the occurrence of density-driven gravity currents (or underflows) in the Chicago Sanitary and Ship Canal near Lemont, Ill., used the 15-min up-looking ADCP dataset, preprocessed as described in the initial processing section above. Daily mean discharge data for the Chicago Sanitary and Ship Canal near Lemont, Ill. (05536890), the Calumet Sag Channel near Route 83 at Sag Bridge, Ill. (05536700), and the Little Calumet River at South Holland, Ill. (05536290; fig. 1), were extracted from the USGS National Water Information System (https://doi.org/10.5066/F7P55KJN) database for use in the analysis. The water-quality data used in the analysis included USGS and MWRD stations on the CAWS (fig. 1). Edited data from the temperature and specific conductance strings deployed in the Chicago Sanitary and Ship Canal near Lemont, Ill. (05536890), Chicago Sanitary and Ship Canal at Western Avenue at Chicago, Ill. (05536137), and Calumet Sag Channel near Route 83 at Sag Bridge, Ill. (05536700), were extracted from the USGS National Water Information System database at their native, 10-min time steps (fig. 1). MWRD provided hourly temperature and specific conductance data for the Chicago Sanitary and Ship Canal at Loomis Street (left bank), Cicero Avenue (left bank), and the B&O Railroad Bridge (center), and for the Calumet Sag Channel at Cicero Avenue (left bank) and Route 83 (left bank). MWRD also provided daily outfall discharge, temperature, and chloride concentrations for the Stickney and Calumet Water Reclamation Plants (WRPs) for the period of interest (available from http://www.mwrd.org). Daily meteorological data for the area were downloaded from the National Climatic Data Center (https://www.ncdc.noaa.gov) for station USC00111577 Chicago Midway Airport 3 SW, Illinois, US, for the period of interest.

The period of interest for the analysis was from January 29, 2015, to July 10, 2017. Data before 2015 could not be used in this analysis because the USGS temperature and specific conductance strings on the CAWS were not installed until December 2014. The temperature and specific conductance data from the Chicago Sanitary and Ship Canal near Lemont, Ill., and Western Avenue at Chicago, Ill., and the Calumet Sag Channel near Route 83 at Sag Bridge, Ill., and the up-looking ADCP data were interpolated to a common 10-min time step starting January 29, 2015, at 13:00 and ending July 10, 2017, at 19:30.

Following the methods of Jackson (2013), water density was computed at each of the USGS and MWRD water-quality sites from water temperature and specific conductance data following the United Nations Educational, Scientific, and Cultural Organization 1983 equation of state for seawater that is valid for the observed temperatures and salinities (Fofonoff and Millard, 1983). A low salinity correction is applied following Clesceri and others (1999). Density also was computed assuming zero salinity at each site to isolate the effects of temperature on density. All density computations were completed for every 10-min sample. At the USGS sites with temperature and specific conductance strings, vertical profiles of density were computed for every time step after applying a 60-min moving average. Likewise, a 60-min moving average was applied to velocity data from the up-looking ADCP before computing vertical profiles of streamwise velocity. The application of the moving average reduced the variability in the profiles because of instrument noise and other factors.

Finally, to allow a correlation analysis using the full dataset described above, daily mean values were computed for all parameters not already in a daily mean format. These data included the USGS and MWRD water-quality parameters (temperature, specific conductance, and density) and the up-looking ADCP data (streamwise velocity, temperature at the transducer head, and slope of the lower part of the velocity profile).

Index-Velocity Rating Development for the Up-Looking Acoustic Doppler Current Profiler

The USGS streamgage on the Chicago Sanitary and Ship Canal near Lemont, Ill. (05536890; fig. 1), uses index-velocity ratings and stage-area (SA) ratings to compute continuous records of discharge from the AVM and ADVM velocity data (each instrument has a pair of index-velocity and SA rating curves). With the addition of an up-looking ADCP in 2014, it is possible to develop an index-velocity rating for this instrument. However, the potential for hysteresis in the index-velocity rating is higher for an instrument measuring only in the center of the channel, especially downstream from a confluence like Sag Junction, because the horizontal velocity distribution may change for the same discharge depending on the discharge ratio of the two converging channels upstream (Jackson and others, 2013).

An index-velocity rating curve (M1) for the up-looking ADCP was developed following the guidance of Levesque and Oberg (2012). A total of 26 discharge measurements made at the site by the USGS between February 11, 2014, and July 10, 2017, were used in rating development (see appendix 1, tables 1.1 and 1.2). The measurements spanned a discharge range of 347 to 11,138 ft^3/s and typically contained 12 or more transects across the channel due to unsteadiness often present in the flow. The discharge from each measurement was divided

by the rated area to compute a mean channel velocity (V_{mean}, in feet per second). The rated area (A, in square feet) was computed from the time-weighted mean gage height (GH, in feet) using SA rating 3.1 (eq. 1).

$$A=164.68\times GH-71.021 \quad (1)$$

The index velocity (V_{indx}) from the up-looking ADCP was computed by first time-averaging 1-min velocity profiles over the period of the boat-mounted ADCP discharge measurement (typically about 38 min for 12 transects) and then computing the arithmetic mean of streamwise velocity in bins 3 to 18, or about 6 to 21 ft above the canal bed. A fixed averaging range was used rather than a dynamic averaging range because the total range of stage is small (3.54 ft during the 3.4-year period of record used for rating development) relative to the depth of the canal (about 25 ft), and the near-surface data can have occasional outliers. This method produced a single V_{indx} for each discharge measurement. The M1 index-velocity rating curve was developed using an ordinary least squares (OLS) regression between V_{indx} and V_{mean}.

In addition to computing the M1 index-velocity rating curve based on multiple-transect discharge measurements, a second index-velocity rating curve (S1) was computed based on individual transects from each multiple-transect discharge measurement (see appendix 1, table 1.2). This single-transect rating development was suggested by the seventh LMDA TRC as a possible method to better capture unsteadiness in the flow (Espey and others, 2014). This was accomplished by treating each transect as a separate measurement of discharge and computing an associated V_{mean} and V_{index} for each transect in the same manner as described above. This method produces many more points to define the index-velocity rating (332 compared to 26) and covers a larger range of discharge (−17 to 11,354 ft^3/s) but has a substantially shorter averaging period (about 3 min per transect compared to about 38 min for a typical 12-transect measurement). Although using individual transects provides more data points and captures the unsteadiness during a 12-transect measurement in the index-velocity rating, the short 3-min averaging period of the up-looking ADCP data generally results in more variability in the velocity profile and index velocity and more uncertainty in the single-transect measurement of discharge (and thus more variability in V_{mean}).

Direct Computation of Discharge

The USGS streamgage on the Chicago Sanitary and Ship Canal near Lemont, Ill. (05536890; fig. 1), uses index-velocity and SA ratings to compute continuous records of discharge from the AVM and ADVM velocity measurements at this study site. With the addition of an up-looking ADCP in 2014, it is possible to use the vertical velocity profile from the up-looking ADCP and the transverse velocity profile from the ADVM to compute a direct estimate of discharge without the need for an index-velocity rating (the SA rating is still required). Although there are multiple possible methods for direct computation of discharge from these two instruments, the approach used for this site resembles the velocity profile method (Le Coz and others, 2008) but modified to use measured, rather than theoretical, vertical profiles of streamwise velocity.

Open-channel flow theory dictates that the depth-averaged velocity for a velocity profile that conforms to the logarithmic "law of the wall" (hereafter log law) occurs at about 6/10ths of the depth from the water surface. The log law is defined as

$$\frac{u}{u*}=\frac{1}{\kappa}\ln\left(\frac{z}{z_0}\right) \quad (2)$$

where

u is the streamwise velocity at a height (z) above the bed, in feet per second,
$u*$ is the shear velocity, in feet per second,
κ is von Karman's constant (about 0.41; unitless), and
z_0 is the roughness height, in feet.

For the log law, the depth-averaged velocity is at a height above the bed of $z=0.37\times H$, where H is the water depth. Because the ADVM is at a fixed height above the bed (about 14 ft above the bed depending on the reference bed elevation) and the mean depth of flow at the site is about 25 ft, the transverse velocity profile measured by the ADVM is generally not at $z=0.37\times H$ but is closer to $z=0.56\times H$ and varies with flow depth. Jackson and others (2013) determined that the ADVM-measured velocities were about 5 percent higher than the depth-averaged velocity (fig. 8). With this knowledge, the vertical profile of streamwise velocity from the up-looking ADCP can be fit with the log law and used to estimate the velocity ratio (V_r), a "correction" applied to the ADVM velocities to make the shifted ADVM transverse velocity profile representative of the depth-averaged velocity profile, ultimately yielding an estimate of the mean velocity for the cross section V_{mean}. The measured GH for a given period can be used to compute area (A) using SA rating 3.1 (eq. 1). A directly computed discharge (Q_{DC}) can be computed from $Q_{DC}=V_{mean}\times A$. This method does not require the use of an index-velocity rating.

Although this method of estimating discharge from these two instruments is relatively straightforward, it relies on the assumption that the vertical velocity profile follows the log law. Jackson and others (2012) determined that instantaneous and short-term averaged vertical velocity profiles can be noisy and deviated from a logarithmic profile, whereas long-term, time-averaged profiles tended to be logarithmic. This difference presents issues in computing discharge using this method at typical 10- to 15-min intervals used at many USGS streamgages. To overcome this limitation, the V_r for non-logarithmic profiles can be computed from the velocity measured by the up-looking ADCP at the ADVM elevation (V_{UL_ADVM}) and the depth-averaged velocity measured by the up-looking ADCP over bins 3 to 18 (V_{UL_DAV}).

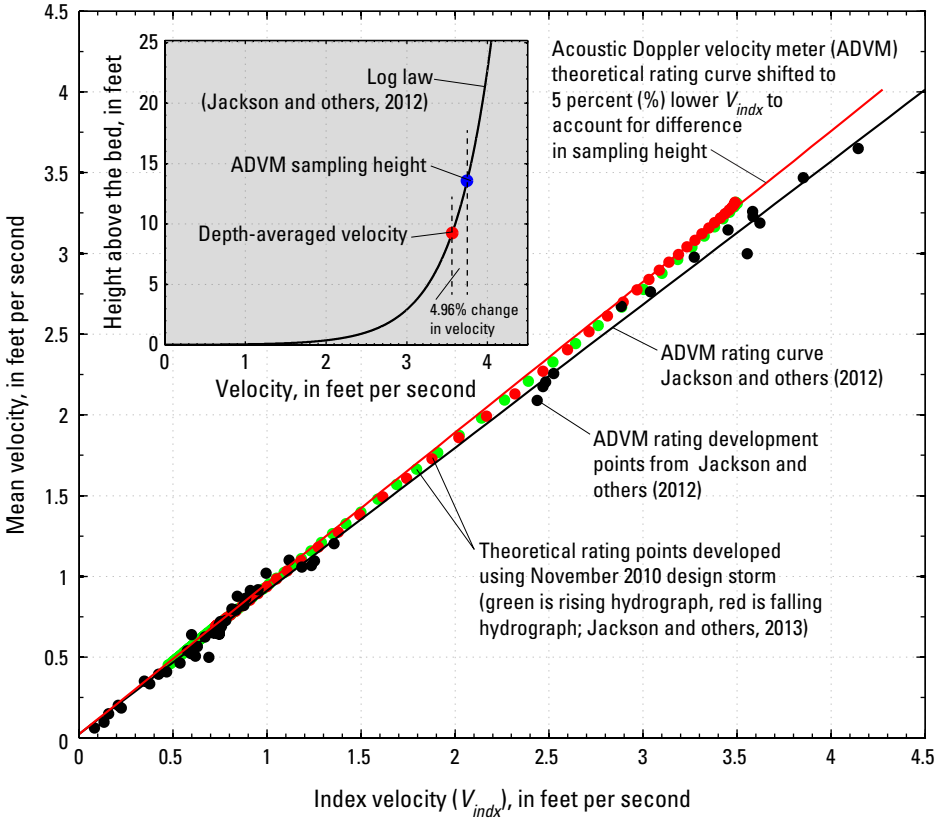

Figure 8. The acoustic Doppler velocity meter index-velocity rating curves (observed and theoretical) and the relation between the depth-averaged velocity and the acoustic Doppler velocity meter sampling height above the canal bed for the U.S. Geological Survey streamgage on the Chicago Sanitary and Ship Canal near Lemont, Illinois (05536890). Modified from Jackson and others (2013, fig. 14).

The depth-averaged velocity is computed by integrating the velocity profile over bins 3 to 18 and dividing by the distance between bins 3 and 18 (14.765 ft). Inherent in this method is the assumption that the true depth-averaged velocity is equivalent to the layer-averaged velocity over bins 3 to 18. Therefore, the V_r is computed using two different methods depending on the applicability (fit) of the log law to the time-averaged vertical profile of streamwise velocity at each time step:

$$V_r = \frac{V_{log\,0.37}}{V_{log\,ADVM}} \text{ for } R^2 \geq 0.95 \text{ and } u^* > 0, \quad (3)$$

$$V_r = \frac{V_{UL\_DAV}}{V_{UL\_ADVM}} \text{ for } R^2 < 0.95 \text{ or } u^* < 0, \quad (4)$$

where

$V_{log0.37}$ is the streamwise velocity, in feet per second, at a height of $0.37 \times H$ above the bed computed using a log-law fit to the velocity profile from the up-looking ADCP;

$V_{logADVM}$ is the streamwise velocity, in feet per second, at a height of the ADVM above the bed computed using a log-law fit to the velocity profile from the up-looking ADCP;

V_{UL_DAV} is the depth-averaged streamwise velocity, in feet per second, computed from the velocity profile from the up-looking ADCP over bins 3 to 18;

V_{UL_ADVM} is the streamwise velocity, in feet per second, at the elevation of the ADVM computed from the velocity profile from the up-looking ADCP using linear interpolation;

H is the average flow depth, in feet, over the averaging period;

R^2 is the coefficient of determination for the log-law fit to the streamwise velocity profile from the up-looking ADCP (unitless);

u^* is the shear velocity, in feet per second, estimated from the log-law fit to the streamwise velocity profile from the up-looking ADCP;

Correction of the ADVM velocity data using V_r to obtain the most accurate and robust estimate of the mean cross-sectional velocity V_{mean} required some iteration. One approach was to fit the beta distribution (Seo and Baek, 2004) to each of the ADVM 15-min transverse velocity profiles with the no-slip condition applied at the banks (Jackson and others, 2013). This method produced an estimate of the mean velocity at the elevation of the ADVM (V_β) and mean cross-sectional velocity can be computed as $V_{mean}=V_r \times V_\beta$. However, this method underestimated discharge by 100 to 200 ft^3/s for the daily, monthly, and annual mean flows. Ultimately, the method that produced the best results used the index velocity from the ADVM (V_{iADVM}) to compute the mean cross-sectional velocity

$$V_{mean}=V_r \times V_{iADVM} \quad (5)$$

The use of V_{iADVM} improves computational efficiency because every transverse velocity profile does not have to be fit with the beta distribution. Instead, V_{iADVM} is the simple arithmetic average of the velocity in the nine cells of the ADVM. Although this method uses V_{iADVM}, it does not rely on an index-velocity rating curve for computation of discharge.

The 15-min time-averaged velocity profiles from the up-looking ADCP were used in conjunction with the 1-min time-averaged ADVM profiles and 10-min time-averaged *GH* to compute Q_{DC} using the methods described above. The period of comparison was between January 14, 2014, and July 10, 2017. The 1-min ADVM velocity and discharge data were time-averaged over the same period as the 15-min up-looking ADCP data, whereas the 10-min *GH* data were linearly interpolated at the 15-min time stamps of the up-looking ADCP data. SA rating 3.1 (eq. 1) was used to compute the rated area. To ensure that time-averaging and interpolation of data did not result in substantial errors in the computed discharge record, ADVM index-velocity rating 3.1 was applied to the time-averaged velocity data, the SA rating 3.1 was applied to the interpolated *GH*, and the ADVM discharge record was reproduced with a median error of less than 1 ft^3/s. This confirmed no substantial errors were introduced in the process of producing 15-min ADVM and *GH* data. Finally, both the ADVM discharge data and the directly computed discharge data were averaged over each day, month, and year of the period of comparison to allow comparison of daily, monthly, and annual mean flows.

Tow Passage Videos

Recordings from the barge-detection camera were first screened for validity and any video clips without vessels (triggered by rain, spider webs, or other motion in the field-of-view) were removed. Video files from the camera are archived on a USGS server in Urbana, Ill., and were reviewed by USGS personnel. Data including date, time, tow configuration, loading, direction of travel, bow type (rake or box), and any other relevant information were recorded in a spreadsheet for each video file. Still shots from typical daytime and nighttime videos can be seen in figure 9. About 15 percent of the videos lacked sufficient length or clarity for full analysis, but generally some data could be gleaned from the videos (such as direction of travel and tow width; for example, a two-barge wide tow of unknown length moving upstream).

Statistical Analyses

Statistical analyses were performed using Matlab R2015b (Mathworks, 2015). For analysis of underflows, the Kolmogorov-Smirnov test, a non-parametric test, was used to test normality of response and explanatory variables. The response variables tested were not normally distributed, so a Spearman's rank correlation analysis was used to determine significant associations. The strength of an association between response and explanatory variables is given by the Spearman's rank correlation coefficient (ρ), which is always between −1 and 1. Associations are defined as very weak (|ρ|=0.00 to 0.19), weak (|ρ|=0.20 to 0.39), moderate (|ρ|=0.40 to 0.59), strong (|ρ|=0.60 to 0.79), and very strong (|ρ|=0.80 to 1.0), where |ρ| is the absolute value of the Spearman's rank correlation coefficient. Positive associations (response variable increases with an increase in the explanatory variable) have $\rho>0$, while negative associations (response variable decreases with an increase in the explanatory variable) have $\rho<0$. Comparison of discharge records used a suite of statistical tests. The t-test was used to compare the daily, monthly, and annual means of each record to determine if they are statistically different. A sign test was performed using the difference between the two records to determine if the daily, monthly, and annual means are statistically different from zero. Finally, a two-sample Kolmogorov-Smirnov test and quantile-quantile plots were used to compare the distributions of the two discharge records. All statistical tests were performed at a significance level of 5 percent, unless otherwise noted.

Figure 9. Still images extracted from video from the barge-detection camera on July 2, 2016, at 12:46:30 (upstream-bound tow) and July 3, 2016, at 00:02:45 (downstream-bound tow) at the U.S. Geological Survey streamgage on the Chicago Sanitary and Ship Canal near Lemont, Illinois (05536890).

Characterizing Variability in Vertical Profiles of Streamwise Velocity

This section presents the results of the data collection and analyses described in the "Methods" section beginning with the evolution of the vertical profile of streamwise velocity for unsteady flows. Evidence of the formation of density-driven underflows in the Chicago Sanitary and Ship Canal near Lemont, Ill., is presented, followed by a correlation analysis to identify possible triggers that initiate the underflows.

Evolution of Vertical Profiles of Streamwise Velocity during Unsteady Flows

In general, as discharge in the Chicago Sanitary and Ship Canal increases, the vertical profile of streamwise velocity becomes less uniform, develops higher gradient profiles with the near-surface velocity increasing faster than the near-bed velocity, and becomes more logarithmic in shape (fig. 10). For discharges less than 5,000 ft^3/s (discharges computed from 1-min ADVM data), the water-surface elevation varies by only 0.31 ft (fig. 10; table 1), the up-looking ADCP velocity profiles are relatively uniform (neglecting the near-bed flow acceleration discussed below), and an increase in discharge of 1,000 ft^3/s produces an increase in velocity of about 0.25 ft/s over most of the vertical profile. As the discharge increases from 5,000 to 11,000 ft^3/s, the median water-surface elevation decreases by 0.7 ft, velocity profiles begin to show steeper gradients, and mean velocity increases by about 0.33 ft/s per 1,000-ft^3/s increase in discharge (fig. 10; table 1). Between 11,000 and 12,000 ft^3/s, the median water-surface elevation reaches a local minimum, and the velocity profile shows the greatest change in mean velocity with an increase of about 0.5 ft/s over a 1,000-ft^3/s increase in discharge. At a discharge above 12,000 ft^3/s, the median water-surface elevation increases with increasing discharge, and the gradient in the velocity profile increases with velocity (and discharge), with the near-surface velocity increasing faster than the near-bed

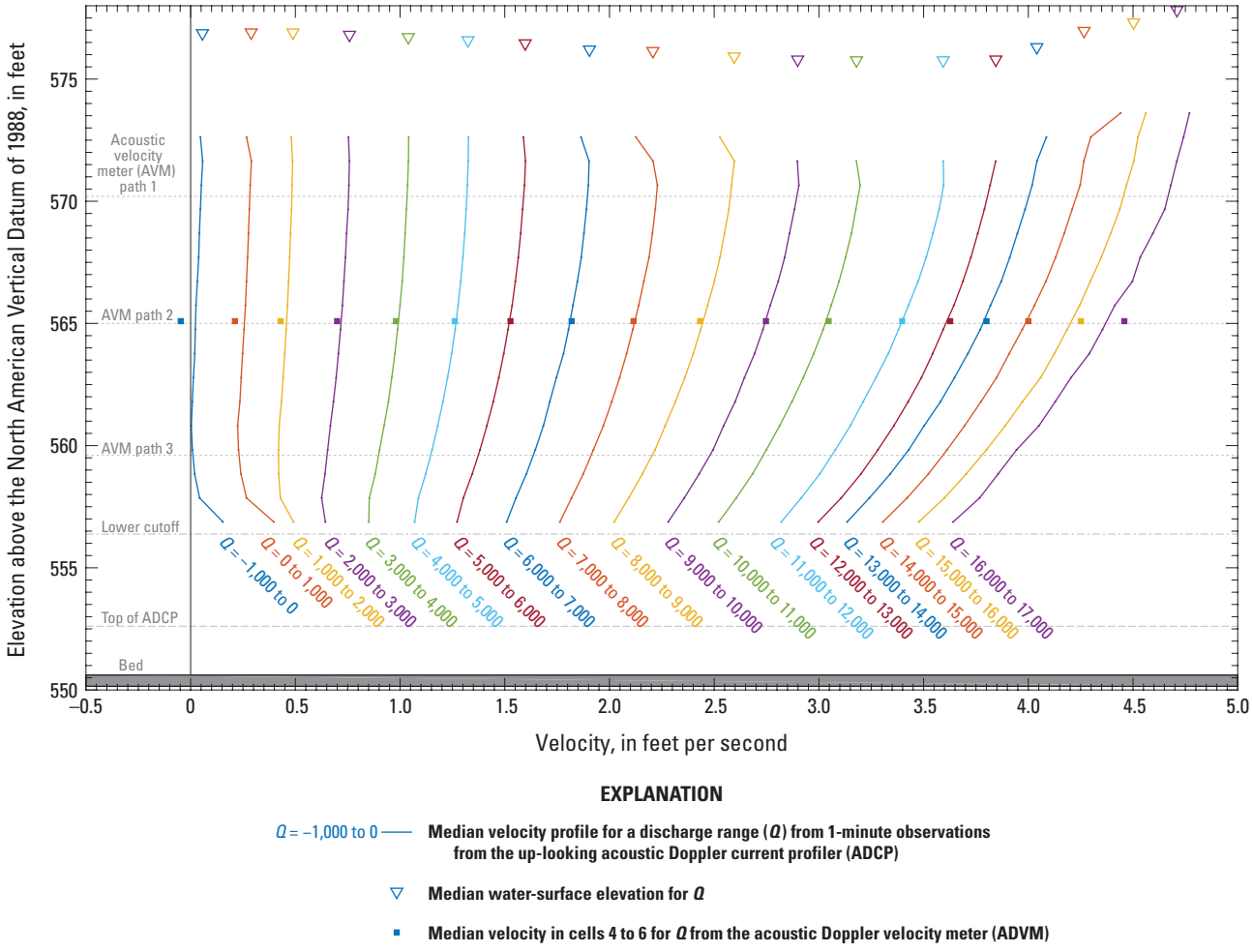

Figure 10. Median streamwise velocity profiles from the up-looking acoustic Doppler current profiler (ADCP) as a function of discharge at the U.S. Geological Survey streamgage on the Chicago Sanitary and Ship Canal near Lemont, Illinois (05536890), January 14, 2014, to July 10, 2017.

velocity. Log law fits to 15-min profiles tended to be most appropriate for moderate to high flows; at least 70-percent of the profiles adhere to a log law for discharge ranges above 5,000 ft^3/s (based on a coefficient of determination threshold of 0.95; table 1).

The median velocity computed for the 1-min ADVM data in cells 4 to 6 (between 60 and 105 ft from the right bank) at 565.1 ft (NAVD 88; the elevation of the ADVM) shows excellent agreement with the up-looking ADCP profiles for discharge ranges between 4,000 to 15,000 ft^3/s (fig. 10). The ADVM shows a slightly lower median velocity than the up-looking ADCP for discharges below 4,000 ft^3/s and a slightly higher median velocity than the up-looking ADCP at discharges above 15,000 ft^3/s (fig. 10). Although the differences at high discharge may be due to a smaller number of profiles (table 1), the number of profiles is not the issue for discharges less than 4,000 ft^3/s.

A more plausible explanation for the difference between the ADVM and up-looking ADCP median velocities at low discharge is the physical separation between the ADVM and up-looking ADCP (fig. 2) combined with unsteady flows dominated by negative upstream surges induced by the filling of Lockport Lock (fig. 7). As the ambient discharge in the Chicago Sanitary and Ship Canal drops, the relative magnitude of the lockage surge increases (fig. 7). For example, at an ambient discharge of 1,200 ft^3/s, a lockage surge can increase the flow about 2,000 ft^3/s (or 167 percent) compared to a lockage surge at an ambient discharge of 4,000 ft^3/s, which increases the flow about 1,200 ft^3/s (or 30 percent). Therefore, the effect of lockage surges is greater as the ambient canal discharge decreases. Because a lockage surge propagating upstream will reach the ADVM before it reaches the up-looking ADCP, ADVM discharge and ADVM velocity are generally in phase, whereas ADVM discharge and up-looking ADCP velocity are

Table 1. Summary of up-looking acoustic Doppler current profiler data used to compute median streamwise velocity profiles for a range of discharge (fig. 10) at the U.S. Geological Survey streamgage on the Chicago Sanitary and Ship Canal near Lemont, Illinois (05536890), January 14, 2014, to July 10, 2017.

[The parent dataset contains 1-minute time-averaged profiles (n=1,723,858). NAVD 88, North American Vertical Datum of 1988. A negative discharge indicates upstream flow towards Lake Michigan]

Discharge range, in cubic feet per second	Median discharge, in cubic feet per second	Number of profiles	Median water-surface elevation, in feet above the NAVD 88	Aspect ratio (A_r) (width/depth)	Percent of 15-minute profiles fitting a log-law profile[1]
−1,000 to 0	−148	6,597	576.89	6.16	0.3
0 to 1,000	771	114,262	576.90	6.16	0.9
1,000 to 2,000	1,516	563,427	576.90	6.16	4.5
2,000 to 3,000	2,453	481,184	576.82	6.18	18.1
3,000 to 4,000	3,431	281,811	576.73	6.20	36.0
4,000 to 5,000	4,423	152,514	576.59	6.24	54.0
5,000 to 6,000	5,369	62,876	576.47	6.26	70.7
6,000 to 7,000	6,391	22,810	576.22	6.33	74.3
7,000 to 8,000	7,477	14,172	576.14	6.35	80.4
8,000 to 9,000	8,447	9,796	575.94	6.40	85.3
9,000 to 10,000	9,519	7,103	575.80	6.43	94.0
10,000 to 11,000	10,425	6,193	575.77	6.44	96.2
11,000 to 12,000	11,528	4,988	575.76	6.44	95.2
12,000 to 13,000	12,401	3,970	575.79	6.43	92.4
13,000 to 14,000	13,495	3,734	576.30	6.31	100.0
14,000 to 15,000	14,434	2,862	576.98	6.14	91.9
15,000 to 16,000	15,304	1,141	577.32	6.07	100.0
16,000 to 17,000	16,196	101	577.84	5.95	100.0

[1]Based on a coefficient of determination of at least 0.95.

slightly out of phase because of the physical separation of the two instruments. Both instruments are averaged over the same 1-min interval during the passage of a lockage surge, resulting in a difference in velocity between the two instruments. Velocity and discharge will peak at the up-looking ADCP slightly after the peaks occur at the ADVM, resulting in higher up-looking ADCP velocity than ADVM velocity for the same ADVM discharge. Because the effect of lockage surges is greater as the ambient canal discharge decreases, the difference between the ADVM and up-looking ADCP velocities increases as discharge decreases (fig. 10).

The effect of the instrument separation is most pronounced during flow reversals. Full flow reversals that produce a negative (upstream) discharge are most commonly associated with a shutdown of the flow at Lockport Dam to "pond" water for release and power generation when utility rates are favorable (Duncker and Johnson, 2015). Stopping flow at Lockport Dam produces a positive surge that propagates upstream. Like the negative surge, the positive surge will reach the ADVM before it reaches the up-looking ADCP. This can result in a negative velocity and discharge at the ADVM but a positive velocity at the up-looking ADCP for the same 1-min averaging period. Because the positive surges that produce flow reversals always propagate upstream, this artifact of instrument separation does not go away with averaging and leads to the observation of a positive up-looking velocity profile for negative discharge and ADVM velocity (fig. 10). More analysis of lockage surges and the effect of instrument separation is discussed later in this section.

In general, the Chicago Sanitary and Ship Canal near Lemont, Ill. (05536890), exhibits an inverse stage-discharge relation over the range 0 to 12,000 ft^3/s but changes to a positive stage-discharge relation above 12,000 ft^3/s (fig. 10; table 1). This behavior is characteristic of the operation of the canal by MWRD, which draws down the water level in the CAWS in anticipation of high-precipitation events by releasing water at Lockport Dam and Lockport Controlling Works (fig. 1). The drawdown lowers the water-surface elevation while increasing discharge (fig. 10). High-precipitation events can rapidly supply runoff to the canal creating an increase in stage and discharge, thus producing a positive stage-discharge relation. The approximate 12,000-ft^3/s transition between these two regimes seems to be related to the operational constraints of the waterway. Specifically, the minimum water level in the Chicago Sanitary and Ship Canal at the Lockport Controlling Works is 10.0 ft below the Chicago City Datum (CCD) to maintain minimal navigational depths of the channel, as required by 33 Code of Federal Regulations 207.420 and 33 Code of Federal Regulations 207.425 (MWRD, 2013). This constraint, combined with the methodical operation of the flows at Lockport Dam and Lockport Controlling Works, results in a maximum discharge of about 12,000 ft^3/s at a water level of −10.0 ft (CCD) at Lockport Controlling Works.

As an example, consider the high-flow event in April 2013. During this event, the CAWS was overwhelmed by runoff, and water had to be released (backflowed) to Lake Michigan to keep Chicago from flooding (Duncker and Johnson, 2015). Before the backflows, the water level in the Chicago Sanitary and Ship Canal was drawn down. The drawdown started at 15:50 (CST) on April 17, 2013, reached a steady state at 20:00 (CST), and remained at this state until 23:00 (CST). During this 3-hour (h) period, the water level at Lockport Controlling Works was held steady at −10.0 ft (CCD), the stage and discharge at Lemont were relatively steady (mean Q=11,940 ft^3/s; standard deviation Q=100 ft^3/s; maximum change in stage=0.08 ft), and all 9 pit gates at Lockport Dam and 5 of 7 sluice gates at Lockport Controlling Works were fully open. At 23:40 (CST), heavy precipitation caused stage in the canal to rapidly rise (5 ft in 6 h at Lemont), and backflows to the lake commenced on April 18, 2013, at 5:05 (CST) and lasted about 11 h. After the backflows, there was an extended 8-h period on April 19, 2013, between 04:50 and 12:50 (CST) in which all 9 pit gates at Lockport Dam and all 7 sluice gates at Lockport Controlling Works were fully open to release as much water as possible from the CAWS. During this period, the stage at Lemont varied only 0.07 ft while the stage of the Chicago River in downtown Chicago held steady at more than 4 ft above normal (pre-event) water levels. Discharge in the canal near Lemont also was steady for this period with a mean discharge of 14,380 ft^3/s and a standard deviation of 92 ft^3/s. This event nicely demonstrates that the operation of the waterway by MRWD and the lower limit of −10.0 ft (CCD) for the water level in the canal at Lockport Controlling Works results in a maximum drawdown discharge of about 12,000 ft^3/s, and any additional substantial runoff to the canal will result in an increase in stage.

The median vertical profiles of streamwise velocity for discharge ranging from 6,000 to 12,000 ft^3/s have a velocity maximum that is well below the water surface at heights above the bed of 0.79H to 0.83H (fig. 10). The aspect ratios (Ar) of the Chicago Sanitary and Ship Canal near Lemont, Ill. (05536890), are relatively low (5.95 to 6.44; table 1) and close to the threshold for a narrow channel (Ar<5) where the velocity distribution is three-dimensional and the velocity maximum is below the free surface (Bonakdari and others, 2008). However, the discharge range 6,000 to 12,000 ft^3/s in the canal is primarily due to drawdown events, which lowers the water-surface elevation and produces the largest aspect ratios at this site. Despite having lower aspect ratios, median velocity profiles at discharges less than 6,000 ft^3/s and greater than 12,000 ft^3/s do not show consistent evidence of a submerged velocity maximum (neglecting the near-bed increase in velocity for Q<3,000 ft^3/s, which is addressed below). The depth of these velocity maxima below the water surface are substantially deeper than predictions from empirical equations based on Ar (Wang and others, 2001; Yang and others, 2004; Bonakdari and others, 2008) and are more characteristic of a narrower channel with an Ar of about 3.5. The cause of these submerged velocity maxima remains unclear.

Median profiles at lower discharge (Q<3,000 ft^3/s) show near-bed velocities increasing below 557 ft (NAVD 88) or within about 6.4 ft above the canal bed (fig. 10). In fact, the median profiles show the maximum velocity for the lowest three discharge classes (Q<2,000 ft^3/s) have the velocity maximum at the bottom of the profile. It is important to note that these median profiles are made up of more than 684,000 individual 1-min average profiles (563,427 of these profiles are in the 1,000 to 2,000 ft^3/s range; see table 1). Therefore, these near-bed velocity maxima are not simply anomalies in the dataset, but rather they are evidence of a dominant process of flow acceleration near the canal bed, and can be seen at discharges as high as 6,000 ft^3/s. The cause of this near-bed acceleration will be examined in detail later in this section and in the "Underflows" section.

When the data are grouped seasonally, an inflection point in the median streamwise velocity profile and an increase in near-bed velocities are evident for flows as high as 5,000 ft^3/s during the winter, but these features do not exist in the summer (figs. 11 and 12; tables 2 and 3). The seasonal dependence of these features suggests that these near-bed velocity anomalies are real, are driven by environmental factors, and are not caused by flow disturbance by the ADCP mount on the canal bed. The flow acceleration near the bed and shape of the winter velocity profiles are consistent with profiles of gravity currents (density-driven underflows). Density-driven underflows have been observed elsewhere in the Chicago Sanitary and Ship Canal near Sag Junction (Wang and others, 2016; Jackson, 2016) and in the main branch of the Chicago River (Jackson and others, 2008). Density differences can arise due to variations in temperature and salinity of water in the CAWS.

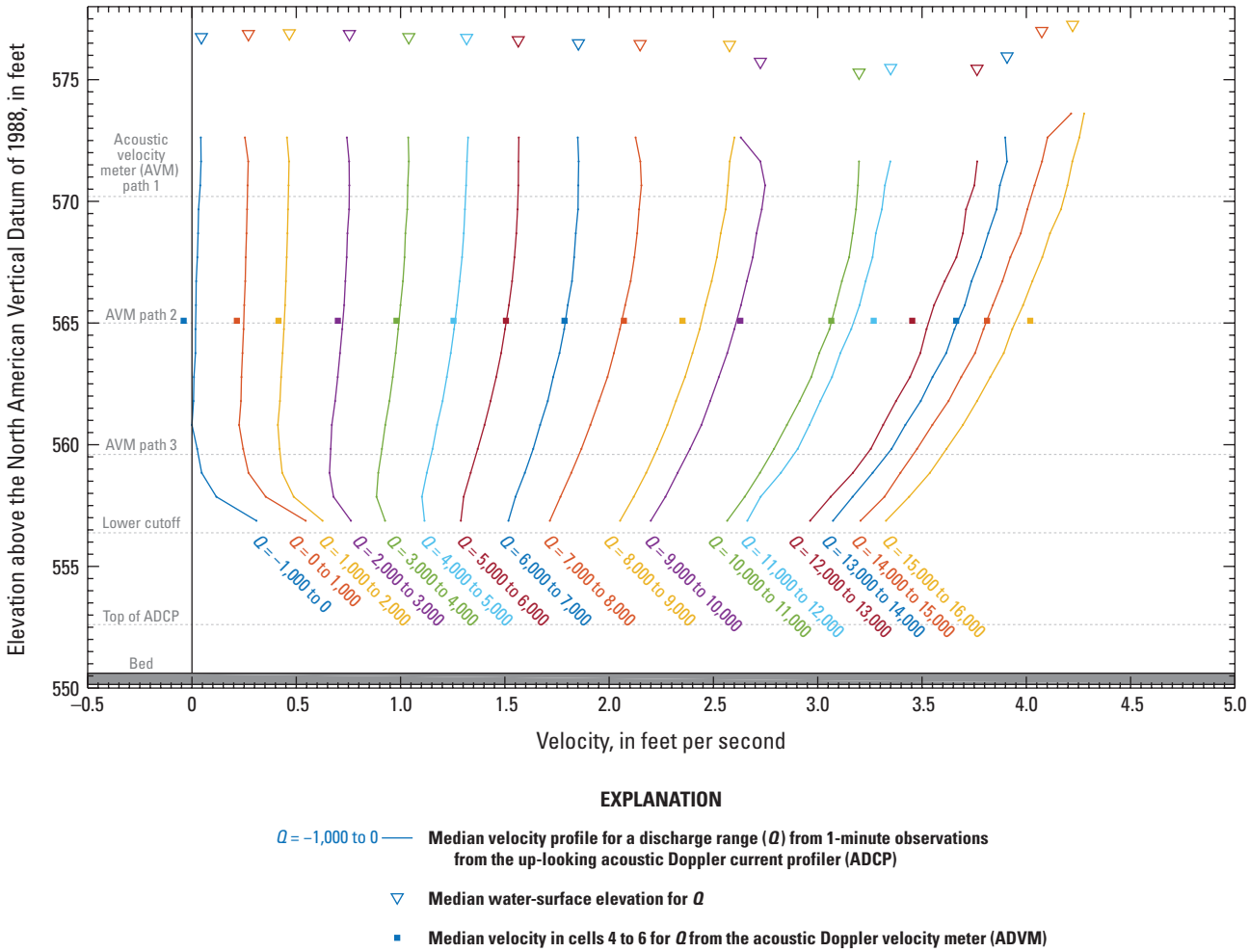

Figure 11. Median streamwise velocity profiles for the winter months (January through March) from the up-looking acoustic Doppler current profiler (ADCP) as a function of discharge at the U.S. Geological Survey streamgage on the Chicago Sanitary and Ship Canal near Lemont, Illinois (05536890), January 14, 2014, to July 10, 2017.

To assess the potential role of temperature in the formation of these underflows, median velocity profiles from the up-looking ADCP were computed as a function of near-bed water temperature as measured by the thermistor on the up-looking ADCP 2 ft above the canal bed (fig. 13). An inflection point in the velocity profile and increase in near-bed velocity was detected for all median profiles with temperatures less than 20 degrees Celsius (fig. 13; table 4). The increase in near-bed velocity was greatest (0.31 ft/s) for the lowest near-bed water temperature (0 to 2 degrees Celsius) and decreased with increasing near-bed water temperature. It is clear from figure 13 and table 4 that the apparent underflows in the Chicago Sanitary and Ship Canal near Lemont, Ill. (05536890), are temperature dependent. These underflows are discussed in detail in the next section.

When the 3.5-year dataset from the up-looking ADCP is sorted into observations on the rising or falling limb of a hydrograph, the median profiles for discharge ranges less than 12,000 ft^3/s show a slightly greater velocity and lower water-surface elevation for the falling limb compared to the rising limb of the hydrograph for the same range of discharge (fig. 14; table 5). For Q<12,000 ft^3/s, the difference in velocity was generally greatest in the upper part of the water column. Overall, the velocity difference was most pronounced between 2,000 to 6,000 ft^3/s. Above 12,000 ft^3/s, there is little to no difference in the velocity profile for the rising and falling limbs. The ADVM data show no consistent variation in velocity between the rising and falling limbs. Any differences observed are smaller in magnitude than those observed for the up-looking ADCP. For all the discharge ranges, the median discharge and number of profiles used to compute the median velocity profiles are nearly equal for the rising and falling limbs (table 5).

The matching filter described in the methods section allowed the identification of 8,545 lockage surges during the up-looking ADCP period of analysis. The assessment of

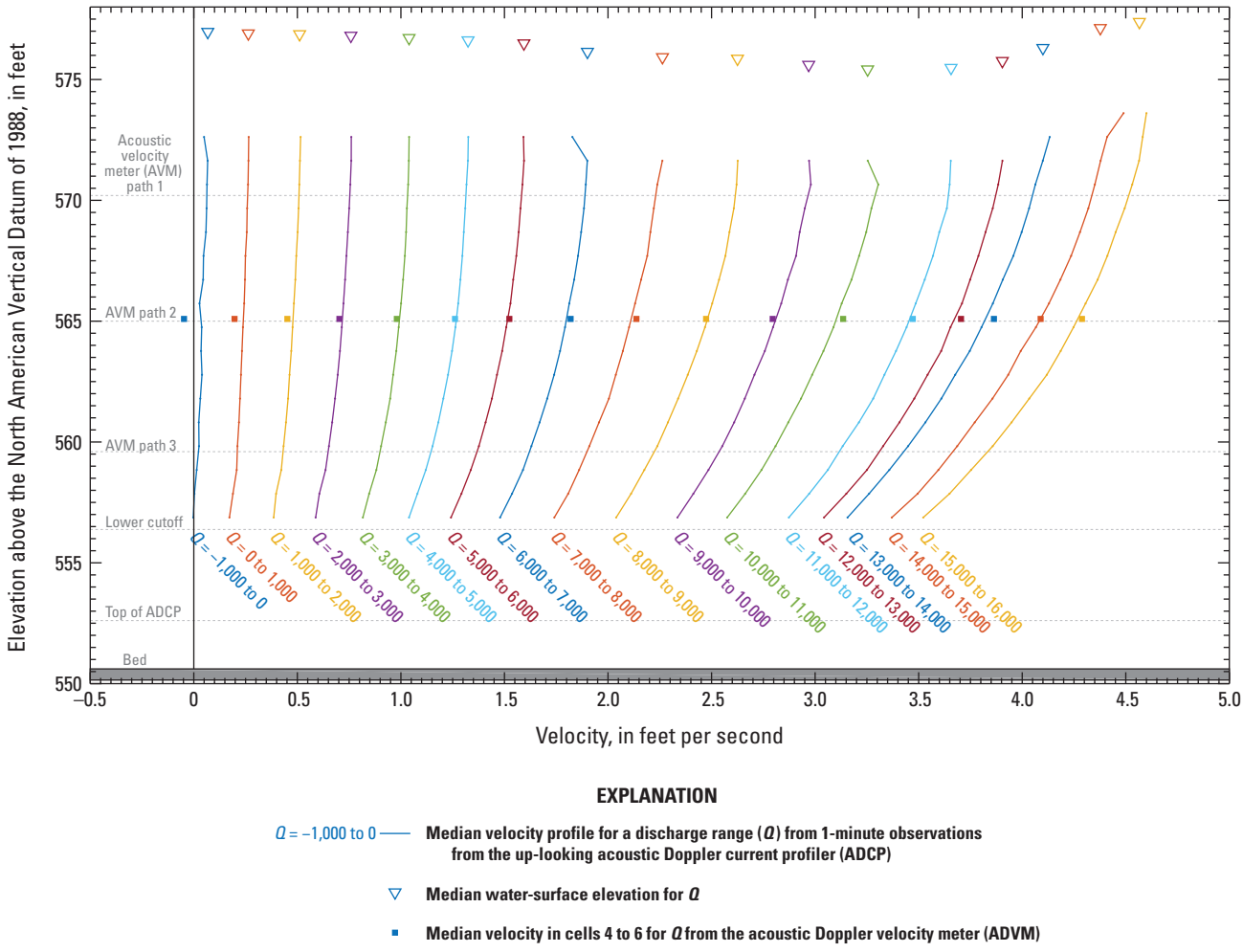

Figure 12. Median streamwise velocity profiles for the summer months (July through September) from the up-looking acoustic Doppler current profiler (ADCP) as a function of discharge at the U.S. Geological Survey streamgage on the Chicago Sanitary and Ship Canal near Lemont, Illinois (05536890), January 14, 2014, to July 10, 2017.

differences between the rising and falling limbs of a hydrograph was repeated using only observations during these lockage surges. During a lockage surge, the velocity is higher and the water-surface elevation is slightly lower on the falling limb of the surge compared to the rising limb for the same discharge (fig. 15; table 6). These results are consistent with the analysis of the entire dataset presented above. However, compared to the analysis of the entire dataset, the lockage surges show a greater overall difference in velocity between the rising and falling limbs. The difference in velocity can be as much as five times that observed for the entire dataset (for the same discharge range) and is most pronounced for discharge in the 1,000 to 2,000 ft^3/s range and the upper part of the water column. The ADVM data show some slight differences in velocity between the two limbs of lockage surges, but the differences are much smaller in magnitude and not consistently higher velocity on the falling limb.

The observation that vertical profiles of streamwise velocity from the up-looking ADCP are generally higher (faster) on the falling limb of a hydrograph compared to the rising limb for the same discharge requires further discussion. In unsteady flows, laboratory experiments and numerical models have shown that hysteresis in the stage-discharge relation can lead to a phase (time) shift between the peak discharge and the peak stage as the flood wave passes a fixed site in the channel (Song and Graf, 1996; Nezu and Sanjou, 2006; Bareš and others, 2008; Bombar, 2016). Velocity peaks are first followed by discharge and then stage (Song and Graf, 1996; Bareš and others, 2008). This can lead to observations of higher velocity on the rising limb compared to the falling limb for the equal water depth (Song and Graf, 1996; Nezu and others, 1997; Bagherimiyab, 2012; Langhi and others, 2013; Ma and others, 2015). The more rapid the change in discharge, the more deviation was seen between the velocity profiles on

Table 2. Summary of up-looking acoustic Doppler current profiler data used to compute median streamwise velocity profiles for a range of discharge during winter months (January through March; fig. 11) at the U.S. Geological Survey streamgage on the Chicago Sanitary and Ship Canal near Lemont, Illinois (05536890), January 14, 2014, to July 10, 2017.

[The parent dataset contains 1-minute time-averaged profiles (n=1,723,858). NAVD 88, North American Vertical Datum of 1988. A negative discharge indicates upstream flow towards Lake Michigan]

Discharge range, in cubic feet per second	Median discharge, in cubic feet per second	Number of profiles	Median water-surface elevation, in feet above the NAVD 88
−1,000 to 0	−145	1,736	576.76
0 to 1,000	800	38,284	576.88
1,000 to 2,000	1,456	214,203	576.91
2,000 to 3,000	2,432	118,159	576.87
3,000 to 4,000	3,451	64,262	576.76
4,000 to 5,000	4,449	34,970	576.72
5,000 to 6,000	5,390	14,564	576.63
6,000 to 7,000	6,408	5,341	576.50
7,000 to 8,000	7,455	2,707	576.47
8,000 to 9,000	8,575	1,520	576.44
9,000 to 10,000	9,375	1,802	575.72
10,000 to 11,000	10,452	733	575.30
11,000 to 12,000	11,582	367	575.47
12,000 to 13,000	12,290	373	575.46
13,000 to 14,000	13,483	448	575.95
14,000 to 15,000	14,523	417	577.00
15,000 to 16,000	15,300	255	577.25

Table 3. Summary of up-looking acoustic Doppler current profiler data used to compute median streamwise velocity profiles for a range of discharge during summer months (July through September; fig. 12) at the U.S. Geological Survey streamgage on the Chicago Sanitary and Ship Canal near Lemont, Illinois (05536890), January 14, 2014, to July 10, 2017.

[The parent dataset contains 1-minute time-averaged profiles (n=1,723,858). NAVD 88, North American Vertical Datum of 1988. A negative discharge indicates upstream flow towards Lake Michigan]

Discharge range, in cubic feet per second	Median discharge, in cubic feet per second	Number of profiles	Median water-surface elevation, in feet above the NAVD 88
−1,000 to 0	−162	1,100	576.97
0 to 1,000	729	11,017	576.90
1,000 to 2,000	1,620	98,490	576.87
2,000 to 3,000	2,476	137,125	576.80
3,000 to 4,000	3,417	81,355	576.73
4,000 to 5,000	4,419	43,851	576.61
5,000 to 6,000	5,330	16,099	576.51
6,000 to 7,000	6,366	5,607	576.15
7,000 to 8,000	7,470	3,020	575.91
8,000 to 9,000	8,444	2,836	575.87
9,000 to 10,000	9,554	1,951	575.59
10,000 to 11,000	10,393	2,046	575.41
11,000 to 12,000	11,537	1,801	575.49
12,000 to 13,000	12,483	1,836	575.76
13,000 to 14,000	13,429	1,417	576.32
14,000 to 15,000	14,483	1,127	577.12
15,000 to 16,000	15,336	673	577.39

the rising and falling limbs. In the Chicago Sanitary and Ship Canal near Lemont, Ill., negative upstream surges, induced by lockages at Lockport Lock, generally produce a peak discharge before the water-surface elevation reaches a minimum associated with the negative surge. For the 8,545 lockage surges analyzed, the median time lag between the arrival of the peak *Q* and the minimum stage is 2 min. The median time lag times between the peak *Q* and peak velocity from the ADVM and up-looking ADCP are 0 and 2 min, respectively (Jackson and Johnson, 2018). However, differences less than 1 min cannot be resolved due to the 1-min resolution of the data. The peak up-looking ADCP velocity occurs after the discharge peaks (contrary to the laboratory experiments and numerical models discussed above); however, the two instruments are not colocated. The up-looking ADCP is 170 ft upstream from the ADVM, and a negative upstream lockage surge reaches the ADVM before the up-looking ADCP. For this reason, the peak velocity from the up-looking ADCP was after the peak in the ADVM-derived discharge rather than before it.

In this analysis, the rising and falling limbs of the hydrograph have been defined by the time-rate-of-change of discharge (dQ/dt). Therefore, because stage and up-looking ADCP velocity lag discharge by about 2 min (on average) for lockage surges, points defined on the falling limb of the discharge hydrograph include (on average) 2 min of data before the stage reaches a minimum and the up-looking ADCP velocity reaches a maximum. As a result, the data classified as "falling limb" have generally lower stage and higher up-looking ADCP velocity than data classified as "rising limb." Therefore, the time lag between discharge and stage can account for the slightly lower water-surface elevation computed for the falling limb compared to the rising limb for the lockage surges (table 6). Additionally, the large differences between velocity profiles for the rising and falling limbs seen in figure 15 (and to a lesser extent fig. 14) can be attributed to the spatial separation of the instrumentation and the associated lag time between discharge and up-looking ADCP velocity. With no spatial separation and no resolvable phase shift

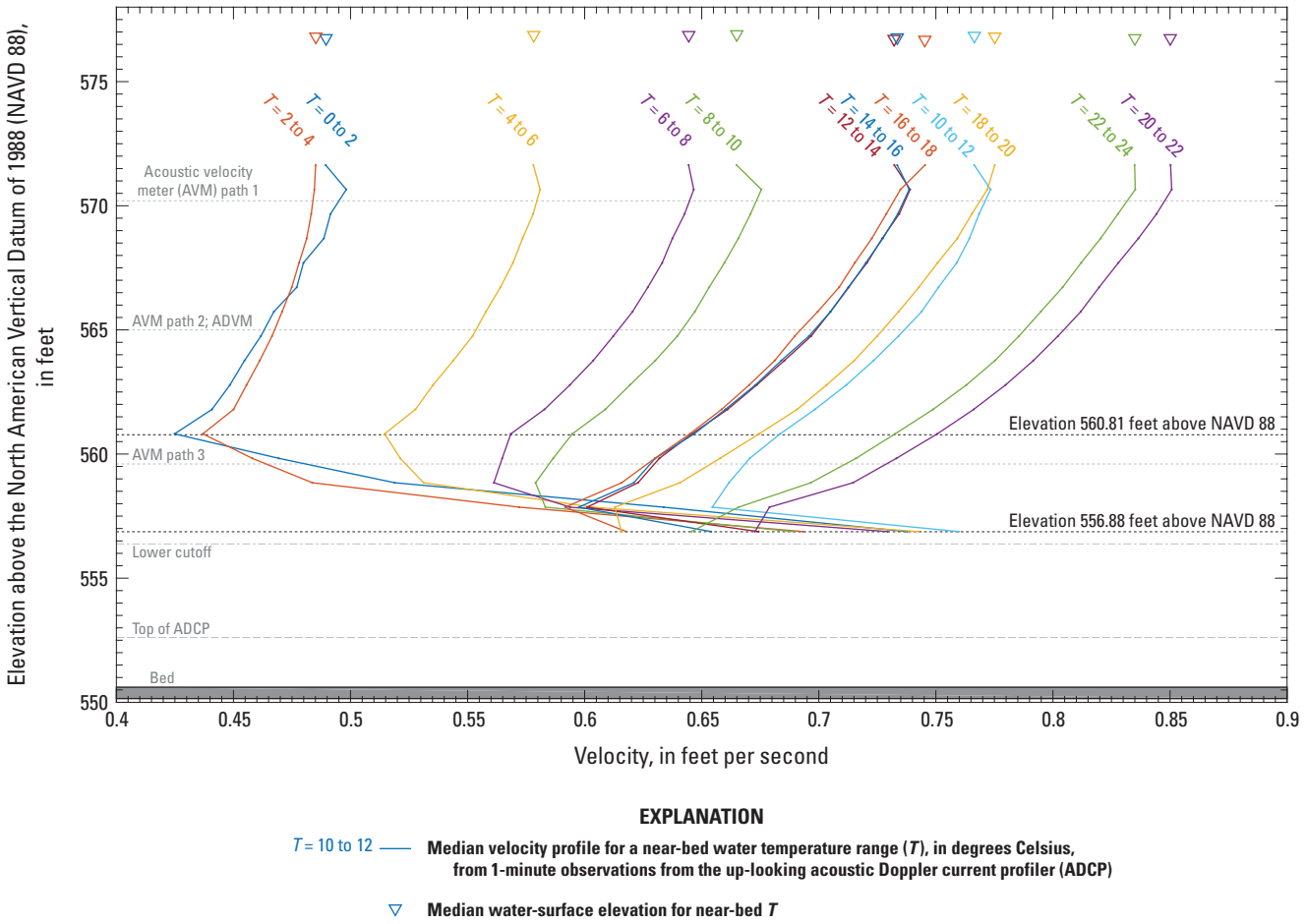

Figure 13. Median streamwise velocity profiles from the up-looking acoustic Doppler current profiler (ADCP) as a function of near-bed water temperature (T), in degrees Celsius, at the U.S. Geological Survey streamgage on the Chicago Sanitary and Ship Canal near Lemont, Illinois (05536890), January 14, 2014, to July 10, 2017.

between discharge and ADVM velocity, it is not surprising the median ADVM velocities for the rising and falling limbs were in general agreement.

Underflows

The near-bed increase in velocity that is prominent in low-flow velocity profiles in the winter months in the Chicago Sanitary and Ship Canal near Lemont, Ill. (05536890), is due to the presence of gravity currents (underflows) (fig. 16). Gravity currents (also called density currents) are driven by density differences between the ambient water and the density of the water in the current (Turner, 1973). If the current is denser than the ambient water, it creates an underflow along the canal bed. Close examination of the density profiles in the canal near Lemont, Ill., reveals that the near-bed increase in velocity is associated with an increase in density near the bed (fig. 16) based on data for two example profiles of underflows that occurred in February 2015. Although the February 15, 2015, underflow (in black) could be caused by higher density water from the Calumet Sag Channel plunging into the Chicago Sanitary and Ship Canal at Sag Junction (the bed of the Calumet Sag Channel is perched about 10 ft above the bed of the canal at the confluence), the February 26, 2015, underflow (in red) is not likely to be driven by Calumet Sag Channel water because the Calumet Sag Channel water had a lower density than the canal during that period. Despite having very similar shaped velocity and density profiles, the February 15, 2015, underflow occurred when the canal near Lemont had a lower density than the Calumet Sag Channel and the canal at Western Avenue; and the February 26, 2015, event occurred when the canal at Lemont had a higher density than the Calumet Sag Channel and the canal at Western Avenue. If it is assumed that the density profile observed on the left bank of the Calumet Sag Channel at USGS streamgage 05536700 is representative of the density profile for the full cross section at this location (fig. 1), then this evidence suggests that water from the Calumet Sag Channel is not solely responsible for formation of density currents in the canal near Lemont, Ill. There must be additional mechanisms driving the observed underflows. The inverted (unstable) density profiles observed on both dates in the canal at Western Avenue indicates that dense water is plunging at this location, potentially driven by loss of heat to the atmosphere. Surface cooling in shallow regions of lakes has been shown to form gravity currents that flow into deeper regions of the lake (Wells and Sherman, 2001). A similar mechanism may be occurring in the largely ice-free canal when winter air temperatures drop below the water temperature.

To characterize the observed underflows in the Chicago Sanitary and Ship Canal near Lemont, Ill. (05536890), the slope of the lower part of the velocity profile from the up-looking ADCP was computed for every 10-min time-averaged profile between January 29, 2015, to July 10, 2017

Table 4. Summary of up-looking acoustic Doppler current profiler data used to compute median streamwise velocity profiles for a range of near-bed water temperature (fig. 13) at the U.S. Geological Survey streamgage on the Chicago Sanitary and Ship Canal near Lemont, Illinois (05536890), January 14, 2014, to July 10, 2017.

[The parent dataset contains 1-minute time-averaged profiles (n=1,723,858). NAVD 88, North American Vertical Datum of 1988; $V_{556.88}$, median velocity at elevation 556.88 feet above the NAVD 88; $V_{560.81}$, median velocity at elevation 560.81 feet above the NAVD 88]

Near-bed water-temperature range, in degrees Celsius	Median discharge, in cubic feet per second	Velocity difference ($V_{556.88}$–$V_{560.81}$), in cubic feet per second	Number of profiles	Median water-surface elevation, in feet above the NAVD 88
0 to 2	1,449	0.31	3,505	576.76
2 to 4	1,539	0.26	87,477	576.80
4 to 6	1,811	0.23	173,760	576.88
6 to 8	2,006	0.16	178,498	576.87
8 to 10	2,156	0.09	130,615	576.92
10 to 12	2,512	0.08	115,056	576.84
12 to 14	2,412	0.03	86,126	576.73
14 to 16	2,416	0.01	114,751	576.77
16 to 18	2,326	−0.03	114,183	576.70
18 to 20	2,467	−0.06	95,038	576.82
20 to 22	2,747	−0.08	191,811	576.76
22 to 24	2,721	−0.09	182,267	576.75

(averaged over the same sampling interval as the temperature and specific conductance probes). The slope, computed using points 3 and 4 in the velocity profile ($Slope_{34}$) and points 4 and 5 in the profile ($Slope_{45}$), is positive when no density current is present and negative when density currents drive an increase in near-bed velocity (fig. 16). The slope sum ($Slope_{sum}=Slope_{34}+Slope_{45}$) also was computed. Before the slope computation, the axes in figure 16 were switched (abscissa: elevation; ordinate: streamwise velocity) so that high negative slopes indicate greater velocity increase near the bed. Therefore, the strongest underflows are characterized by a large negative $Slope_{sum}$. Finally, the presence/absence of an underflow is characterized by the binary variable $Slope_{sign}$, which is taken as the sign of the $Slope_{34}$. The four variables computed from the slope of the lower part of the velocity profile form a set of response variables that can be examined with correlation analysis to examine possible drivers. For correlation analysis, daily mean values of each variable are used.

Potential explanatory variables (daily means) used in the correlation analysis include meteorological data (rainfall, snowfall, snowmelt, air temperature), discharge data (Chicago Sanitary and Ship Canal above and below Sag Junction, Calumet Sag Channel, the Little Calumet River at South Holland, effluent from the Stickney and Calumet WRPs), water temperature, specific conductance, and density at 5 locations in the canal (Loomis Street [MWRD station], Western Avenue [USGS streamgage 05536137], Cicero Avenue [MWRD station], B&O Railroad Bridge [MWRD station], and Lemont, Ill.

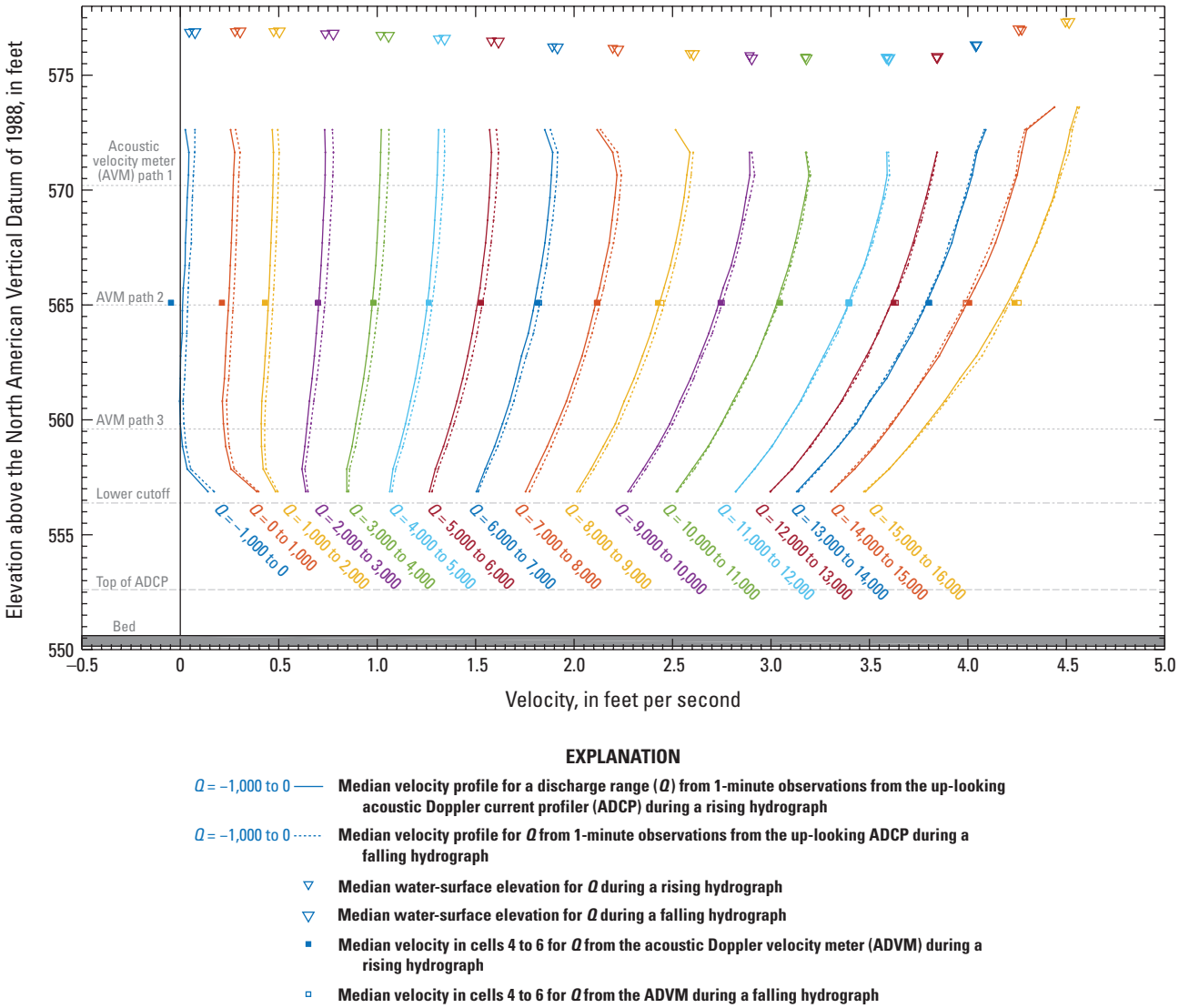

Figure 14. Median streamwise velocity profiles averaged over the rising and falling limbs of the hydrograph from the up-looking acoustic Doppler current profiler (ADCP) as a function of discharge at the U.S. Geological Survey streamgage on the Chicago Sanitary and Ship Canal near Lemont, Illinois (05536890), January 14, 2014, to July 10, 2017.

[USGS streamgage 05536890]) and 3 locations in the Calumet Sag Channel (Cicero Avenue [MWRD station], Route 83 at Sag Bridge, Ill. [USGS streamgage 05536700], and Route 83 [MWRD station]). Additional explanatory variables were formed by computing the density difference between each location and the canal at Lemont. Density differences were computed with and without salinity as a contributing factor to the density. This was necessary because the observed drift in specific conductance sensors led to errors in the computed density at times. The above set of explanatory variables were chosen because they represent the most likely factors to affect the density of the water in the CAWS upstream from Sag Junction.

Density-driven underflows are most prevalent when the air and water temperatures are coldest between October and May, can be present for extended periods of more than 1 month, and are temporarily disrupted by high-flow events (fig. 17). The slope of the lower part of the velocity profile is predominantly negative between October and May and positive the rest of the year (fig. 17*F*). Although high-flow events (about 5,000 ft^3/s or greater) in the Chicago Sanitary and Ship Canal near Lemont, Ill. (05536890), temporarily disrupt the density-driven underflows, examination of the 15-day moving average of the slope sum allows the seasonality of the phenomenon to be seen. Between October and May, the persistence of the underflows seems to be most dependent upon the canal discharge. Higher discharge produces greater turbulence, which temporarily disrupts the formation of the underflow through vertical mixing. After the high flows cease and the stratification returns, the underflows return in the canal.

To better understand the drivers behind the formation of these underflows, a correlation analysis was performed. In general, underflows in the Chicago Sanitary and Ship Canal near Lemont, Ill. (USGS streamgage 05536890), have the strongest association with water temperature and density in the canal at Cicero Avenue (MWRD station; table 7), which is just upstream from the outfall from the Stickney WRP. This correlation may suggest that the underflows at Lemont are due, in part, to formation of gravity currents farther upstream where canal water and water from the Stickney WRP outfall

Table 5. Summary of up-looking acoustic Doppler current profiler data used to compute median streamwise velocity profiles for a range of discharge and classified by rising and falling limbs of the hydrograph (fig. 14) at the U.S. Geological Survey streamgage on the Chicago Sanitary and Ship Canal near Lemont, Illinois (05536890), January 14, 2014, to July 10, 2017.

[The parent dataset contains 1-minute time-averaged profiles (n=1,723,858). NAVD 88, North American Vertical Datum of 1988. A negative discharge indicates upstream flow towards Lake Michigan]

Discharge range, in cubic feet per second	Median discharge, in cubic feet per second (rising limb)	Median discharge, in cubic feet per second (falling limb)	Number of profiles, (rising limb)	Number of profiles, (falling limb)	Median water-surface elevation, in feet above the NAVD 88 (rising limb)	Median water-surface elevation, in feet above the NAVD 88 (falling limb)
−1,000 to 0	−149	−149	3,008	3,220	576.89	576.88
0 to 1,000	770	771	51,650	55,803	576.90	576.90
1,000 to 2,000	1,518	1,521	261,671	278,151	576.90	576.90
2,000 to 3,000	2,453	2,454	223,174	246,625	576.83	576.81
3,000 to 4,000	3,434	3,429	131,414	145,643	576.74	576.72
4,000 to 5,000	4,424	4,421	73,121	77,349	576.60	576.58
5,000 to 6,000	5,376	5,364	30,687	31,517	576.48	576.46
6,000 to 7,000	6,391	6,391	11,464	11,156	576.24	576.20
7,000 to 8,000	7,480	7,474	7,021	7,029	576.16	576.11
8,000 to 9,000	8,442	8,453	4,906	4,826	575.96	575.93
9,000 to 10,000	9,524	9,515	3,478	3,575	575.87	575.73
10,000 to 11,000	10,430	10,417	3,008	3,149	575.79	575.74
11,000 to 12,000	11,526	11,528	2,458	2,506	575.78	575.72
12,000 to 13,000	12,390	12,412	1,975	1,974	575.78	575.80
13,000 to 14,000	13,497	13,491	1,886	1,833	576.30	576.30
14,000 to 15,000	14,453	14,418	1,415	1,434	576.97	576.99
15,000 to 16,000	15,298	15,311	559	580	577.31	577.33

interact. All four response variables have strong, significant associations with these two water-quality parameters in the canal at Cicero Avenue (water temperature: Spearman's rank correlation coefficient (ρ)=0.693 to 0.794, probability (p) value<0.001, n=811; density: ρ=−0.684 to −0.794, p-value<0.001, n=811). Air temperature, especially daily minimum, also was strongly associated with underflows in the canal near Lemont (ρ=0.668 to 0.745, p-value<0.001, n=884), but rainfall, snowfall, and snowmelt were very weakly to weakly associated (table 7). The strongest association with discharge was in the canal upstream from Sag Junction (ρ=0.676, p-value<0.001, n=865), whereas the remainder of the discharge variables, except for the Calumet WRP outfall and the Little Calumet River at South Holland, were moderately and strongly associated with underflows. Water temperature at all sites was strongly associated with underflows in the canal near Lemont (ρ=0.647 to 0.794, p<0.001, n=810 to 884), and temperature differences between each site and Lemont had the strongest association for two Calumet Sag Channel sites at Route 83 (ρ=−0.629 to −0.709, p<0.001, n=807 and 879). Specific conductance was moderately to strongly associated with underflows; the strongest association was in the canal at B&O Railroad Bridge (ρ=−0.632 to −0.716, p<0.001, n=810). Except for the canal at Western Avenue and the Calumet Sag Channel at Route 83 (USGS), the water density in the canal and Calumet Sag Channel was strongly associated with the

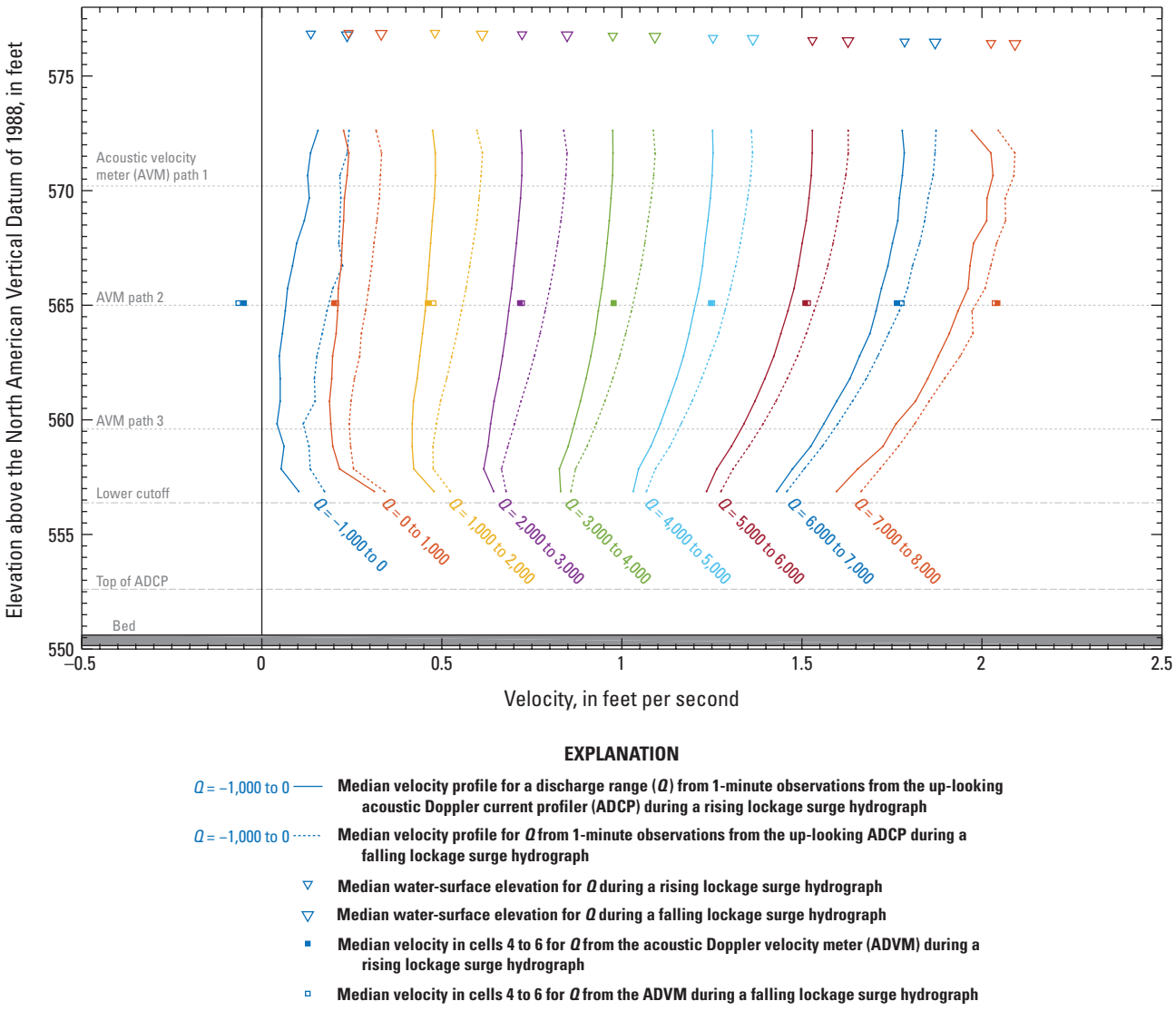

Figure 15. Median streamwise velocity profiles averaged over the rising and falling limbs of lockage surges from the up-looking acoustic Doppler current profiler (ADCP) as a function of discharge at the U.S. Geological Survey streamgage on the Chicago Sanitary and Ship Canal near Lemont, Illinois (05536890), January 14, 2014, to July 10, 2017.

formation of underflows in the canal near Lemont (table 7). However, density differences between each site and the canal at Lemont were only weakly to moderately associated for the two Calumet Sag Channel sites at Route 83 and the canal at B&O Railroad Bridge (table 7). Associations with density differences were improved for sites upstream in the canal if salinity was neglected.

Table 6. Summary of up-looking acoustic Doppler current profiler data used to compute median streamwise velocity profiles for a range of discharge and classified by rising and falling limbs of the hydrograph for lockage surges only (fig. 15) at the U.S. Geological Survey streamgage on the Chicago Sanitary and Ship Canal near Lemont, Illinois (05536890), January 14, 2014, to July 10, 2017.

[The parent dataset contains 1-minute time-averaged profiles (n=1,723,858). A total of 8,545 lockage surges were analyzed. NAVD 88, North American Vertical Datum of 1988. A negative discharge indicates upstream flow towards Lake Michigan]

Discharge range, in cubic feet per second	Median discharge, in cubic feet per second (rising limb)	Median discharge, in cubic feet per second (falling limb)	Number of profiles, (rising limb)	Number of profiles, (falling limb)	Median water-surface elevation, in feet above the NAVD 88 (rising limb)	Median water-surface elevation, in feet above the NAVD 88 (falling limb)
−1,000 to 0	−184	−229	204	204	576.85	576.77
0 to 1,000	727	756	3,260	3,314	576.88	576.83
1,000 to 2,000	1,638	1,681	23,868	27,017	576.87	576.82
2,000 to 3,000	2,532	2,529	44,164	60,820	576.80	576.77
3,000 to 4,000	3,447	3,430	39,827	50,014	576.74	576.71
4,000 to 5,000	4,401	4,391	20,111	22,316	576.65	576.63
5,000 to 6,000	5,365	5,351	7,638	7,975	576.56	576.53
6,000 to 7,000	6,319	6,294	1,815	1,670	576.49	576.46
7,000 to 8,000	7,393	7,356	380	310	576.42	576.39

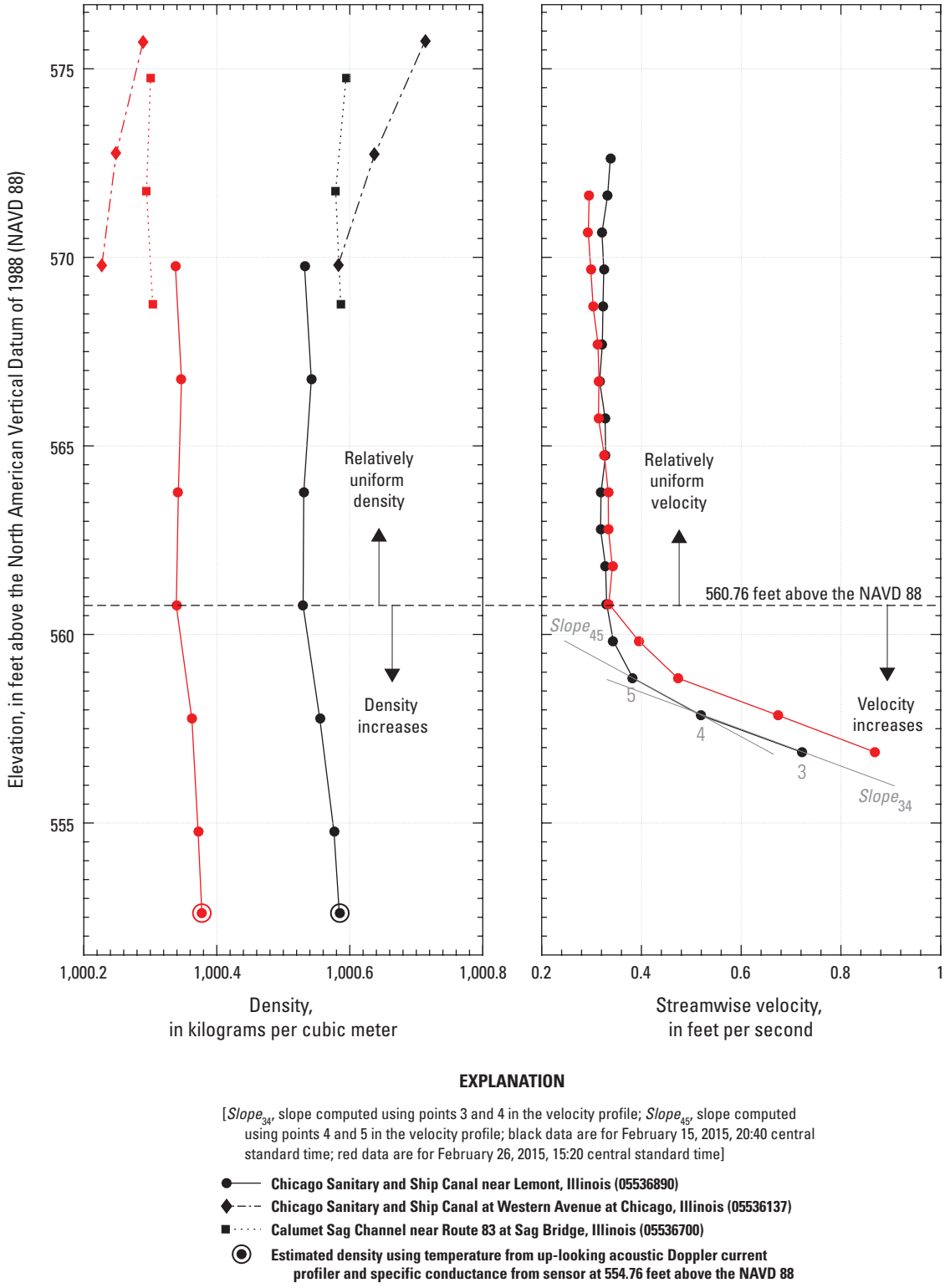

Figure 16. Vertical profiles of density and streamwise velocity at the U.S. Geological Survey streamgage on the Chicago Sanitary and Ship Canal near Lemont, Illinois (05536890), for two underflow events on February 15 and 26, 2015 (black and red, respectively). Density profiles in the Calumet Sag Channel and Chicago Sanitary and Ship Canal at Western Avenue are shown for reference.

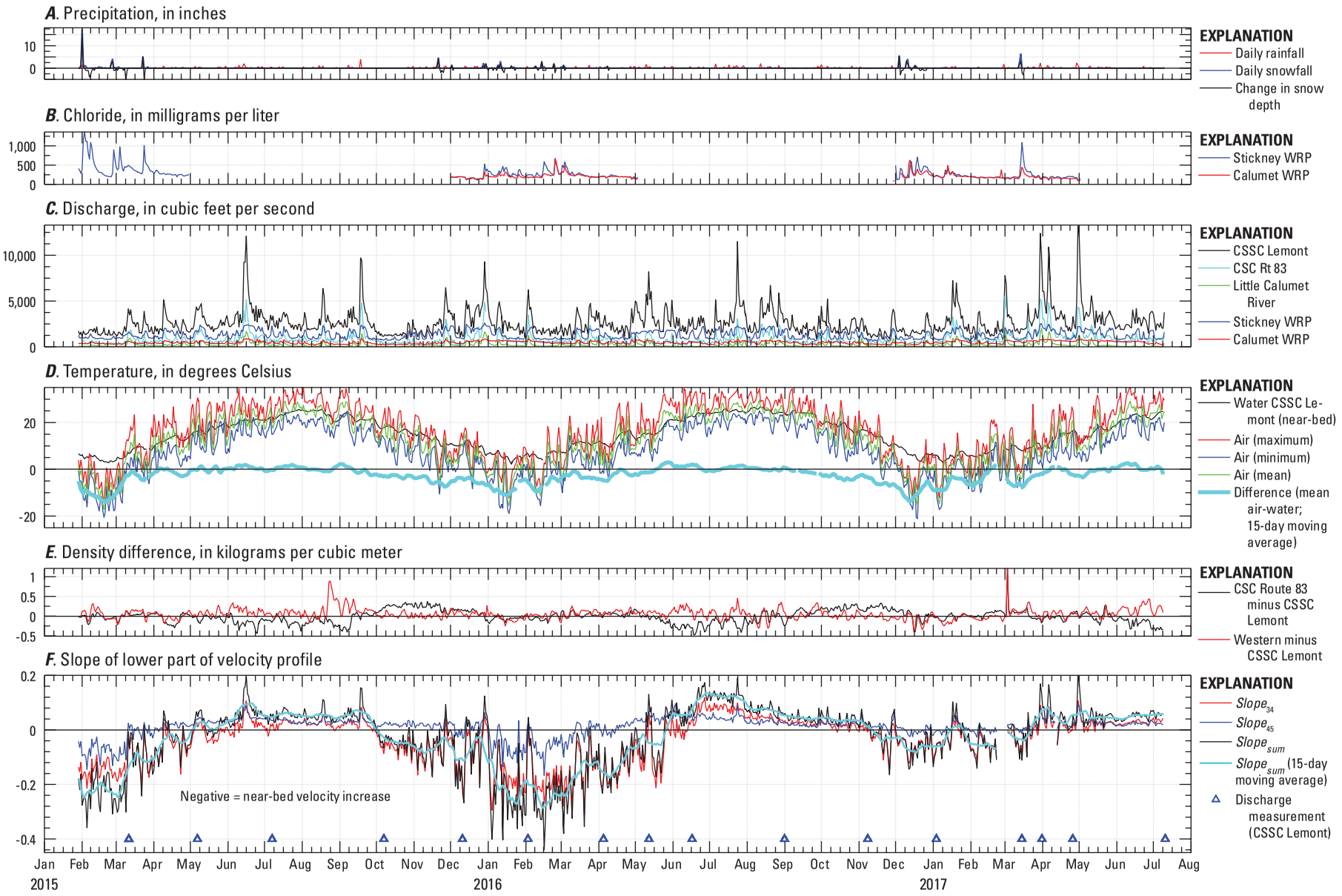

Figure 17. Time series of meteorological, water-reclamation plant effluent, and water density data for comparison to underflow events, January 2015–July 2017. *A*, precipitation. *B*, chloride. *C*, discharge. *D*, temperature. *E*, density difference. *F*, slope of lower part of velocity profile. [WRP, Water Reclamation Plant; CSSC, Chicago Sanitary and Ship Canal; Rt, Route; CSC, Calumet Sag Channel; $Slope_{34}$, slope computed using points 3 and 4 in the velocity profile; $Slope_{45}$, slope computed using points 4 and 5 in the velocity profile; $Slope_{sum}$, sum of $Slope_{34}$ and $Slope_{45}$]

Table 7. Spearman's rank correlation coefficients between underflow response variables and potential explanatory variables.

[n, number of observations; $Slope_{sum}$, sum of $Slope_{34}$ and $Slope_{45}$; $Slope_{34}$, slope between points 3 and 4 in the velocity profile; $Slope_{45}$, slope between points 4 and 5 in the velocity profile; $Slope_{sign}$, sign of $Slope_{34}$; p-value, probability value for testing the null hypothesis of no correlation; <, less than; CSSC, Chicago Sanitary and Ship Canal; CSC, Calumet Sag Channel; WRP, water reclamation plant; MWRD, Metropolitan Water Reclamation District of Greater Chicago; USGS, U.S. Geological Survey]

Potential explanatory variable and station (fig. 1)	n	Response variable							
		$Slope_{sum}$		$Slope_{34}$		$Slope_{45}$		$Slope_{sign}$	
		Spearman's rank correlation coefficient	p–value	Spearman's rank correlation coefficient	p–value	Spearman's rank correlation coefficient	p–value	Spearman's rank correlation coefficient	p–value
Meteorological data									
Daily rainfall	884	0.170	<0.001	0.151	<0.001	0.204	<0.001	0.133	<0.001
Daily snowfall	884	−0.288	<0.001	−0.271	<0.001	−0.298	<0.001	−0.220	<0.001
Daily snowmelt	882	0.103	0.002	0.092	0.006	0.117	<0.001	0.081	0.017
Air temperature (minimum)	884	0.745	<0.001	0.730	<0.001	0.668	<0.001	0.692	<0.001
Air temperature (maximum)	884	0.693	<0.001	0.674	<0.001	0.634	<0.001	0.647	<0.001
Air temperature (mean)	884	0.726	<0.001	0.710	<0.001	0.656	<0.001	0.677	<0.001
Discharge data									
Discharge, CSSC near Lemont	884	0.581	<0.001	0.529	<0.001	0.632	<0.001	0.448	<0.001
Discharge, CSC Channel at Route 83	865	0.465	<0.001	0.446	<0.001	0.421	<0.001	0.364	<0.001
Discharge, CSSC upstream of Sag Junction	865	0.581	<0.001	0.519	<0.001	0.676	<0.001	0.445	<0.001
Discharge, Little Calumet River at South Holland	884	0.097	0.004	0.047	0.167	0.203	<0.001	0.006	0.857
Discharge, Stickney WRP outfall	884	0.447	<0.001	0.389	<0.001	0.537	<0.001	0.321	<0.001
Discharge, Calumet WRP outfall	884	0.234	<0.001	0.213	<0.001	0.239	<0.001	0.199	<0.001
Temperature data									
Water temperature, CSSC at Loomis	844	0.751	<0.001	0.738	<0.001	0.663	<0.001	0.695	<0.001
Water temperaure, CSSC at Western	884	0.767	<0.001	0.758	<0.001	0.669	<0.001	0.711	<0.001
Water temperature, CSSC at Cicero	811	0.794	<0.001	0.783	<0.001	0.693	<0.001	0.732	<0.001
Water tempeature, CSSC at B&O Railroad	810	0.738	<0.001	0.731	<0.001	0.647	<0.001	0.677	<0.001
Water temperature, CSSC near Lemont (near bed)	879	0.755	<0.001	0.747	<0.001	0.659	<0.001	0.703	<0.001
Water tempeature, CSC at Cicero	849	0.754	<0.001	0.742	<0.001	0.670	<0.001	0.707	<0.001
Water temperature, CSC at Route 83 (MWRD station)	812	0.771	<0.001	0.767	<0.001	0.664	<0.001	0.710	<0.001
Water temperature, CSC at Route 83 (USGS station)	884	0.768	<0.001	0.756	<0.001	0.679	<0.001	0.713	<0.001

Table 7. Spearman's rank correlation coefficients between underflow response variables and potential explanatory variables.—Continued

[n, number of observations; $Slope_{sum}$, sum of $Slope_{34}$ and $Slope_{45}$; $Slope_{34}$, slope between points 3 and 4 in the velocity profile; $Slope_{45}$, slope between points 4 and 5 in the velocity profile; $Slope_{sign}$, sign of $Slope_{34}$; p-value, probability value for testing the null hypothesis of no correlation; <, less than; CSSC, Chicago Sanitary and Ship Canal; CSC, Calumet Sag Channel; WRP, water reclamation plant; MWRD, Metropolitan Water Reclamation District of Greater Chicago; USGS, U.S. Geological Survey]

Potential explanatory variable and station (fig. 1)	n	Response variable							
		$Slope_{sum}$		$Slope_{34}$		$Slope_{45}$		$Slope_{sign}$	
		Spearman's rank correlation coefficient	p–value	Spearman's rank correlation coefficient	p–value	Spearman's rank correlation coefficient	p–value	Spearman's rank correlation coefficient	p–value
Temperature difference data									
Temperature difference, air (mean) minus water (CSSC near Lemont)	879	0.464	<0.001	0.435	<0.001	0.470	<0.001	0.420	<0.001
Temperature difference, CSSC Lemont minus CSSC Loomis	839	0.005	0.876	0.005	0.890	0.028	0.412	0.033	0.347
Temperature difference, CSSC Lemont minus CSSC Western	879	−0.285	<0.001	−0.273	<0.001	−0.249	<0.001	−0.221	<0.001
Temperature difference, CSSC Lemont minus CSSC Cicero	806	−0.521	<0.001	−0.491	<0.001	−0.507	<0.001	−0.419	<0.001
Temperature difference, CSSC Lemont minus CSSC B&O Railroad	806	0.635	<0.001	0.611	<0.001	0.621	<0.001	0.604	<0.001
Temperature difference, CSSC Lemont minus CSC Cicero	844	−0.383	<0.001	−0.359	<0.001	−0.393	<0.001	−0.379	<0.001
Temperature difference, CSSC Lemont minus CSC Route 83 (MWRD station)	807	−0.709	<0.001	−0.673	<0.001	−0.694	<0.001	−0.629	<0.001
Temperature difference, CSSC Lemont minus CSC Route 83 (USGS station)	879	−0.698	<0.001	−0.663	<0.001	−0.679	<0.001	−0.638	<0.001
Specific conductance data									
Specific conductance, CSSC at Loomis	844	−0.702	<0.001	−0.705	<0.001	−0.578	<0.001	−0.652	<0.001
Specific conductance, CSSC at Western	884	−0.703	<0.001	−0.715	<0.001	−0.565	<0.001	−0.661	<0.001
Specific conductance, CSSC at Cicero	811	−0.698	<0.001	−0.711	<0.001	−0.547	<0.001	−0.668	<0.001
Specific conductance, CSSC at B&O Railroad	810	−0.716	<0.001	−0.710	<0.001	−0.632	<0.001	−0.654	<0.001
Specific conductance, CSSC near Lemont (near bed)	884	−0.655	<0.001	−0.667	<0.001	−0.519	<0.001	−0.637	<0.001
Specific conductance, CSC at Cicero	849	−0.642	<0.001	−0.633	<0.001	−0.563	<0.001	−0.589	<0.001
Specific conductance, CSC at Route 83 (MWRD station)	812	−0.627	<0.001	−0.625	<0.001	−0.539	<0.001	−0.580	<0.001
Specific conductance, CSC at Route 83 (USGS station)	884	−0.593	<0.001	−0.595	<0.001	−0.492	<0.001	−0.556	<0.001

Table 7. Spearman's rank correlation coefficients between underflow response variables and potential explanatory variables.—Continued

[*n*, number of observations; $Slope_{sum}$, sum of $Slope_{34}$ and $Slope_{45}$; $Slope_{34}$, slope between points 3 and 4 in the velocity profile; $Slope_{45}$, slope between points 4 and 5 in the velocity profile; $Slope_{sign}$, sign of $Slope_{34}$; *p*-value, probability value for testing the null hypothesis of no correlation; <, less than; CSSC, Chicago Sanitary and Ship Canal; CSC, Calumet Sag Channel; WRP, water reclamation plant; MWRD, Metropolitan Water Reclamation District of Greater Chicago; USGS, U.S. Geological Survey]

Potential explanatory variable and station (fig. 1)	*n*	Response variable							
		$Slope_{sum}$		$Slope_{34}$		$Slope_{45}$		$Slope_{sign}$	
		Spearman's rank correlation coefficient	*p*–value	Spearman's rank correlation coefficient	*p*–value	Spearman's rank correlation coefficient	*p*–value	Spearman's rank correlation coefficient	*p*–value
Density data									
Density, CSSC at Loomis	844	−0.758	<0.001	−0.749	<0.001	−0.662	<0.001	−0.698	<0.001
Density, CSSC at Western	884	0.190	<0.001	0.167	<0.001	0.237	<0.001	0.184	<0.001
Density, CSSC at Cicero	811	−0.794	<0.001	−0.788	<0.001	−0.684	<0.001	−0.735	<0.001
Density, CSSC at B&O Railroad	810	−0.749	<0.001	−0.743	<0.001	−0.658	<0.001	−0.690	<0.001
Density, CSSC near Lemont (near bed)	884	−0.764	<0.001	−0.759	<0.001	−0.662	<0.001	−0.711	<0.001
Density, CSSC near Lemont (near bed; assuming zero salinity)	879	−0.755	<0.001	−0.747	<0.001	−0.659	<0.001	−0.703	<0.001
Density, CSC at Cicero	849	−0.778	<0.001	−0.765	<0.001	−0.690	<0.001	−0.725	<0.001
Density, CSC at Route 83 (MWRD station)	812	−0.780	<0.001	−0.778	<0.001	−0.668	<0.001	−0.722	<0.001
Density, CSC at Route 83 (USGS station)	884	−0.347	<0.001	−0.332	<0.001	−0.296	<0.001	−0.348	<0.001
Density difference data									
Density difference, CSSC Loomis minus CSSC Lemont	844	0.208	<0.001	0.197	<0.001	0.224	<0.001	0.216	<0.001
Density difference, CSSC Western minus CSSC Lemont	884	0.190	<0.001	0.167	<0.001	0.237	<0.001	0.184	<0.001
Density difference, CSSC Cicero minus CSSC Lemont	811	−0.066	0.060	−0.064	0.071	−0.035	0.323	−0.050	0.151
Density difference, CSSC B&O Railroad minus CSSC Lemont	810	0.359	<0.001	0.373	<0.001	0.269	<0.001	0.409	<0.001
Density difference, CSC Cicero minus CSSC Lemont	849	−0.000	0.996	0.031	0.361	−0.068	0.049	0.019	0.590
Density difference, CSC Route 83 (MWRD station) minus CSSC Lemont	812	−0.420	<0.001	−0.390	<0.001	−0.390	<0.001	−0.364	<0.001
Density difference, CSC Route 83 (USGS station) minus CSSC Lemont	884	−0.347	<0.001	−0.332	<0.001	−0.296	<0.001	−0.348	<0.001

Table 7. Spearman's rank correlation coefficients between underflow response variables and potential explanatory variables.—Continued

[n, number of observations; $Slope_{sum}$, sum of $Slope_{34}$ and $Slope_{45}$; $Slope_{34}$, slope between points 3 and 4 in the velocity profile; $Slope_{45}$, slope between points 4 and 5 in the velocity profile; $Slope_{sign}$, sign of $Slope_{34}$; p-value, probability value for testing the null hypothesis of no correlation; <, less than; CSSC, Chicago Sanitary and Ship Canal; CSC, Calumet Sag Channel; WRP, water reclamation plant; MWRD, Metropolitan Water Reclamation District of Greater Chicago; USGS, U.S. Geological Survey]

Potential explanatory variable and station (fig. 1)	n	Response variable							
		$Slope_{sum}$		$Slope_{34}$		$Slope_{45}$		$Slope_{sign}$	
		Spearman's rank correlation coefficient	p–value	Spearman's rank correlation coefficient	p–value	Spearman's rank correlation coefficient	p–value	Spearman's rank correlation coefficient	p–value
Density difference data (assuming zero salinity)									
Density difference (zero salinity), CSSC Loomis minus CSSC Lemont	839	0.501	<0.001	0.474	<0.001	0.514	<0.001	0.441	<0.001
Density difference (zero salinity), CSSC Western minus CSSC Lemont	879	0.402	<0.001	0.371	<0.001	0.448	<0.001	0.347	<0.001
Density difference (zero salinity), CSSC Cicero minus CSSC Lemont	806	0.288	<0.001	0.267	<0.001	0.322	<0.001	0.233	<0.001
Density difference (zero salinity), CSSC B&O Railroad minus CSSC Lemont	806	0.586	<0.001	0.582	<0.001	0.524	<0.001	0.597	<0.001
Density difference (zero salinity), CSC Cicero minus CSSC Lemont	844	0.087	0.011	0.093	0.007	0.068	0.048	0.048	0.164
Density difference (zero salinity), CSC Route 83 (MWRD station) minus CSSC Lemont	807	−0.347	<0.001	−0.334	<0.001	−0.282	<0.001	−0.332	<0.001
Density difference (zero salinity), CSC Route 83 (USGS station) minus CSSC Lemont	879	−0.395	<0.001	−0.390	<0.001	−0.321	<0.001	−0.401	<0.001

Implications for Streamgaging Practices

Two methods for computing discharge from the up-looking ADCP are presented, and the results of both methods are compared to the ADVM discharge record. This section concludes with the results from an analysis of the effect of commercial tows on flows and discharge measurements in the Chicago Sanitary and Ship Canal near Lemont using the up-looking ADCP for identification of loaded-tow passages and the barge-detection camera as ground-truth data.

Index-Velocity Ratings

Index-velocity ratings for the up-looking ADCP were developed using multiple-transect discharge measurements (Levesque and Oberg, 2012) and single-transect discharge measurements to account for the highly unsteady flow in the canal. The following sections present the index-velocity ratings developed using each method and the data in tables 1.1 and 1.2 in appendix 1. Statistics of the regressions, plots of residuals, and comparisons of the computed 10-min discharge record from the up-looking ADCP and ADVM (primary index-velocity instrument) for January 14, 2014, to July 10, 2017, also are presented.

Index-Velocity Rating M1—Developed with Multiple-Transect Discharge Measurements

A simple-linear index-velocity rating was developed using ordinary least squares (OLS) regression based on 26 multiple-transect discharge measurements (index-velocity rating M1; fig. 18). The statistics of the regression (table 8) indicate a coefficient of determination (R^2) of 0.995, suggesting only about 0.005 percent of the variance in computed-mean velocity (from the index-velocity rating) is not explained by the variance in the measured-mean velocity. The standard error of the estimate (0.058 ft/s) is less than 6 percent of the average mean channel velocity used to develop the rating. Although the *p*-value for the intercept is greater than 0.05 (suggesting the intercept may not be significantly different from zero; table 8), the OLS-determined intercept is retained at a non-zero value and not forced through zero in accordance with Levesque and Oberg (2012).

Examining the residuals indicates equal variance about zero and no observable trends with respect to observed discharge, index velocity, stage, and measurement date (fig. 19). The residuals are presented in terms of difference between

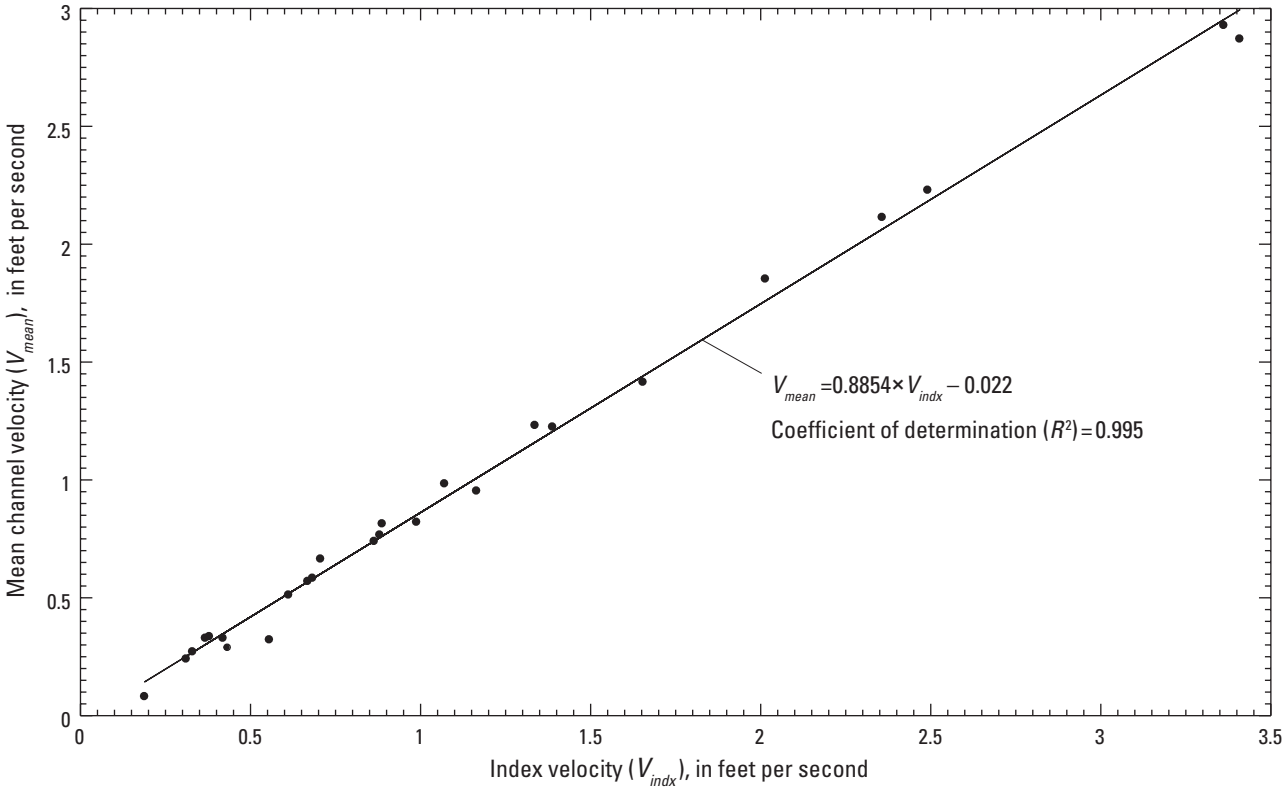

Figure 18. Index-velocity rating M1 developed using multiple-transect discharge measurements and the up-looking acoustic Doppler current profiler deployed at the U.S. Geological Survey streamgage on the Chicago Sanitary and Ship Canal near Lemont, Illinois (05536890), February 11, 2014, to July 10, 2017.

Table 8. Results of a simple-linear regression for the up-looking acoustic Doppler current profiler index-velocity rating M1 using multiple-transect discharge measurements at the U.S. Geological Survey streamgage on the Chicago Sanitary and Ship Canal near Lemont, Illinois (05536890).

[*R*, correlation coefficient; R^2, coefficient of determination; ANOVA, analysis of variance; DF, degrees of freedom; SS, sum of squares; MS, mean square; F, F-test statistic; <, less than; --, not applicable; t Stat, t-test statistic; *p*-value, probability value for the regression coefficient; Lower 95%, lower value for 95-percent confidence limit; Upper 95%, upper value for 95-percent confidence limit]

Regression statistics	
Multiple *R*	0.997483
R^2	0.994973
Adjusted R^2	0.994764
Standard error	0.058089
Observations	26

ANOVA

	DF	SS	MS	F	Significance F
Regression	1	16.029900	16.029900	4,750.534187	<0.000001
Residual	24	0.080984	0.003374	--	--
Total	25	16.110884	--	--	--

	Coefficients	Standard error	t Stat	*p*-value	Lower 95%	Upper 95%
Intercept	−0.022045	0.018490	−1.192270	0.2448109126	−0.060205	0.016116
Slope	0.885398	0.012846	68.924119	<0.000001	0.858886	0.911911

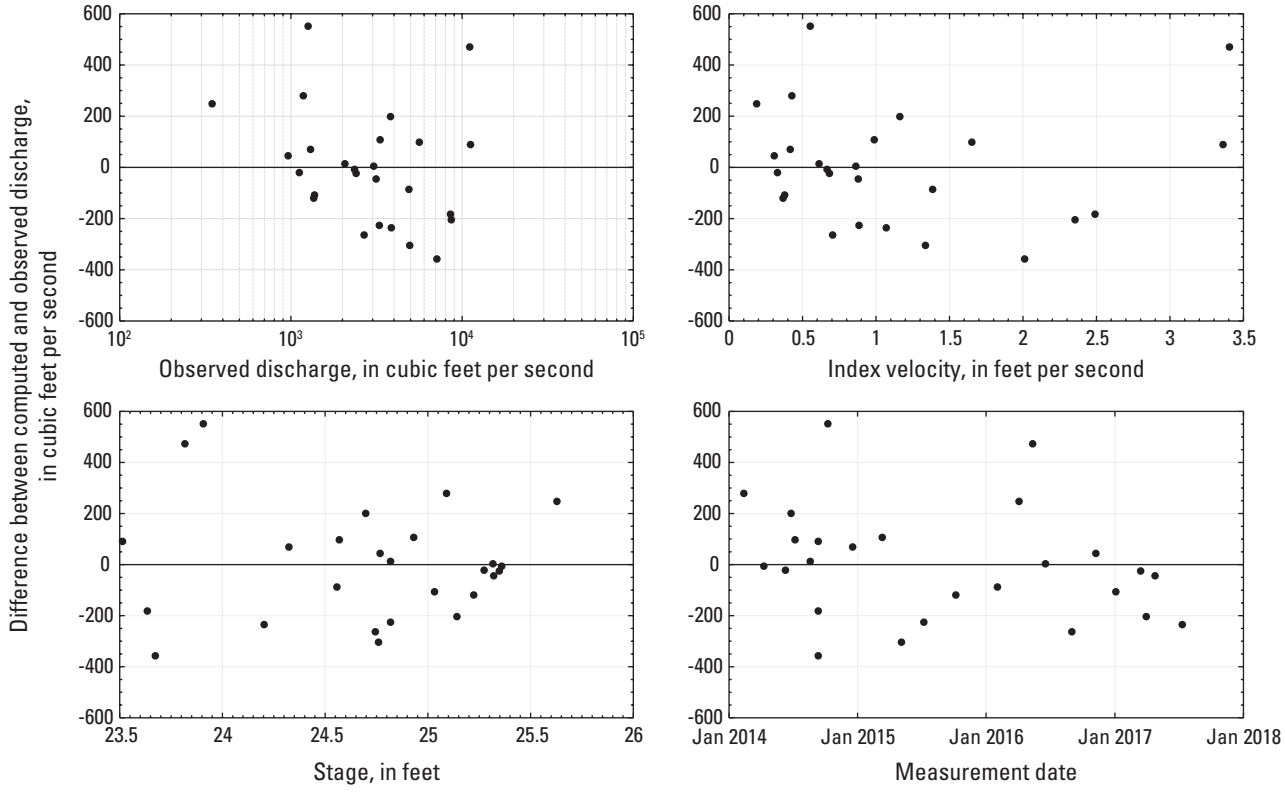

Figure 19. Residuals of the multiple-transect based index-velocity rating curve M1 developed for the up-looking acoustic Doppler current profiler deployed at the U.S. Geological Survey streamgage on the Chicago Sanitary and Ship Canal near Lemont, Illinois (05536890), February 11, 2014, to July 10, 2017.

computed and observed discharge rather than mean channel velocity to give a better understanding of the magnitude of the residuals relative to the primary product of this streamgage (discharge). The residuals have no major outliers, and their magnitudes are generally less than 400 ft^3/s (with two exceptions). Overall, the residual plots and statistics of the regression suggest the simple-linear regression in figure 18 is an appropriate and robust index-velocity rating for the up-looking ADCP. It should be noted, however, that mean channel velocities at this site can approach 4 ft/s (Jackson and others, 2012), and the M1 rating in figure 18 only extends to 3.4 ft/s. Therefore, the M1 rating curve may not adequately capture the highest flows observed at this site.

The 10-min computed discharge using the M1 index-velocity rating curve for the up-looking ADCP, for the period of record for this instrument at the time of this analysis (January 14, 2014, to July 10, 2017), compares well to the computed discharge record from the primary index-velocity instrument (the ADVM) for the same period. Visual comparison of timeseries in figure 20 for a short period in 2014 shows the M1 rating for the up-looking ADCP captures the highly variable flow in the canal including lockage surges, low flows, and periodic high-flow events of variable magnitude. However, some of the high flows are underestimated by the M1 rating curve as are the peak flows from lockage surges.

Although computed discharge differences are subtle, the cumulative effect of this underestimation may be significant. When daily, monthly, and annual mean flows are computed for each instrument and compared, the M1 up-looking ADCP index-velocity rating produces a lower mean discharge compared to the ADVM at each of these three averaging periods (table 9). Underestimation of the discharge relative to the ADVM is most pronounced for high daily mean flows (greater than 5,000 ft^3/s; fig. 21). However, at a significance level of 5 percent, the means and distributions of daily, monthly, and annual mean discharges computed using the ADVM index-velocity and up-looking ADCP M1 index-velocity rating are not significantly different (table 9). At each time scale, a two-sample t-test was used to determine if the dataset means are equal. In each case, the null hypothesis that two samples have equal means was accepted at the 5-percent significance level. Additionally, the data distributions were compared using a two-sample Kolmogorov-Smirnov test and, in each case, the null hypothesis that the two samples come from the same

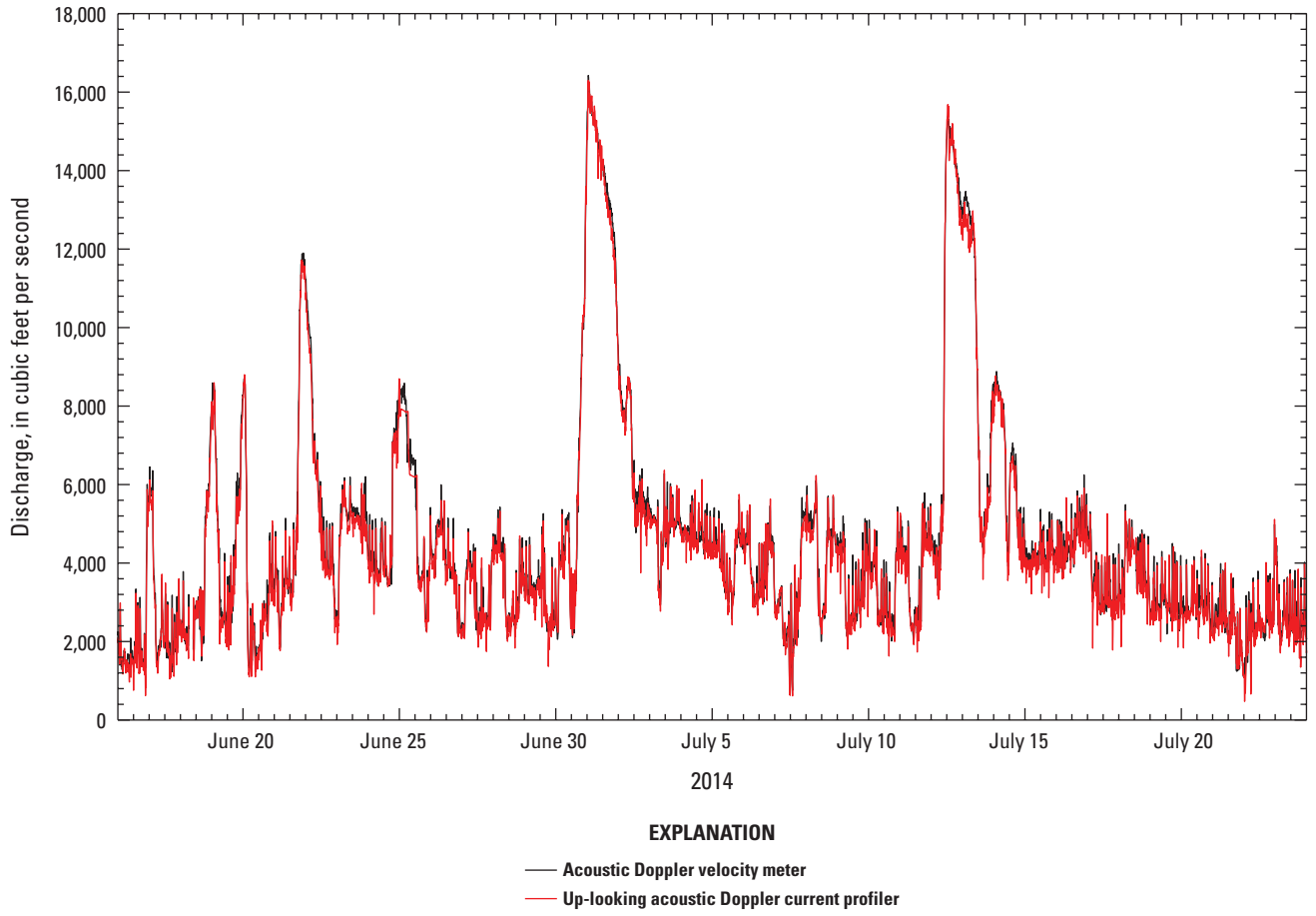

Figure 20. Comparison of computed discharge at the U.S. Geological Survey streamgage on Chicago Sanitary and Ship canal near Lemont, Illinois (05536890), from the acoustic Doppler velocity meter index-velocity rating and the up-looking acoustic Doppler current profiler multiple-transect based index-velocity rating M1 for an example period in 2014.

continuous distribution was accepted at the 5-percent significance level. To further illustrate this equality in distributions, quantile-quantile plots are shown in figure 22 for each time scale for January 14, 2014, to July 10, 2017. Data with equal distributions will fall along the $Y_{quantile}=X_{quantile}$ line, where the quantiles for the upward-looking ADCP computed discharge (Y) equal the quantiles for the ADVM computed discharge (X). The data from the ADVM index-velocity and up-looking ADCP M1 index-velocity methods indicate no substantial deviation from this line. The distribution for the daily mean discharge is highly skewed, whereas the distributions for monthly and annual mean discharges are generally symmetric.

Differences in computed discharge were computed for each pair of daily, monthly, and yearly mean values for the two methods (ADVM index velocity and ADCP M1 index velocity), plotted in boxplots (fig. 23), and compared using a two-sided sign test (table 9). The two-sided sign test analyzes the differences and determines if dataset 1 is generally larger (or smaller, or different) than dataset 2. At the 5-percent significance level, the sign test indicates that the computed daily mean discharges for the up-looking ADCP M1 index-velocity rating are lower than the ADVM index-velocity discharges (median difference of −40.6 ft^3/s). However, monthly and annual mean discharges computed using the up-looking ADCP M1 index-velocity rating are not statistically different from the ADVM index-velocity method when evaluated with the same sign test at the 5-percent significance level. Therefore, despite having median differences of −24.1 and −41.9 ft^3/s for the monthly and annual mean discharges, respectively, these differences could be attributed to chance and are not statistically significant. This finding suggests that temporal averaging of the data on a monthly and annual basis reduces the variability between the two datasets, thus making any differences statistically insignificant.

Index-Velocity Rating S1—Developed with Single-Transect Discharge Measurements

A simple-linear index-velocity rating was developed using OLS regression based on 332 single-transect discharge measurements (index-velocity rating S1; fig. 24) to determine if the up-looking ADCP IV rating can be improved using single transects to better account for unsteady flows in the canal. The statistics of the regression (table 10) indicate a slightly lower, but negligible, difference in the R^2 for the S1 rating (R^2=0.991) compared to the M1 rating (R^2=0.995). The standard error of the estimate for the S1 rating (0.074 ft/s) is greater than the standard error for the M1 rating (0.058 ft/s). The p-values for the slope and intercept are less than 0.05, suggesting confidence in the OLS coefficients at the 5-percent significance level. In general, developing an index-velocity rating for the up-looking ADCP using single transects does not improve the rating. Differences in the slopes and intercepts of the ratings occur in the thousandths place for both coefficients, suggesting the M1 and S1 ratings are nearly identical.

Examining the residuals indicates greater variance (nearly double) in the S1 rating (fig. 25) compared to the M1 rating (fig. 19). Although there are no observable trends in the residuals with respect to stage and time, there does seem to be a slight trend in the residuals with respect to observed discharge and index velocity. The residuals seem to be negatively skewed for observed discharges between 4,000 and 9,000 ft^3/s and index velocities between 1.75 to 2.5 ft/s. Although a compound-linear rating with a break at an index velocity of about 1.8 ft/s may provide a slight improvement in the rating, given the geometry of the channel, no historical overbank flows at the site, and sparsity of data at and above the apparent breakpoint, a compound-linear rating is not advisable at this time. If future measurements in this range continue to show a possible break point, then revision of the S1 rating to include a compound-linear rating may be necessary.

Table 9. Comparison of daily, monthly, and annual mean discharge computed using the multiple-transect based index-velocity rating M1 from the up-looking acoustic Doppler current profiler and acoustic Doppler velocity meter index-velocity rating for January 14, 2014, to July 10, 2017, at the U.S. Geological Survey streamgage on the Chicago Sanitary and Ship Canal near Lemont, Illinois (05536890).

[n, number of samples; Q_{UL}, computed discharge from the up-looking acoustic Doppler current profiler; Q_{ADVM}, computed discharge from the acoustic Doppler velocity meter; t-test (p-value), two-sample t-test result (5-percent significance level) and associated probability p-value; sign test (p-value), two-sided sign test result (5-percent significance level) and associated p-value; Kolmogorov-Smirnov test (p-value), two-sample Kolmogorov-Smirnov test result (5-percent significance level) and associated p-value]

Statistical test	Daily mean discharge	Monthly mean discharge	Annual mean discharge
n	1,203	42	4
Median difference ($Q_{UL}-Q_{ADVM}$), in cubic feet per second	−40.6	−24.1	−41.9
T-test (p-value)	Pass (0.5798)	Pass (0.8455)	Pass (0.8028)
Sign test (p-value)	Fail (1.4075×10^{-9})	Pass (0.0884)	Pass (0.6250)
Kolmogorov-Smirnov test (p-value)	Pass (0.3906)	Pass (0.9874)	Pass (0.9969)

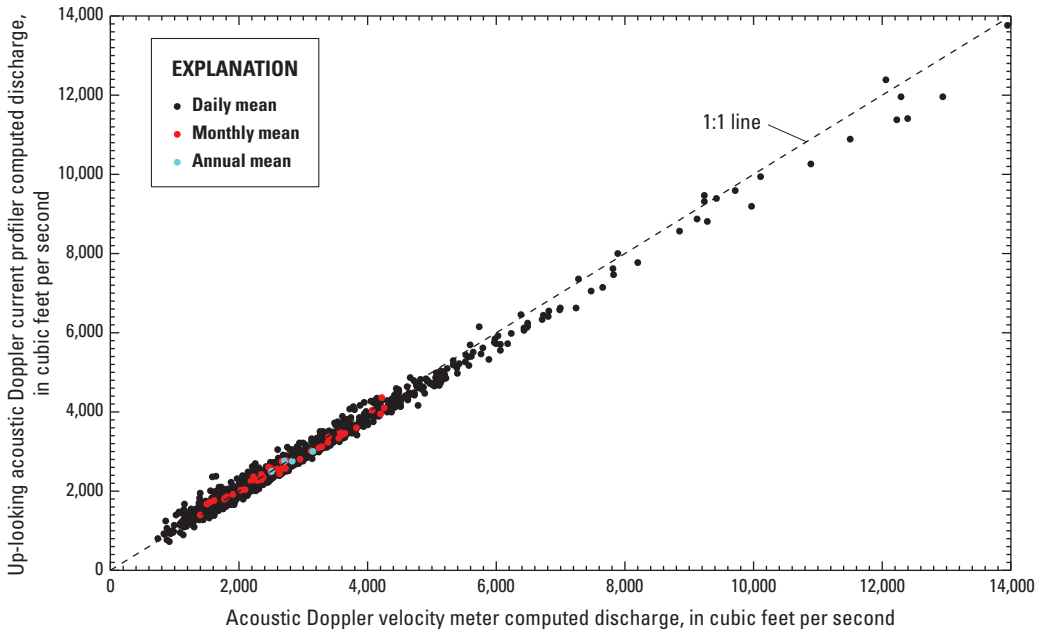

Figure 21. Daily, monthly, and annual mean discharge at the U.S. Geological Survey streamgage on the Chicago Sanitary and Ship canal near Lemont, Illinois (05536890), computed using the acoustic Doppler velocity meter index-velocity rating and the up-looking acoustic Doppler current profiler multiple-transect based index-velocity rating M1 for January 14, 2014, to July 10, 2017.

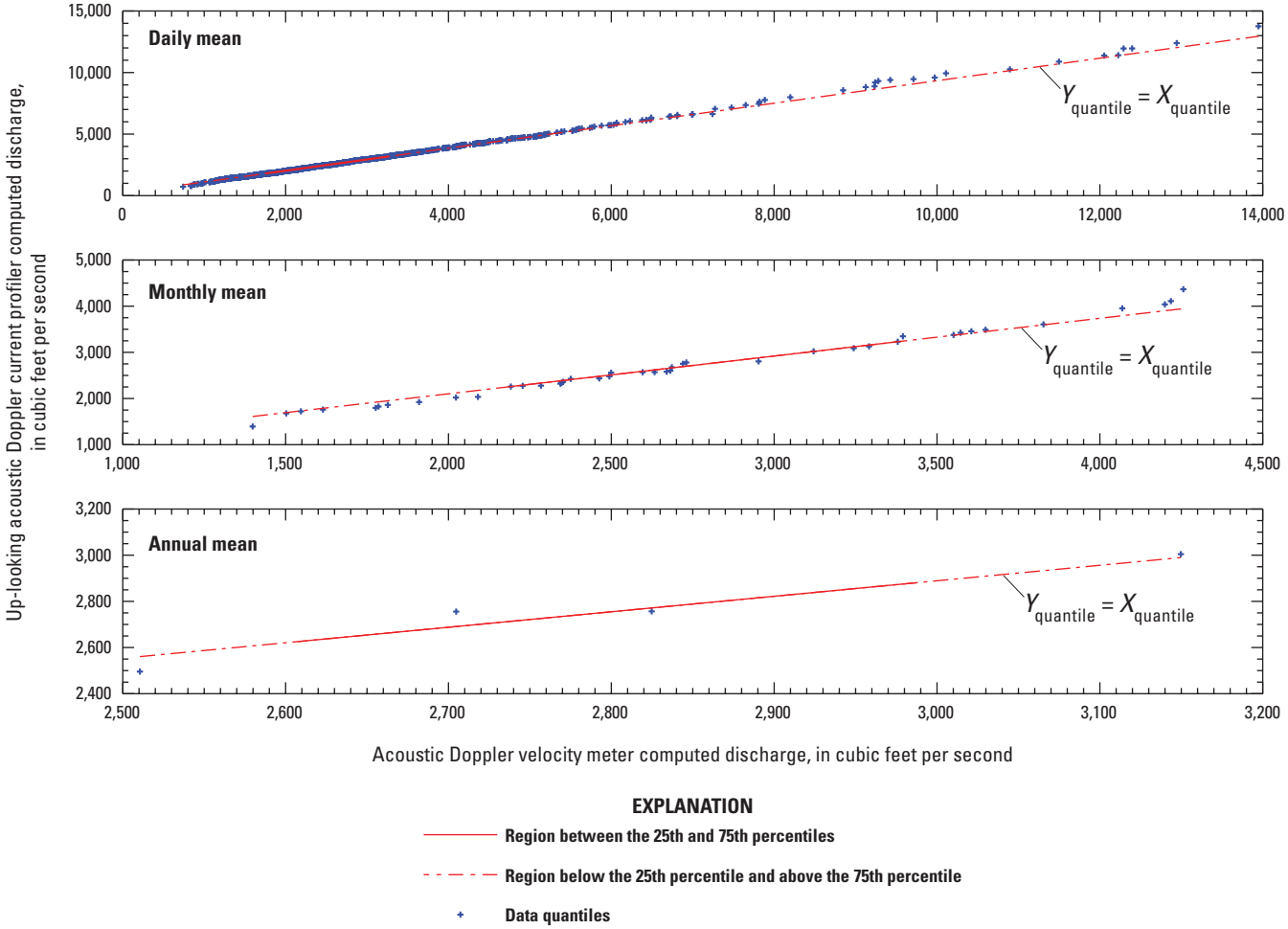

Figure 22. Computed daily, monthly, and annual mean discharges for the acoustic Doppler velocity meter (X) and up-looking acoustic Doppler current profiler (Y; multiple-transect based index-velocity rating curve M1) deployed at the U.S. Geological Survey streamgage on the Chicago Sanitary and Ship Canal near Lemont, Illinois (05536890), January 14, 2014, to July 10, 2017.

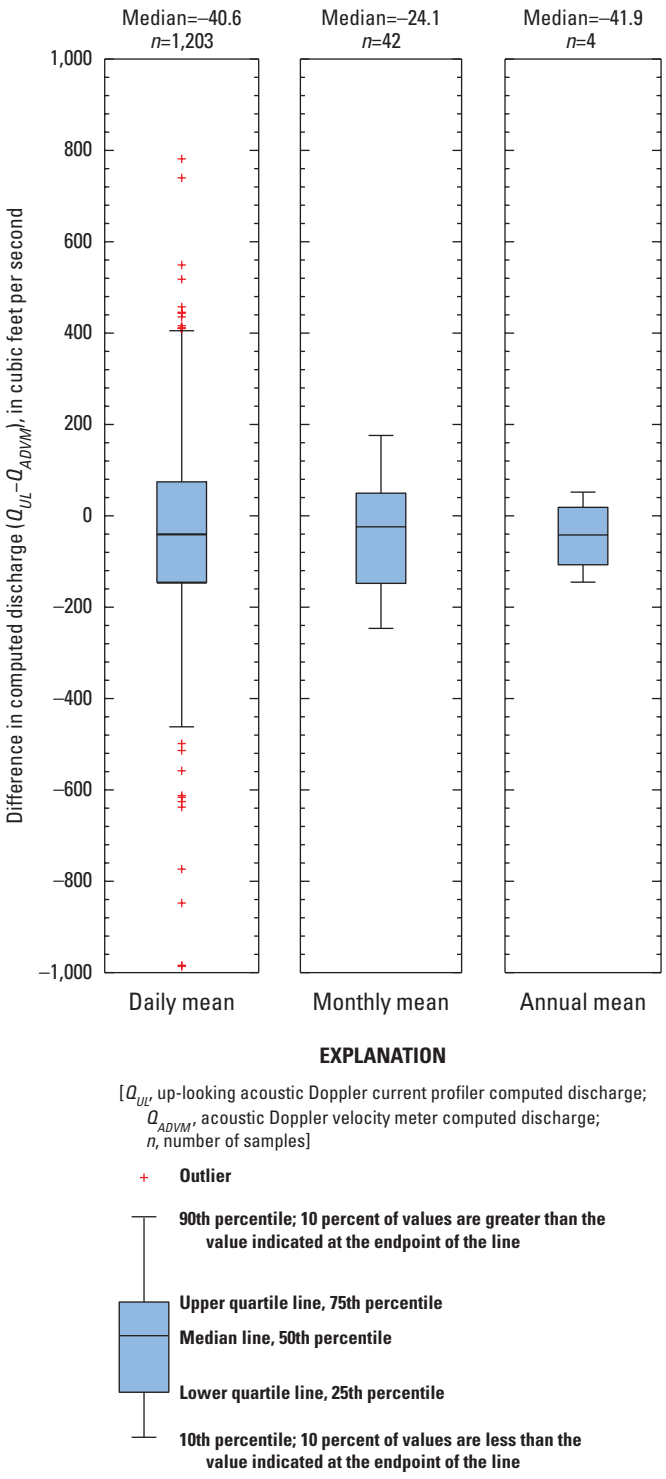

Figure 23. Difference in daily, monthly, and annual mean discharge at the U.S. Geological Survey streamgage on the Chicago Sanitary and Ship canal near Lemont, Illinois (05536890), computed using the up-looking acoustic Doppler current profiler multiple-transect based index-velocity rating M1 and the acoustic Doppler velocity meter index-velocity rating for January 14, 2014, to July 10, 2017.

The 10-min computed discharge, using the S1 index-velocity rating curve for the up-looking ADCP for the period of record for this instrument at the time of this analysis (January 14, 2014, to July 10, 2017), compares well to the computed discharge record from the primary index-velocity instrument (ADVM) for the same period. This result was expected due to the nearly identical S1 and M1 rating curves. Like the M1 rating, the S1 rating produces a computed discharge record that captures the highly variable flow in the canal including lockage surges, low flows, and periodic high-flow events of variable magnitude, but underestimates some of the high flows and the peak flows from lockage surges (fig. 26).

Like the M1 rating, the S1 up-looking ADCP index-velocity rating produces a lower mean discharge compared to the ADVM for daily, monthly, and annual averaging periods (table 11), with the most pronounced difference for high daily mean flows (greater than 5,000 ft^3/s; fig. 27). Two-sample Kolmogorov-Smirnov tests (table 11) and quantile-quantile plots (fig. 28) for each averaging period suggest the S1 and ADVM computed discharge records have equal distributions (like the results from the M1 rating). However, the S1 rating produces slightly smaller median difference in the daily, monthly, and annual mean flows (−34.9, −18.6, and −36.2, respectively; fig. 29; table 11). Like the M1 rating results, only the daily mean flow difference is statistically significant at the 5-percent significance level based on the sign test. Despite the slightly better agreement with the computed discharge from the ADVM, the differences produced by the S1 rating are small and do not justify (at the time of this publication in 2018) a deviation from current practices and the development of an index-velocity rating for the up-looking ADCP based on single-transect measurements.

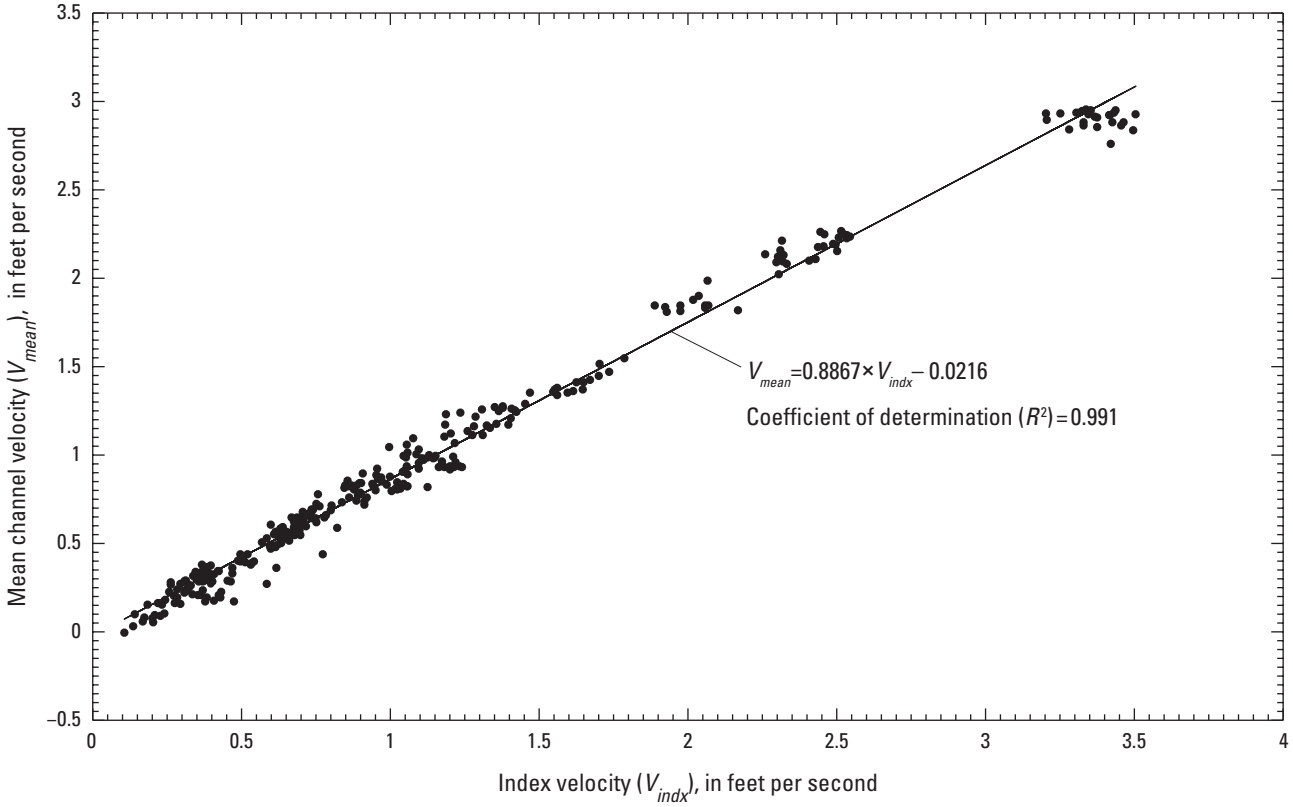

Figure 24. Index-velocity rating S1 developed using single-transect discharge measurements and the up-looking acoustic Doppler current profiler deployed at the U.S. Geological Survey streamgage on the Chicago Sanitary and Ship Canal near Lemont, Illinois (05536890), February 11, 2014, to July 10, 2017.

Table 10. Results of a simple-linear regression for the up-looking acoustic Doppler current profiler index-velocity rating S1 using single-transect discharge measurements at the U.S. Geological Survey streamgage on the Chicago Sanitary and Ship Canal near Lemont, Illinois (05536890).

[*R*, correlation coefficient; R^2, coefficient of determination; ANOVA, analysis of variance; DF, degrees of freedom; SS, sum of squares; MS, mean square; F, F-test statistic; --, not applicable; t Stat, t-test statistic; *p*-value, probability value for the regression coefficient; Lower 95%, lower value for 95-percent confidence limit; Upper 95%, upper value for 95-percent confidence limit]

Regression statistics	
Multiple *R*	0.995388
R^2	0.990798
Adjusted R^2	0.990770
Standard error	0.074069
Observations	332

ANOVA					
	DF	**SS**	**MS**	**F**	**Significance F**
Regression	1	194.926405	194.926405	35,530.1057142409	0
Residual	330	1.810457	0.005486	--	--
Total	331	196.736862	--	--	--

	Coefficients	**Standard error**	**t Stat**	***p*-value**	**Lower 95%**	**Upper 95%**
Intercept	−0.021593	0.006651	−3.246627	0.0012876971	−0.034677	−0.008510
Slope	0.886677	0.004704	188.494312	0	0.877424	0.895931

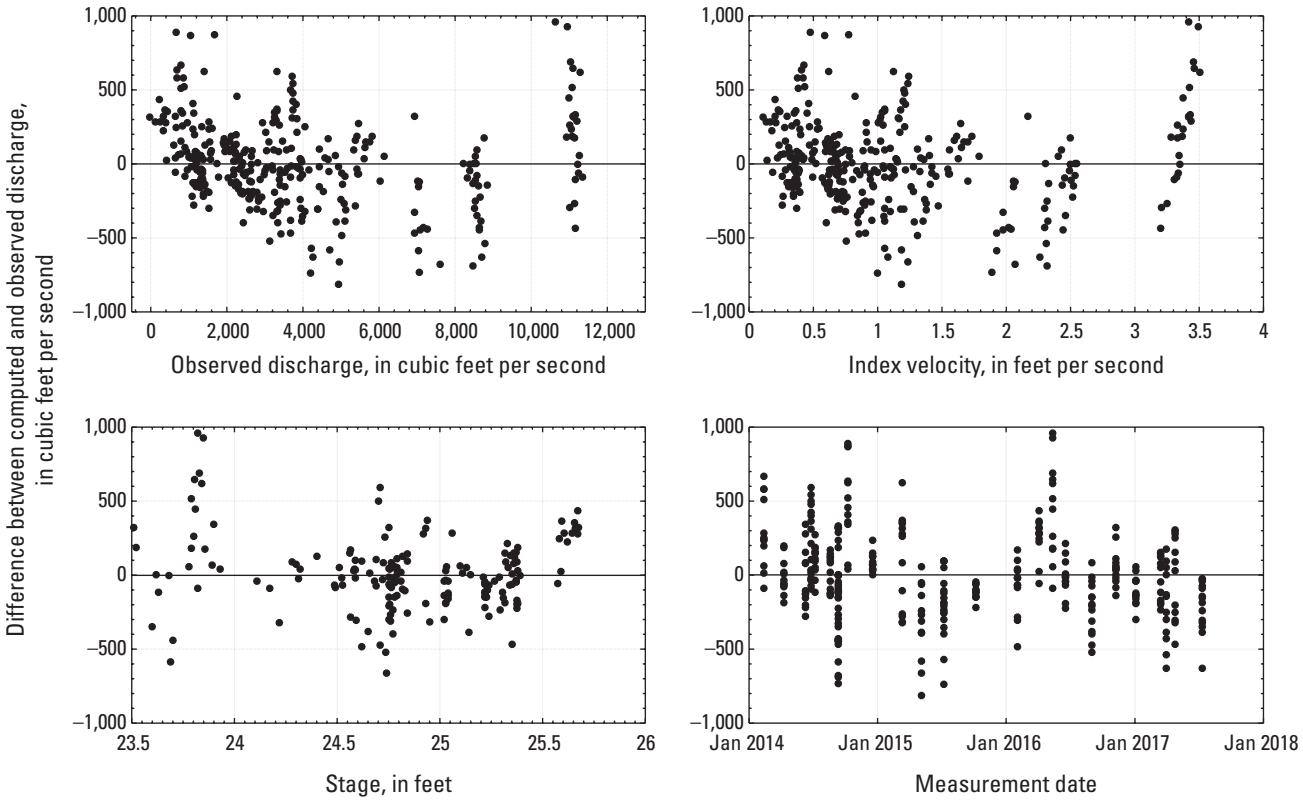

Figure 25. Residuals of the single-transect based index-velocity rating curve S1 developed for the up-looking acoustic Doppler current profiler deployed at the U.S. Geological Survey streamgage on the Chicago Sanitary and Ship Canal near Lemont, Illinois (05536890), February 11, 2014, to July 10, 2017.

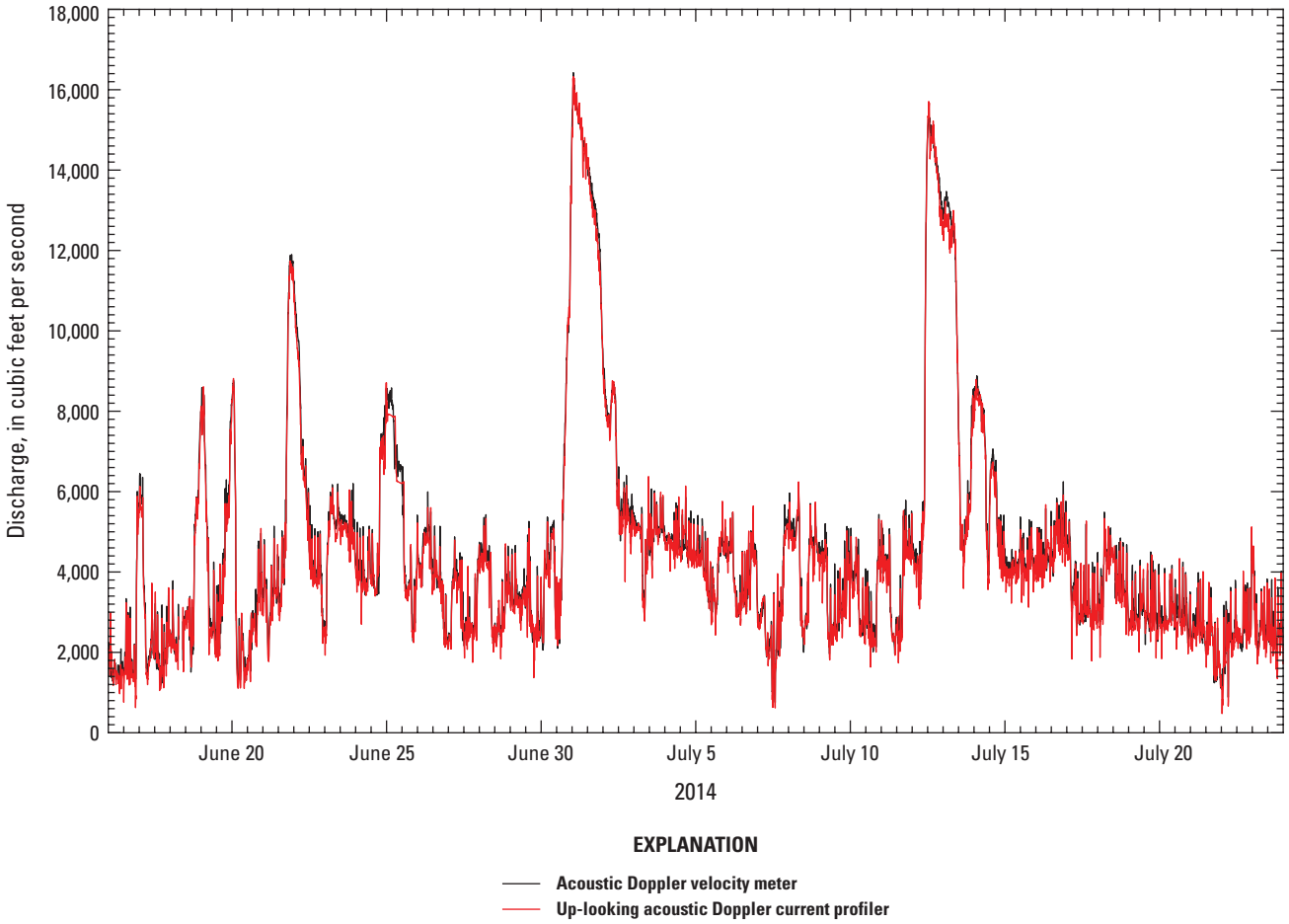

Figure 26. Comparison of computed discharge at the U.S. Geological survey streamgage on Chicago Sanitary and Ship canal near Lemont, Illinois (05536890), from the acoustic Doppler velocity meter index-velocity rating and the up-looking acoustic Doppler current profiler single-transect based index-velocity rating S1 curve for an example period in 2014.

Table 11. Comparison of daily, monthly, and annual mean discharge computed using the single-transect based index-velocity rating S1 from the up-looking acoustic Doppler current profiler and acoustic Doppler velocity meter index-velocity rating for January 14, 2014, to July 10, 2017, at the U.S. Geological Survey streamgage on the Chicago Sanitary and Ship Canal near Lemont, Illinois (05536890).

[*n*, number of samples; Q_{UL}, computed discharge from the up-looking acoustic Doppler current profiler; Q_{ADVM}, computed discharge from the acoustic Doppler velocity meter; t-test (*p*-value), two-sample t-test result (5-percent significance level) and associated *p*-value; sign test (*p*-value), two-sided sign test result (5-percent significance level) and associated probability *p*-value; Kolmogorov-Smirnov test (*p*-value), two-sample Kolmogorov-Smirnov test result (5-percent significance level) and associated *p*-value]

Statistical test	Daily mean discharge	Monthly mean discharge	Annual mean discharge
n	1,203	42	4
Median difference (Q_{UL}–Q_{ADVM}), in cubic feet per second	−34.9	−18.6	−36.2
T-test (*p*-value)	Pass (0.6458)	Pass (0.8726)	Pass (0.8284)
Sign test (*p*-value)	Fail (4.3020×10^{-8})	Pass (0.1641)	Pass (0.6250)
Kolmogorov-Smirnov test (*p*-value)	Pass (0.3630)	Pass (0.9874)	Pass (0.9969)

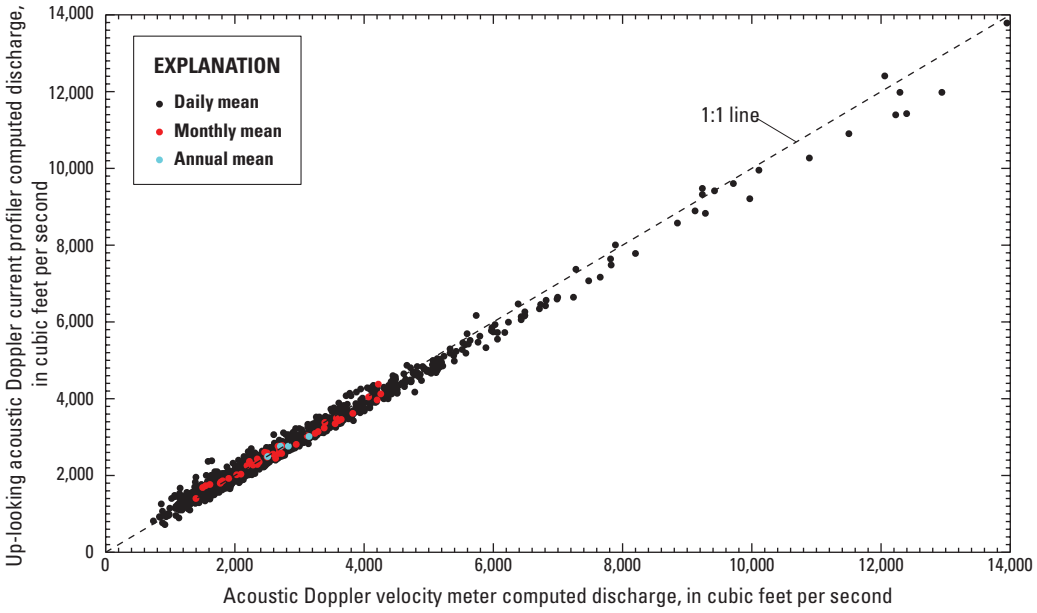

Figure 27. Daily, monthly, and annual mean discharge at the U.S. Geological Survey streamgage on the Chicago Sanitary and Ship canal near Lemont, Illinois (05536890), computed using the acoustic Doppler velocity meter index-velocity rating and the up-looking acoustic Doppler current profiler single-transect based index-velocity rating S1 for January 14, 2014, to July 10, 2017.

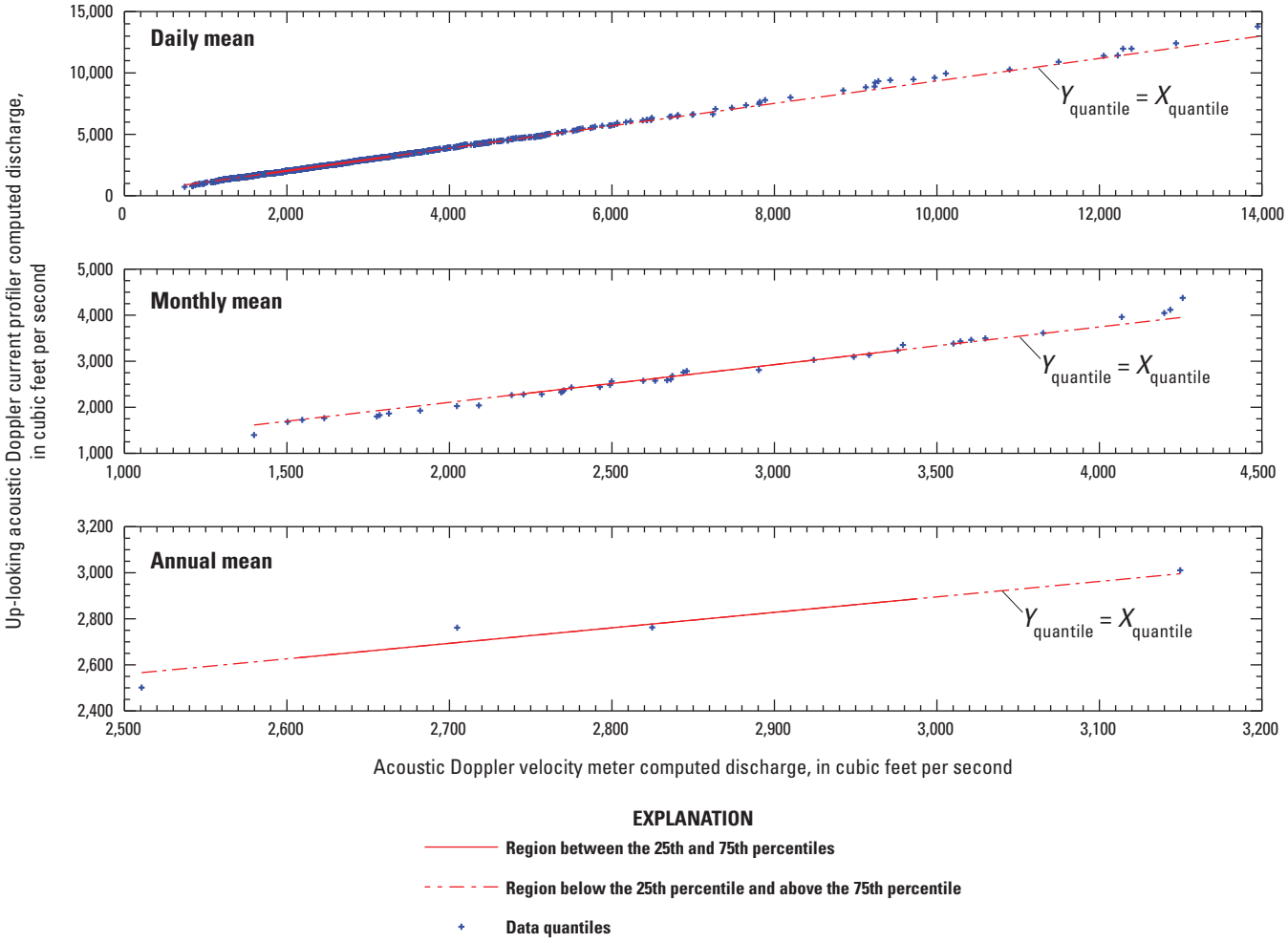

Figure 28. Computed daily, monthly, and annual mean discharges for the acoustic Doppler velocity meter (X) and up-looking acoustic Doppler current profiler (Y; single-transect based index-velocity rating S1) deployed at the U.S. Geological Survey streamgage on the Chicago Sanitary and Ship Canal near Lemont, Illinois (05536890), January 14, 2014, to July 10, 2017.

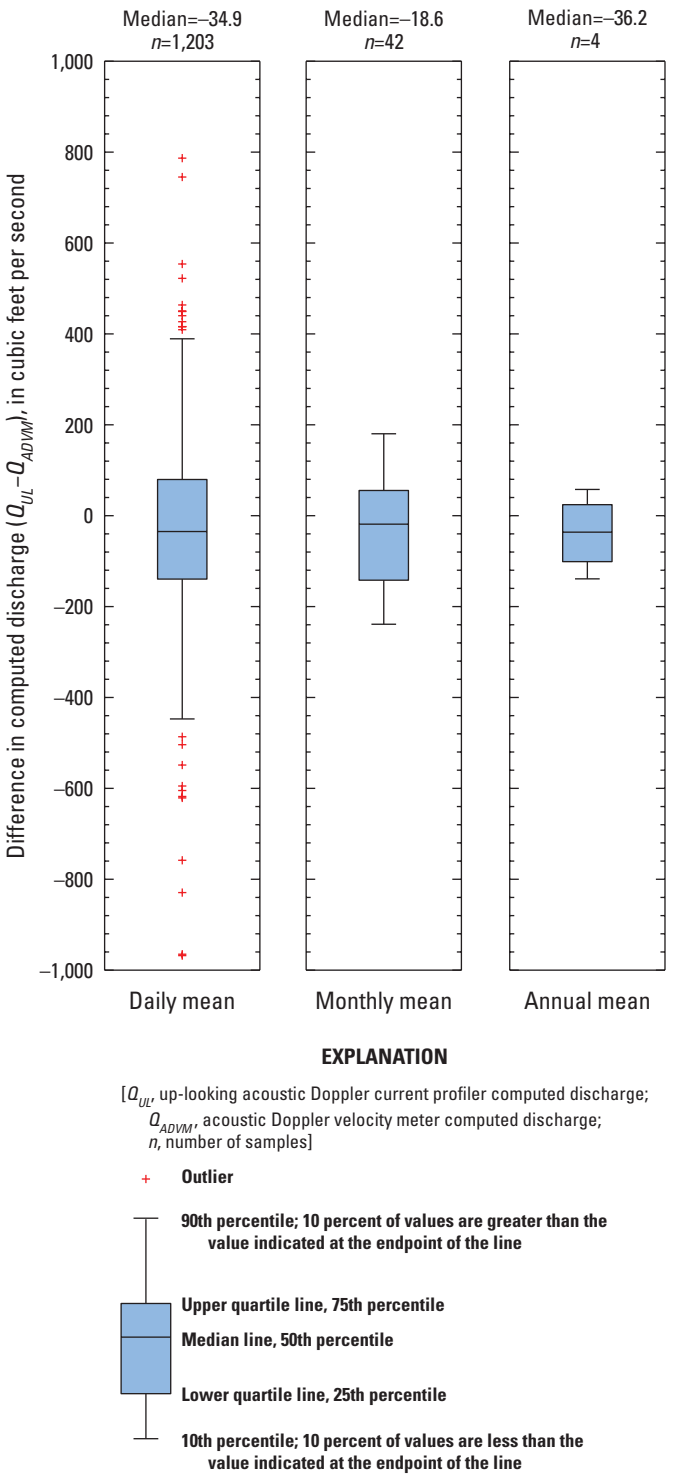

Figure 29. Difference in daily, monthly, and annual mean discharge at the U.S. Geological Survey streamgage on the Chicago Sanitary and Ship canal near Lemont, Illinois (05536890), computed using the up-looking acoustic Doppler current profiler single-transect based index-velocity rating S1 and the acoustic Doppler velocity meter index-velocity rating for January 14, 2014, to July 10, 2017.

Direct Computation of Discharge

Direct computation of discharge from the up-looking ADCP and ADVM velocity profiles relies upon application of the velocity correction factor (V_r), computed from the vertical profile of streamwise velocity, to the transverse profile of streamwise velocity from the ADVM. The highly unsteady and variable flows in the Chicago Sanitary and Ship Canal combined with variability in the velocity profiles because of instrument uncertainty produced substantial variation in the values of V_r for the same flow in the canal. This variability was present for V_r computed from velocity profiles that were logarithmic (eq. 3) and for those that were not (eq. 4). Because of this variability, applying individual correction factors computed for each 15-min velocity profile produced unsatisfactory results in the directly computed discharge record. Therefore, two regression equations were developed for V_r as a function of V_{iADVM}, one for logarithmic profiles and one for non-logarithmic profiles, using median values of V_r computed using equations 3 and 4. Medians were computed in 40 equally sized bins over the range $0 \le V_{iADVM} \le 4.25$ ft/s. The medians and the regression curves are shown in figure 30. The regressions required high-order polynomials, and the coefficients of the regression equations are given in table 12.

The shapes of the regression curves are defined, in part, by the complex hydraulics in the Chicago Sanitary and Ship Canal near Lemont, Ill. Both curves approach a nearly constant V_r between 0.9 and 1.0 for $V_{iADVM} > 0.75$ ft/s and deviate substantially from these values for $V_{iADVM} < 0.75$ ft/s. The velocity ratio is higher for non-log profiles because nearly uniform velocity profiles are common in the canal near Lemont, Ill. The slight deviation for $V_{iADVM} > 3.5$ ft/s, for the log profiles, is likely because the water-surface elevation generally increases with discharge when V_{iADVM} is above 3.5 ft/s (see fig. 10), and V_r is computed using a fixed part of the water column (cells 3 to 18 from the up-looking ADCP). The opposite behavior of the regression curves for $V_{iADVM} < 0.75$ ft/s is primarily due to the effect of underflows for non-log profiles, which increase the velocity in the lower part of the water column and force the velocity ratio above 1 for $V_{iADVM} < 0.25$ ft/s (fig. 30).

For a 1,274-day period of record between January 14, 2014, and July 10, 2017, the direct computation of discharge using the up-looking ADCP, ADVM, and velocity ratio produces a discharge record that compares well to the official discharge record produced using the ADVM index-velocity method (fig. 31). The direct computation method can reproduce high, low, and reverse flows. It also captures the highly variable flows related to passage of lockage surges (figs. 31 and 32). A general trend indicates that the direct computation method slightly overestimates the magnitude of the highest and lowest flows in the first one-half of the record and slightly underestimates the high flows in the second one-half of the record compared to the ADVM index-velocity method. The change occurs on October 1, 2015 (day 625), when a new ADVM index-velocity rating curve was applied.

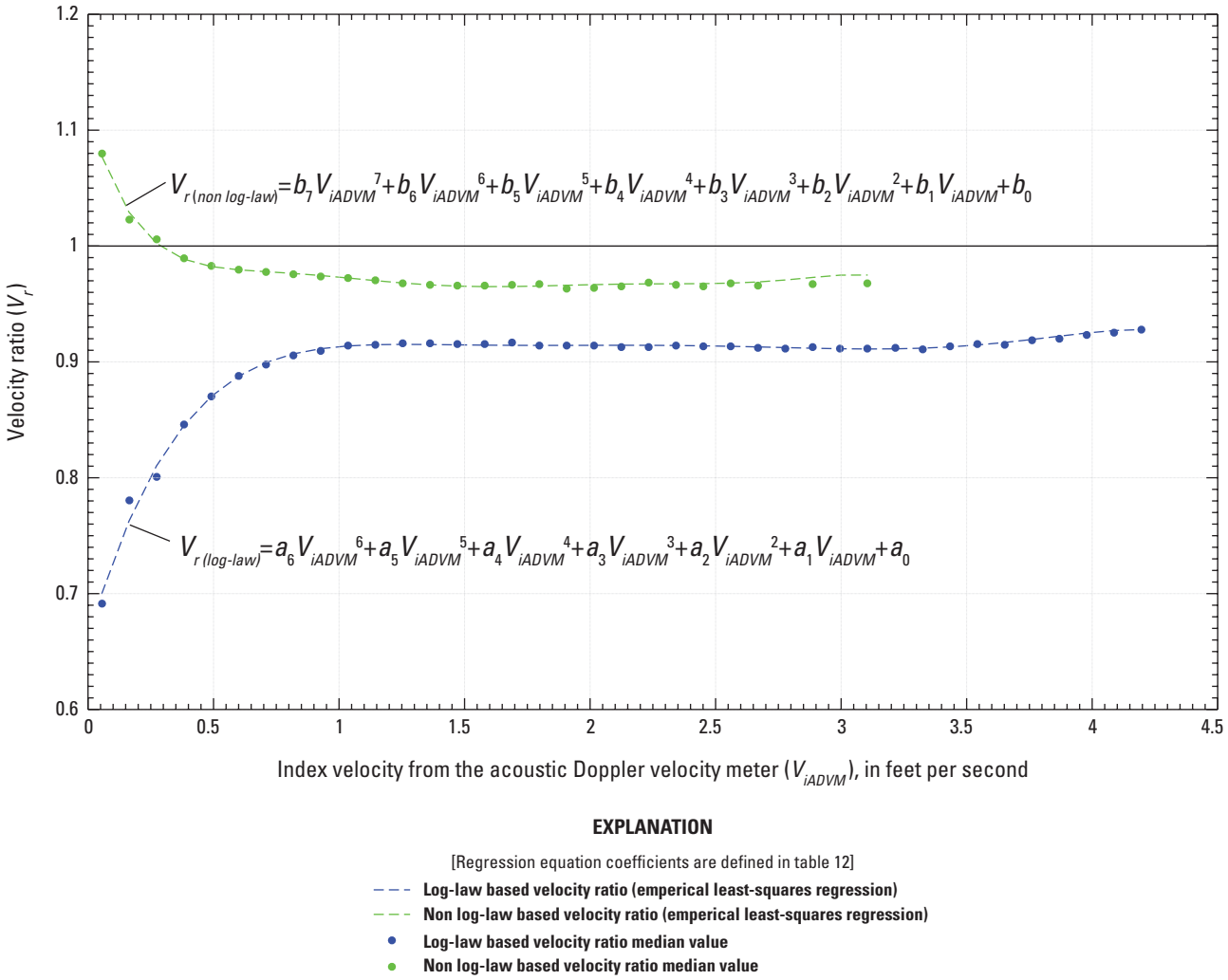

Figure 30. Velocity ratio as a function of the acoustic Doppler velocity meter index velocity for vertical profiles of streamwise velocity that are logarithmic and not logarithmic based on median values of 15-minute vertical velocity profiles from the up-looking acoustic Doppler current profiler from January 14, 2014, to July 10, 2017, at the U.S. Geological Survey streamgage on the Chicago Sanitary and Ship Canal near Lemont, Illinois (05536890), and equations 3 and 4.

Table 12. Coefficients of the regression equations for the velocity ratio as a function of the acoustic Doppler velocity meter index velocity (fig. 30) at the U.S. Geological Survey streamgage on the Chicago Sanitary and Ship Canal near Lemont, Illinois (05536890).

[n, number of 15-minute, time-averaged velocity profiles used in regression; R^2, coefficient of determination; a_m, regression coefficient, where m=0 to 6; b_m, regression coefficient, where m=0 to 7; V_r, velocity ratio computed for profiles fitting a log law (log-law) and those that do not (non log-law)]

n	R^2	a_6	a_5	a_4	a_3	a_2	a_1	a_0
				$V_{r\,(log\text{-}law)}$				
27,938	0.994	−0.001955	0.029401	−0.176334	0.540040	−0.891558	0.752256	0.661317

n	R^2	b_7	b_6	b_5	b_4	b_3	b_2	b_1	b_0
					$V_{r\,(non\ log\text{-}law)}$				
94,162	0.994	−0.008444	0.104855	−0.530364	1.404093	−2.080583	1.716948	−0.746853	1.113471

For the range of discharge observed in the Chicago Sanitary and Ship Canal near Lemont, Ill., between January 14, 2014, and July 10, 2017, the ADVM and directly computed daily, monthly, and annual mean discharges compare well. A scatterplot (fig. 33) compares the computed discharge for both methods at the three time scales. The daily mean discharge data cloud lies along the line of equality with some scatter about the line, particularly at higher discharge. Above about 5,000 ft^3/s, the daily mean data separate into two data clouds: one cloud that lies along or slightly to the left of the line of equality and another cloud that plots primarily to the right of the line of equality. The daily mean data that plot to the right of the line of equality were all collected after October 1, 2015, whereas the data that lie along the line of equality were collected before October 1, 2015. Note that October 1, 2015 (day 625), was the date a new ADVM index-velocity rating went into effect. This behavior at high flows is evident in figure 31.

In general, daily mean flows with discharge greater than 5,000 ft^3/s are underestimated by about 5 percent using the direct computation method compared to the ADVM index-velocity method for the period after October 1, 2015 (fig. 34*B*). For the same period, flows less than 2,500 ft^3/s exhibit an overestimation of the discharge using the direct computation method compared to the ADVM index-velocity method, and the percent difference increases with decreasing discharge. Monthly and annual mean flows follow the same trend but have less variability in discharge and percent difference from the ADVM discharge than daily mean flows. For the period before October 1, 2015, the percent difference between the directly computed discharge and ADVM index-velocity discharge is generally less than 5 percent and only exhibits a trend below 1,500 ft^3/s (fig. 34*A*). For these low flows during this period, the direct computation method underestimates the discharge compared to the ADVM index-velocity method, and the percent difference increases with decreasing discharge.

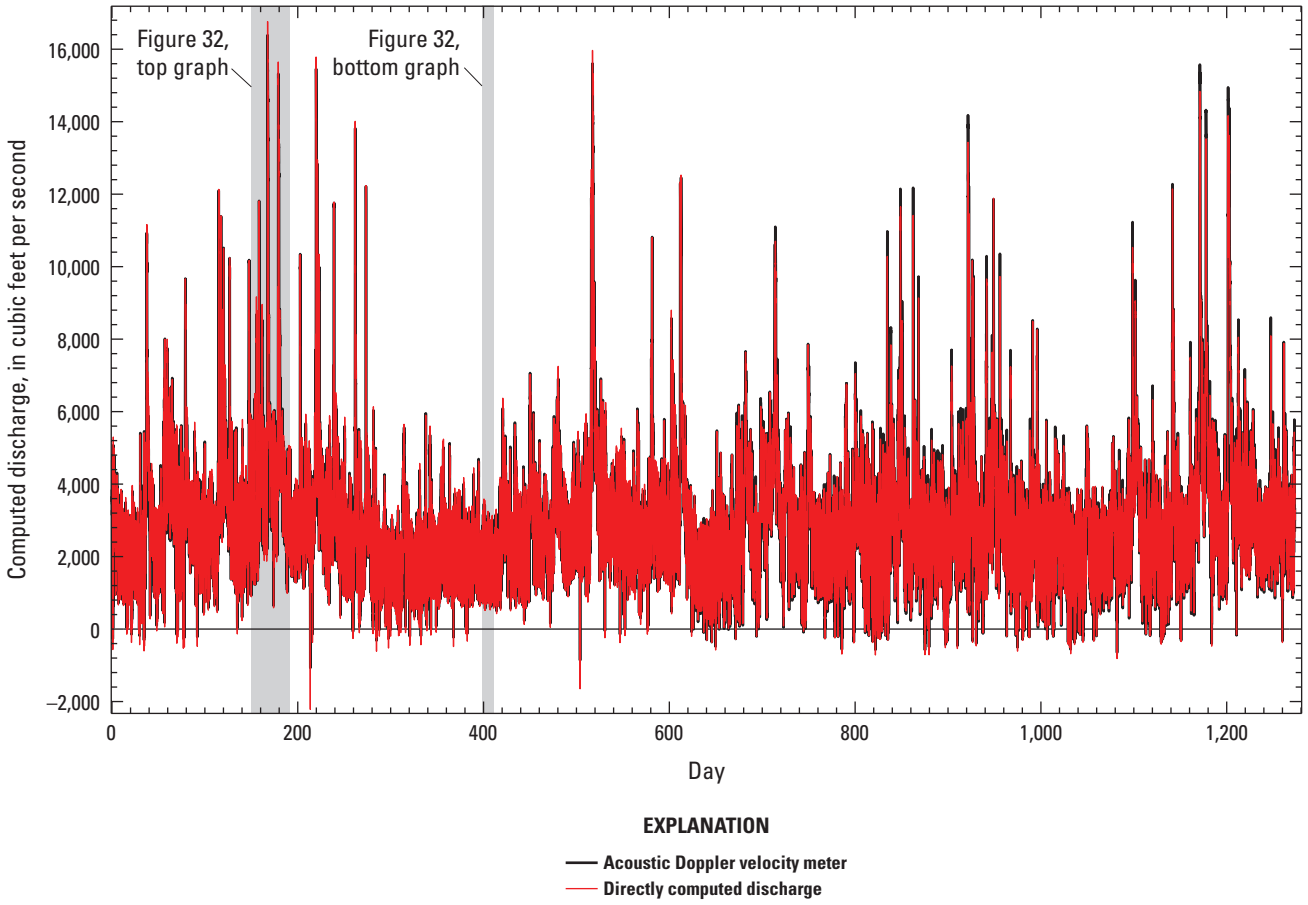

Figure 31. Comparison of computed discharge records from the acoustic Doppler velocity meter (index-velocity method; primary record) and the directly computed discharge for January, 14, 2014, to July 10, 2017, at the U.S. Geological Survey streamgage on the Chicago Sanitary and Ship Canal near Lemont, Illinois (05536890).

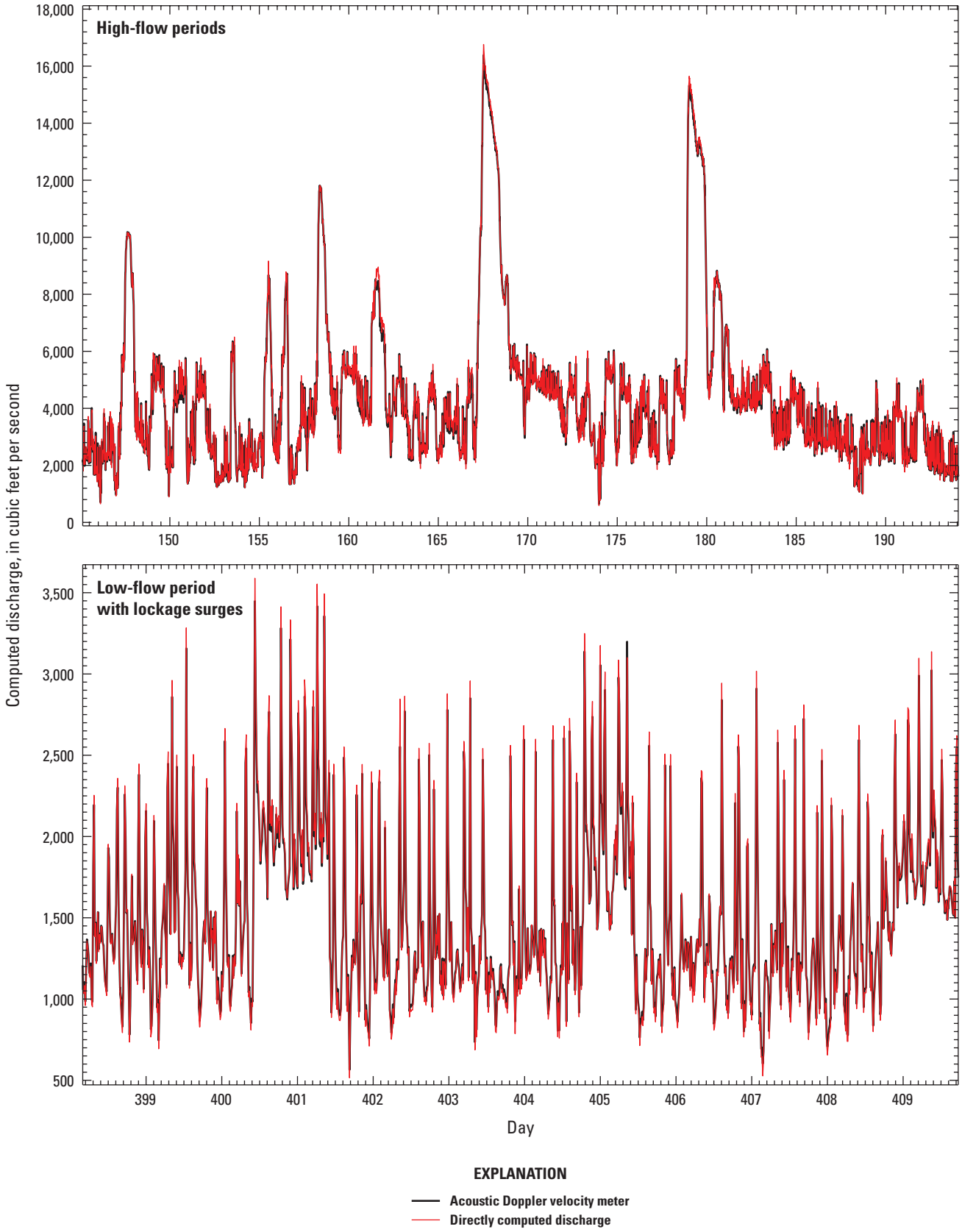

Figure 32. Comparison of computed discharge records from the acoustic Doppler velocity meter (index-velocity method; primary record) and the directly computed discharge for several high-flow periods and a low-flow period with lockage surges at the U.S. Geological Survey streamgage on the Chicago Sanitary and Ship Canal near Lemont, Illinois (05536890).

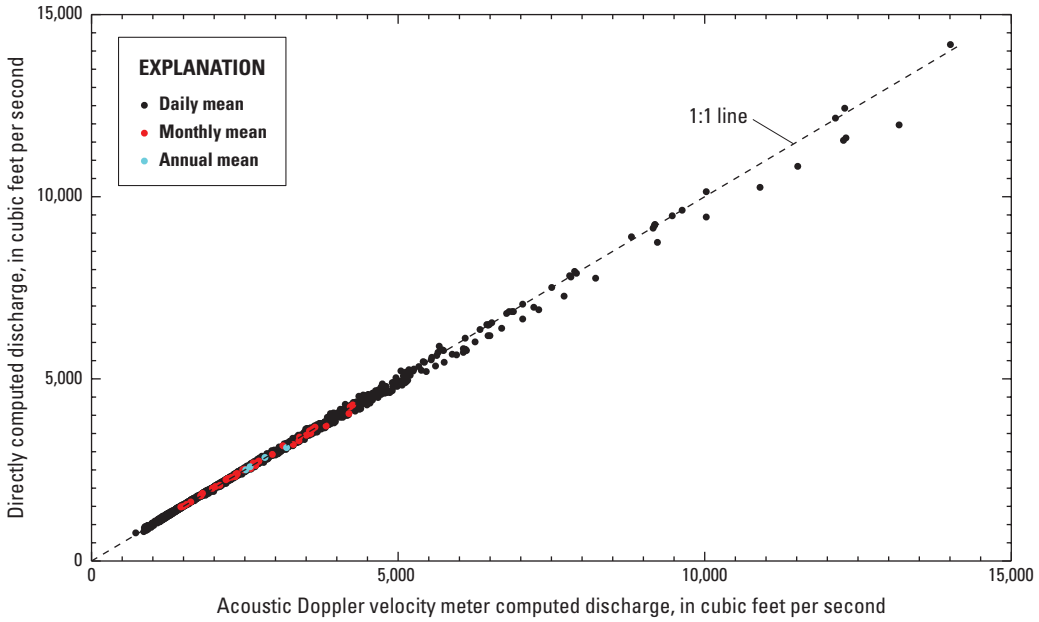

Figure 33. Directly computed discharge versus acoustic Doppler velocity meter computed discharge for daily, monthly, and annual means at the U.S. Geological Survey streamgage on the Chicago Sanitary and Ship Canal near Lemont, Illinois (05536890), January 14, 2014, to July 10, 2017.

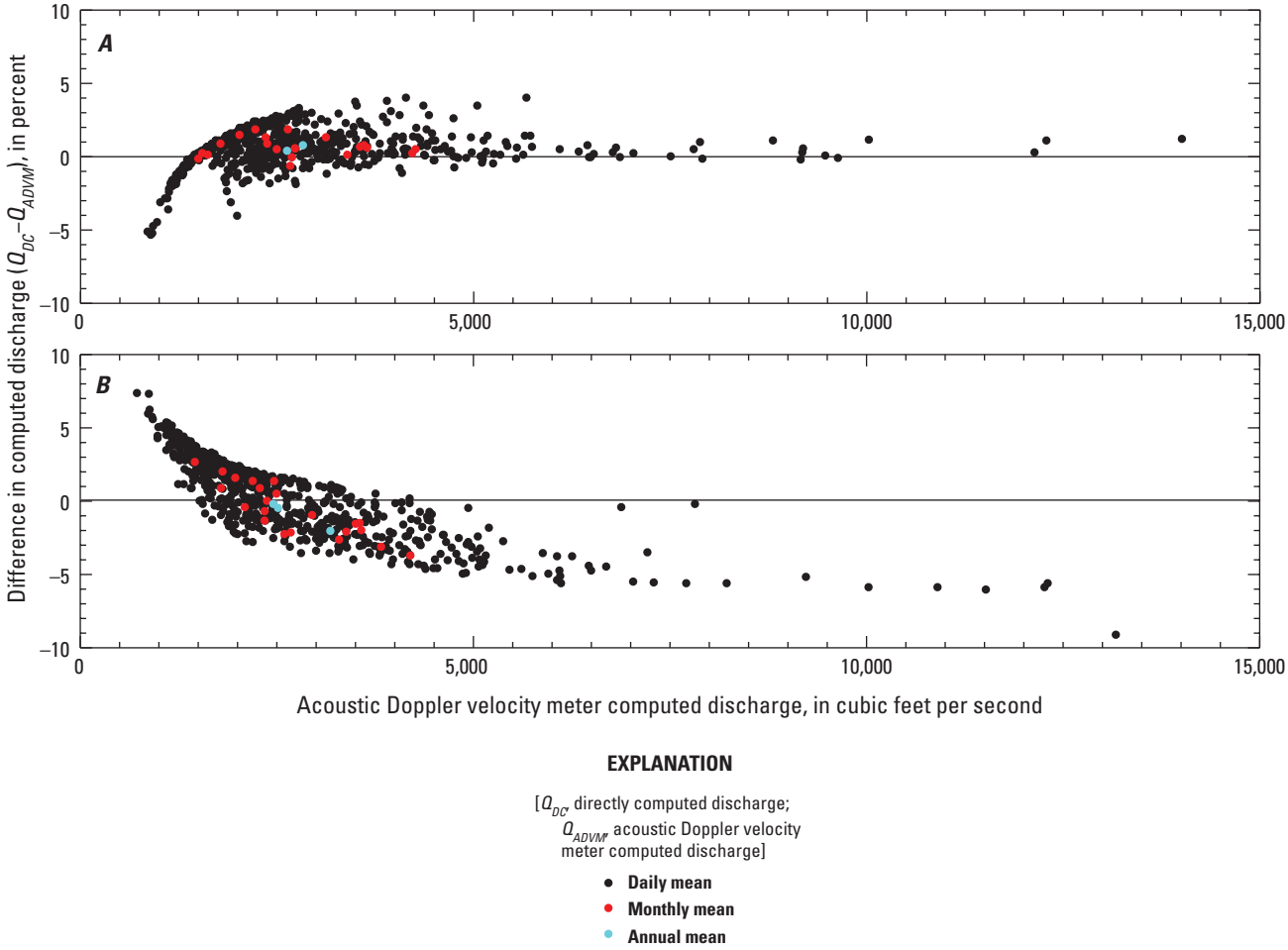

Figure 34. Percent difference between the acoustic Doppler velocity meter discharge and the directly computed discharge for daily, monthly, and annual means as a function of acoustic Doppler velocity meter discharge at the U.S. Geological Survey streamgage on the Chicago Sanitary and Ship Canal near Lemont, Illinois (05536890). *A*, January 14, 2014, to September 30, 2015. *B*, October 1, 2015, to July 10, 2017.

At a significance level of 5 percent, the means and distributions of daily, monthly, and annual mean discharges computed using the ADVM index-velocity and direct computation methods are not significantly different (table 13). At each time scale and for three periods of record, the means were compared with a two-sample t-test, and data distributions were compared using a two-sample Kolmogorov-Smirnov test. In each case, the null hypotheses that the two samples have equal means and come from the same continuous distribution were accepted at the 5-percent significant level (table 13). Further, quantile-quantile plots for each time scale show no significant deviation from the $Y_{quantile}=X_{quantile}$ line, suggesting the data have equal distributions (fig. 35). The distributions for the daily and annual mean discharge are skewed, but the distribution for monthly mean discharges is generally symmetric.

For the period of January 14, 2014, to July 10, 2017, the median difference in the monthly and annual mean flows are 13.0 and −2.2 ft³/s, respectively, yet only the daily mean flow difference (10.5 ft³/s) is statistically significant at the 5-percent significance level based on the sign test (table 13; fig. 36). Therefore, the differences in the monthly and annual mean flows produced by the direct computation method compared to the ADVM index-velocity method are statistically insignificant, and these differences could be attributed to chance.

Slightly different results are yielded when the datasets are broken into two periods. Two-sided sign tests of data before October 1, 2015, suggested the differences between computed discharge for the ADVM index-velocity method and direct computation method were statistically significant at the 5-percent significance level for the daily and monthly time scales (median differences of 11.5 and 16.1 ft³/s for daily and monthly means, respectively; table 13). However, the two-sided sign tests for the period after October 1, 2015, indicated that differences in daily, monthly, and annual mean discharges computed with the direct computation method and ADVM index-velocity method are not statistically significant. For this

Table 13. Comparison of directly computed discharge from the up-looking acoustic Doppler current profiler and acoustic Doppler velocity meter to the acoustic Doppler velocity meter computed discharge (using an index-velocity rating) at the U.S. Geological Survey streamgage on the Chicago Sanitary and Ship Canal near Lemont, Illinois (05536890).

[n, number of samples; Q_{DC}, directly computed discharge from the up-looking acoustic Doppler current profiler and acoustic Doppler velocity meter; Q_{ADVM}, computed discharge from the acoustic Doppler velocity meter; t-test (p-value), two-sample t-test result (5-percent significance level) and associated p-value; sign test (p-value), two-sided sign test result (5-percent significance level) and associated probability p-value; Kolmogorov-Smirnov test (p-value), two-sample Kolmogorov-Smirnov test result (5-percent significance level) and associated p-value]

Statistical test	Daily mean discharge	Monthly mean discharge	Annual mean discharge
Jan. 14, 2014, to July 10, 2017			
n	1,274	43	4
Median difference (Q_{DC}–Q_{ADVM}), in cubic feet per second	10.5	13.0	−2.2
T-test (p-value)	Pass (0.9394)	Pass (0.9762)	Pass (0.9565)
Sign test (p-value)	Fail (1.13×10^{-13})	Pass (0.1263)	Pass (1.0)
Kolmogorov-Smirnov test (p-value)	Pass (0.9948)	Pass (0.9999)	Pass (0.9969)
Jan. 14, 2014, to Sept. 30, 2015			
n	625	21	2
Median difference (Q_{DC}–Q_{ADVM}), in cubic feet per second	11.5	16.1	16.9
T-test (p-value)	Pass (0.8424)	Pass (0.9442)	Pass (0.9164)
Sign test (p-value)	Fail (3.56×10^{-20})	Fail (0.0015)	Pass (0.5)
Kolmogorov-Smirnov test (p-value)	Pass (0.9552)	Pass (0.9999)	Pass (0.8438)
Oct. 1, 2015, to July 10, 2017			
n	649	22	3
Median difference (Q_{DC}–Q_{ADVM}), in cubic feet per second	6.1	−22.4	−11.6
T-test (p-value)	Pass (0.7517)	Pass (0.9022)	Pass (0.9361)
Sign test (p-value)	Pass (0.1820)	Pass (0.5235)	Pass (0.25)
Kolmogorov-Smirnov test (p-value)	Pass (0.9619)	Pass (0.9786)	Pass (0.9762)

period, the median differences between the two methods were 6.1, −22.4, and −11.6 ft³/s for the daily, monthly, and annual mean discharges, respectively (table 13).

It should be noted that before adoption of the direct computation method for direct computation of discharge from the up-looking ADCP and ADVM data based on application of empirically derived velocity ratio functions and applicability of the log-law to the vertical velocity profile, several other methods were tested and determined to be unsuitable for application. Applying a V_r correction to the ADVM data regardless of the goodness of fit (or R^2) of the log law to the vertical velocity profile produced substantial errors in computed discharge. Errors were produced because 77 percent of the 122,100 time-averaged velocity profiles from the up-looking ADCP were not logarithmic (failed to meet the criteria in equation 3), primarily because of the highly unsteady flows in the canal. If one neglects the log law and simply uses equation 4 as the correction for 15-min ADVM data, the high flows in the canal are substantially overestimated. Additionally, fitting the beta distribution to the ADVM 15-min average transverse profiles of streamwise velocity with the no-slip condition applied at the banks (see Jackson and others [2013]) produced an estimate of the mean channel velocity to which V_r can be applied to compute V_{mean}. However, this method substantially underestimated discharge by 182, 200, and 237 ft³/s for the daily, monthly, and annual mean flows, respectively, compared to the ADVM index-velocity method. Ultimately, the computation of the mean cross-sectional velocity that produced the best results was equation 5.

For the purposes of LMDA in which the diversion is assessed based on an annual mean discharge, the use of the proposed direct computation method for computing discharge from the up-looking ADCP and ADVM is an acceptable method and would not result in a significantly different annual mean discharge record. However, the proposed method relies on two instruments being operational (compared to one for

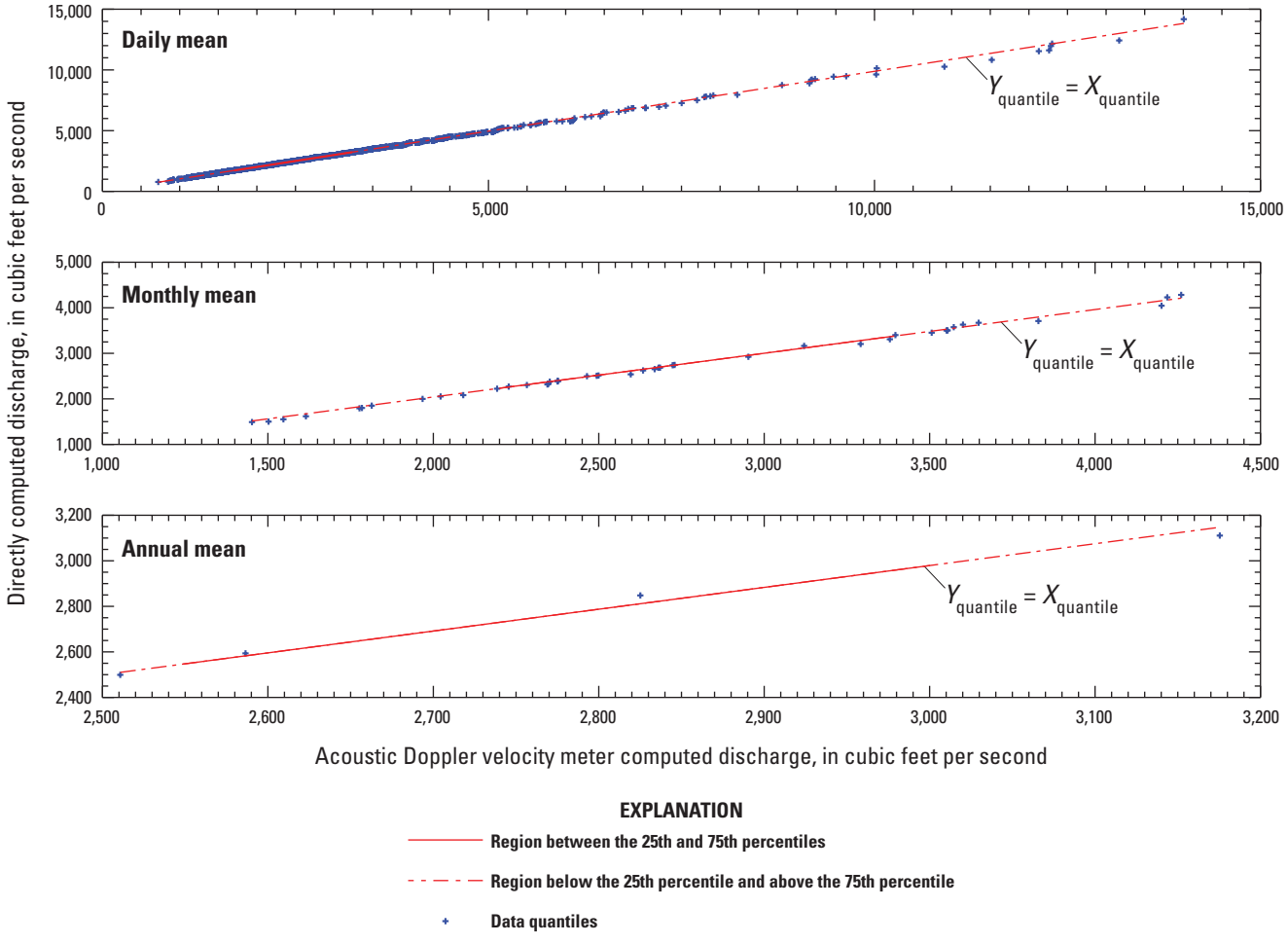

Figure 35. Computed daily, monthly, and annual mean discharges computed using the acoustic Doppler velocity meter index-velocity method (X) and directly computed method (Y) for the U.S. Geological Survey streamgage on the Chicago Sanitary and Ship Canal near Lemont, Illinois (05536890), January 14, 2014, to July 10, 2017.

the index-velocity method), requires regression equations for the velocity ratio (which is more complicated than an index-velocity regression), and has not been proven to yield more accurate records. Therefore, use of this method in place of the index-velocity method is not justified at this time.

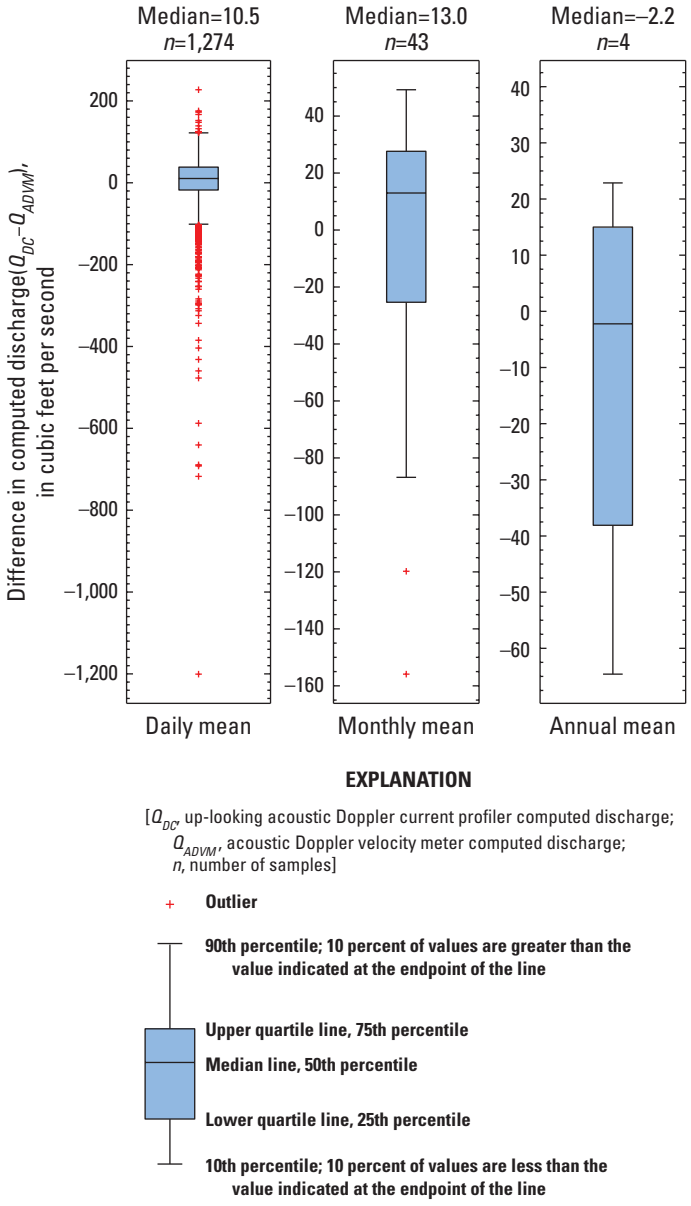

Figure 36. Difference in daily, monthly, and annual mean discharge (directly computed discharge minus discharge measured by the acoustic Doppler velocity meter) at the U.S. Geological Survey streamgage on the Chicago Sanitary and Ship Canal near Lemont, Illinois (05536890), January 14, 2014, to July 10, 2017.

Tow Passages and the Effect on Streamgaging

The barge-detection camera provides excellent ground-truth data to document the passage of commercial tows (hereafter tows, defined as a tow vessel and attached barge raft) through the measurement reach of the Chicago Sanitary and Ship Canal near Lemont, Ill. (05536890). Tow configuration, loading, and direction of travel can be determined for about 85 percent of the videos. The remaining 15 percent of the videos lack sufficient length or quality for analysis and are classified in the data as "insufficient video." With insufficient video, it is not possible to fully characterize the configuration of the tows and the loading; however, direction of travel and width of the barge raft can usually be determined.

Although the video camera with motion detection and night vision is relatively inexpensive, easy to configure, and requires little maintenance other than periodically cleaning lenses and downloading data during site visits, the limitation of this approach to document tow passages lies in the data processing. Video review and data extraction requires playback and interpretation by a person and is prone to human error. The variability in clarity, tow types and configuration, loading, and lighting all make automation of the analysis extremely difficult. Therefore, this approach is not recommended for long-term use in an application where documentation of every tow passage is required. Instead, this approach is best suited for archival of ground-truth data to validate tow passages identified using other methods of detection, such as hydroacoustics, magnetometers, or photoelectric sensors.

Neither the ADVM nor the AVM are currently suitable for barge detection. The ADVM is too deep in the water column to detect tows, and, as was determined by Jackson and others (2012), even fully loaded tows failed to produce consistent, substantial, and prolonged loss of data. Therefore, the ADVM was not a reliable barge-detection instrument. However, path 1 of the AVM (highest in the water column) is consistently blocked by passage of loaded tows making the AVM a possible barge-detection tool. Unfortunately, path 1 of the AVM began intermittently failing on January 17, 2015, which continued until April 8, 2016, when the AVM instrument completely failed. Since most time-of-travel systems such as the AVM are considered obsolete technology, a replacement instrument was difficult to procure. A new AVM is scheduled to be installed in 2018.

Of the three primary hydroacoustic instruments deployed at the USGS streamgage on the Chicago Sanitary and Ship Canal near Lemont, Ill. (05536890), only the up-looking ADCP proved to reliably detect the passage of loaded tows. The reflection of the acoustic beams of the up-looking ADCP off the bottom of a barge can be used to identify the passage of loaded tows. Loaded barges draft about 9 ft, making the sudden change in range of the instrument easily detectable using the receiver signal strength indicator (RSSI) profiles (fig. 37). The RSSI is a measure of the intensity of the sound returned by each acoustic beam. Typically, these peaks are used to determine the range to the water surface; however, the

hard reflection off the bottom of a loaded barge produces a peak that is detectible. Loaded barges are identified when there is a sudden decrease of about 9 ft in the range of the ADCP (fig. 37). The barge-detection algorithm used in this study is comprised of custom RSSI data filter written in Matlab. The algorithm was written in 2016 and provided to the author by Dr. Jessica LeRoy from the USGS (Dr. Jessica LeRoy, USGS, written commun., 2018). The loaded-tow detection algorithm first locates the peaks in the RSSI profile for each 1-min time step. If there is a single peak, and if it is more than five bins from the instrument, the peak is saved. If there are multiple local peaks identified in the RSSI profile (for example fig. 37 at time 13:40), and all are at least five bins from the instrument, the peak nearest the instrument is saved. If the nearest local peak is within five bins from the instrument, the next closest peak is saved (provided it is at least five bins from the instrument). This produces one saved peak for every RSSI profile. Finally, if the saved peak for a profile is within 18 bins of the instrument, the peak is identified as a loaded tow, and the data for that time step are marked as a measurement during passage of a loaded tow.

With loaded-tow passages identified, the algorithm then computes the response of the streamwise velocity in the canal as measured by the up-looking ADCP. The start and end times

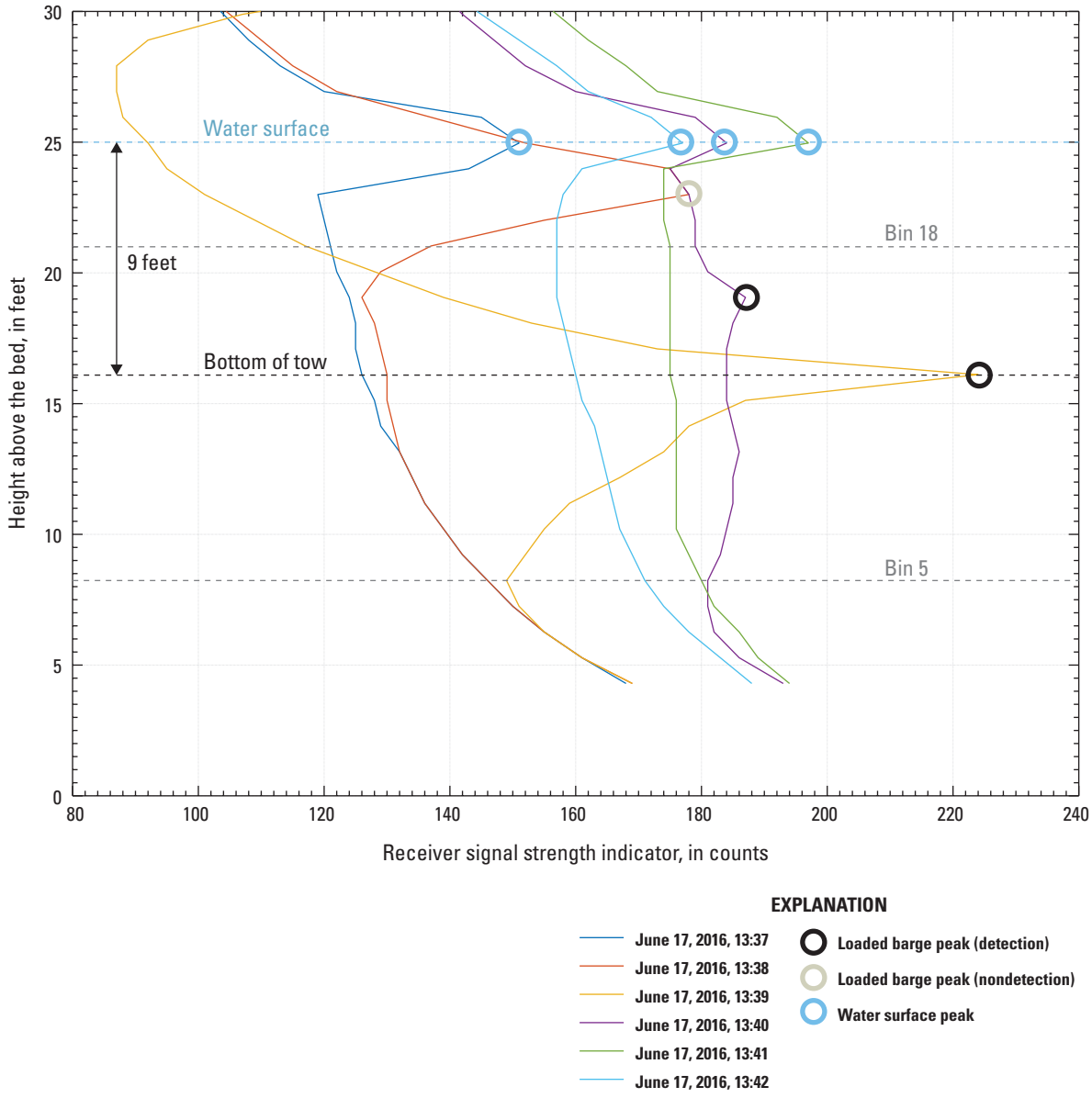

Figure 37. Examples of receiver signal strength indicator profiles during passage of a loaded tow from the up-looking acoustic Doppler current profiler deployed at the U.S. Geological Survey streamgage on the Chicago Sanitary and Ship Canal near Lemont, Illinois (05536890), June 17, 2016.

for each tow passage are determined based on concurrent profiles with barge detections, and the streamwise velocity profiles during each barge passage are time-averaged (yielding a mean profile below the barge) and depth-averaged (yielding an estimate of the mean streamwise velocity below the barge). For each passage, the profiles for the previous four time steps (4 min) and the four time steps after passage are marked, time-averaged, and depth-averaged to estimate the pretow and post-tow streamwise velocity in the canal. Therefore, for each detected tow passage, the algorithm computes a mean streamwise velocity profile and depth-averaged streamwise velocity estimates before, during, and after the passage of the tow. The tow's direction of travel (upstream or downstream) is determined from return flows. Return flows from downstream-bound tows produce a decrease in streamwise velocity or flow reversals below the tow, and upstream-bound tows produce an increase in streamwise velocity below the tow (where positive streamwise velocity is downstream) (Davis and others, 2017). Tow direction of travel can be determined by subtracting the pretow depth-averaged streamwise velocity from the during-tow depth-averaged streamwise velocity. Upstream-bound tows produce a positive velocity difference, whereas down-stream-bound tows produce a negative velocity difference.

Based on ground-truth data from analysis of videos from the barge-detection camera during July 2016, this algorithm is about 64-percent effective at identifying loaded-tow passages (table 14). During this period, the algorithm detected 132 of 206 loaded-tow passages. The algorithm produced 18 false detections possibly because of debris in the water column or wakes from vessels. Of the 74 missed detections of loaded tows, 28 tows (37.8 percent) had mixed loadings (loaded and empty barges) and 38 tows (51.4 percent) were only 1 barge wide. Mixed-loadings and single-wide tows can result in missed detections because the RSSI used by the algorithm is the average of the four beams of the up-looking ADCP. The four beams diverge at 20-degree angles to produce a measurement width (distance between opposite beams) that is equal to about 73 percent of the range from the instrument (18.2 ft for a flow depth of 25 ft). This relatively large measurement region can result in not all the beams hitting the bottom of a loaded tow producing an average RSSI profile that is not characteristic of either the tow or the water surface (see fig. 37, time 13:38 loaded barge peak nondetection). Single-wide tows are relatively narrow (30 ft wide), and not all the beams may hit the bottom of the barge, especially for barges not centered in the canal. Mixed-loading tows can have similar issues produced by some beams hitting the bottom of a loaded tow and some hitting an empty tow. In both cases, the mean RSSI profiles from the four beams may not satisfy the criteria in the algorithm for a loaded tow, so the tow will not be detected.

Table 14. Summary of performance of loaded barge detection algorithm using up-looking acoustic Doppler current profiler data and the barge-detection camera as ground-truth data for July 2016 at the U.S. Geological Survey streamgage on the Chicago Sanitary and Ship Canal near Lemont, Illinois (05536890).

[--, not applicable; mixed loading, barge rafts with loaded and empty barges; atypical configuration, nonstandard barge raft configuration; simultaneous passages, multiple tows passing streamgage at the same time; 1 x 1, barge raft 1 wide by 1 long; 1 wide, barge raft 1 wide; 2 wide, barge raft 2 wide]

Category	Count	Percentage of total loaded tows (from barge-detection camera)	Percentage of total detections	Percentage of missed detections
Barge-detection camera				
Total loaded tows (from barge-detection camera)	206	--	--	--
Algorithm				
Total detections (from algorithm)	224	108.7	--	--
Correct detections	132	64.1	--	--
False detections	18	--	8.0	--
Missed detections	74	35.9	--	--
Missed detections; mixed loading	28	--	--	37.8
Missed detections; atypical configuration	3	--	--	4.1
Missed detections; simultaneous passages	3	--	--	4.1
Missed detections; insufficient video	14	--	--	18.9
Missed detections; 1 x 1	17	--	--	23.0
Missed detections; 1 wide (includes insufficient video)	38	--	--	51.4
Missed detections; 2 wide (includes insufficient video)	2	--	--	2.7

Of the 74 missed detections, 66 of the tows (89.2 percent) fall into the single-wide and mixed-loading categories. The remaining 8 missed detections are due to either atypical configurations of the barge rafts (3 tows), multiple barges passing the gage at the same time (simultaneous passages, 3 tows), and 2 double-wide tows that had insufficient video for analysis (it is suspected these may have been barges with mixed loading).

Application of the loaded-tow detection algorithm to the 1-min up-looking ADCP data from January 14, 2014, to July 10, 2017, identified 7,079 loaded-tow passages. Assuming the July 2016 ground-truth assessment statistics in table 14 are representative of this entire dataset, then about 8 percent of these detections are false detections. If the depth-averaged velocity change during barge passage is screened to remove any values less than 0.07 ft/s (to remove false detections), 311 upstream-bound tow detections and 278 downstream-bound tow detections are removed (totaling 589 detections or 8.3 percent). The remaining 6,490 profiles should therefore primarily consist of detections of loaded tows without mixed loadings and double-wide configurations (tows that are two barges wide). Based on the 35.9 percent of missed detections in table 14, this dataset is missing about 3,600 tows that are primarily made up of single-wide tows and mixed-loading configurations. Nevertheless, the double-wide, fully loaded tows have the most pronounced effect on flows in a confined channel because of their large blocking ratio (ratio of the submerged cross-sectional area of the barge to the cross-sectional area of the channel; see Das and others, 2012). The mean passage duration for a tow was less than 1 min.

Median profiles of the change in streamwise velocity below a loaded tow as it transits through the Chicago Sanitary and Ship Canal past the streamgage near Lemont, Ill. (05536890), show a decrease in streamwise velocity of about 0.45 ft/s for downstream-bound tows and an increase in streamwise velocity of about 0.6 ft/s for upstream-bound tows (fig. 38). In both cases, the profiles are fairly uniform between about 6 ft above the bed (first good bin) to about 3 ft below the barge (about 13 ft above the bed). Both profiles have a maximum velocity change that occurs about halfway between the bed and the bottom of the barge. Within about 3 ft of the bottom of the barge, the magnitude of the velocity difference rapidly decreases. This change is associated with the boundary layer of the barge and the fact that there is a no-slip condition at the bottom of the barge. As the tow moves through the reach, it drags a mass of water with it in the same direction as the tow travel. Davis and others (2016, 2017) determined the thickness of this layer varied with barge speed and was between 3.2 and 4.9 ft based on measurements from the side of a fully loaded barge with a 2 wide by 3 long configuration. This boundary layer thickness is consistent with the observations from the up-looking ADCP as presented in figure 38.

The velocity change reported herein is equivalent to what Davis and others (2017) call the return current velocity corrected for ambient velocity. Although their corrected mean return current velocities are −0.95 and 1.02 ft/s for downstream-bound and upstream-bound tows, respectively, their experiments were done in the Chicago Sanitary and Ship Canal at the Electric Dispersal Barrier System (fig. 1) using a fully loaded tow with a two wide by three long configuration. This configuration represents the largest tows operated in this part of the canal (producing a maximum displacement of water) and generates the greatest magnitude return flows for the same channel cross-sectional area and barge speed. The mean depth-averaged velocity changes (return currents) for the 6,490 tow passages identified in the present analysis are −0.51 and 0.59 ft/s for downstream-bound (n=2,500) and upstream-bound tows (n=3,990), respectively (fig. 39). The median depth-averaged velocity changes (return currents) are −0.47 and 0.54 ft/s for downstream-bound and upstream-bound tows, respectively. The magnitude of these velocity changes are about one-half the magnitude of the observed return currents by Davis and others (2017), despite the cross section of the canal at the two sites being nearly identical. The higher magnitude return currents observed by Davis and others (2017) are not surprising because they tested a configuration with maximum displacement. The present study included loaded tows in virtually every configuration typically operated on the canal, most of which will have a configuration or loading that will generate a smaller magnitude return current than the tow used by Davis and others (2017) for the same tow speed, canal flow, and cross section.

Jackson and others (2012) analyzed 23 tow passages during a short-term up-looking ADCP deployment in May 2008 in the Chicago Sanitary and Ship Canal near Lemont, Ill., and determined a 0.1- to 0.3-ft/s decrease in the reported AVM velocity was associated with downstream-bound tows and an increase in streamwise velocity of 0.2 to 0.5 ft/s for upstream-bound tows. The loading and configuration of the tows was not recorded but likely included loaded and empty barges. In addition, Jackson and others (2012) did not report the velocity change beneath the barge from the up-looking ADCP but rather reported the change in the AVM velocity. The slightly lower magnitude return currents determined by Jackson and others (2012) compared to the present study are likely due, in part, to the inclusion of unloaded tows in the analysis, the small sample size, and the reporting of change in AVM velocities, which are mean velocities for the full cross section at three elevations above the bed and measured at a 44.5-degree angle to the flow (see fig. 2).

In theory, return currents produced by a tow moving at the same speed and corrected for canal flow should be equal in magnitude and opposite in sign for upstream and downstream transit directions as was observed by Davis and others (2017). The slightly higher magnitude velocity changes (return currents) observed for the upstream-bound tows (median=0.54 ft/s) compared to the downstream-bound tows (median=−0.47 ft/s) may be due, in part, to differences in the distribution of tows that were detected moving upstream compared to downstream (fig. 39). A substantially larger number of loaded tows were detected moving upstream (n=3,990) compared to downstream (n=2,500). If the median blockage ratio or tow speed differ between the upstream and downstream

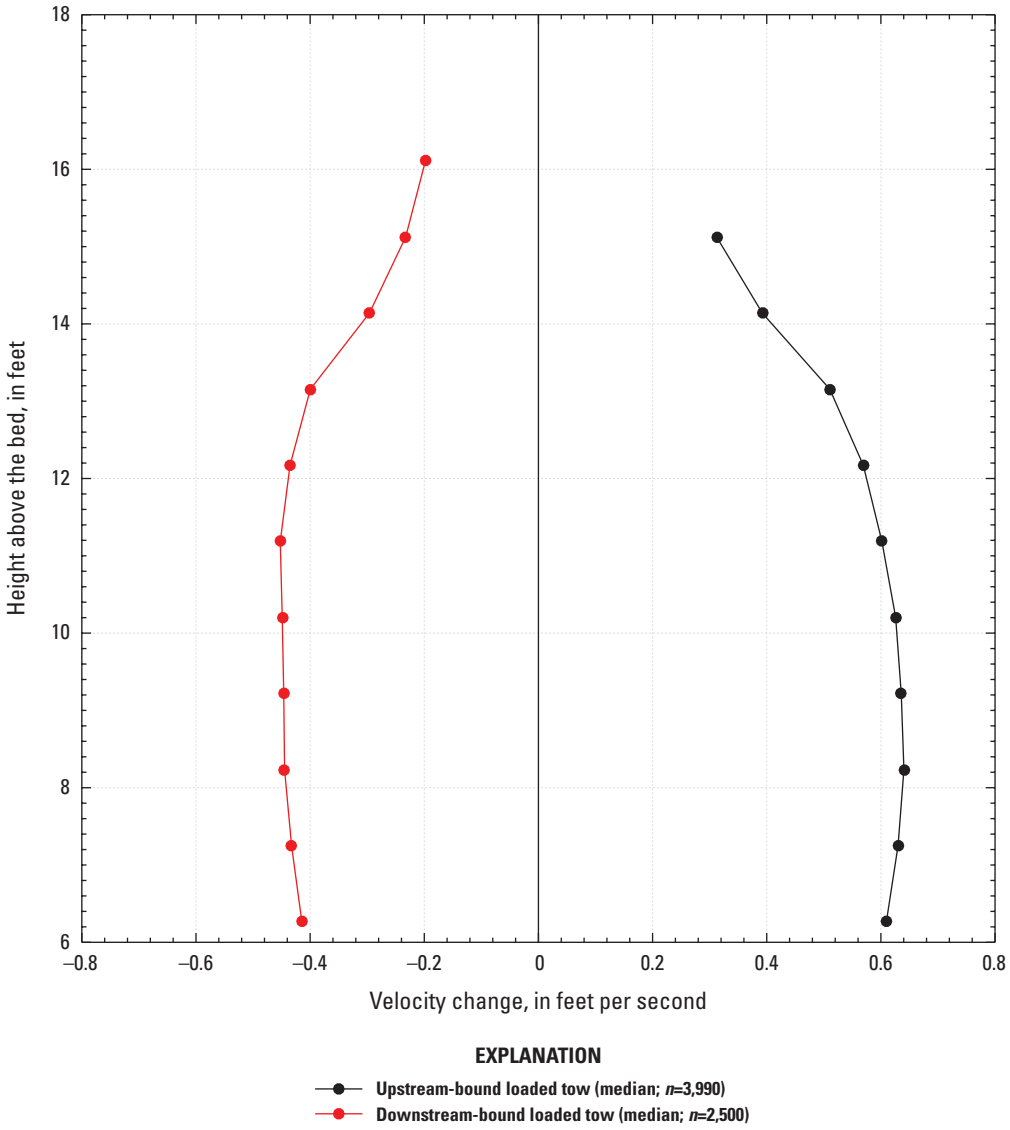

Figure 38. Median profiles of change in streamwise velocity in the water column below a loaded tow vessel relative to the depth-averaged streamwise velocity before the tow passage for upstream-bound and downstream-bound tows at the U.S. Geological Survey streamgage on the Chicago Sanitary and Ship Canal near Lemont, Illinois (05536890), January 14, 2014, to July 10, 2017 [*n*, number of tows].

datasets, the resulting median velocity changes will not be equal in magnitude and opposite in direction. Ground-truth video data do not exist for all the tow passages in this dataset, so it is impossible to evaluate what is causing the slight difference in return current magnitude between upstream and downstream-bound tows. Nevertheless, the difference is small and likely attributed to differences in the number and characteristics of tows moving upstream compared to downstream.

Detection of empty tows is much more difficult than loaded tows because empty tows typically draft less than 2 ft, which is within the range of stage variation in the canal and a similar magnitude to recreational vessels. Empty tows displace substantially less water and generate less disruption to the water column as they transit the measurement reach. The primary disruption caused by empty tows is due to the wake of the vessel and the propeller wash, which entrains air and causes a broad peak in the RSSI profiles. Although this wake can cause some data loss in the near-surface bins of the up-looking ADCP, it also can be used to detect passage of unloaded tows. However, other factors including suspended

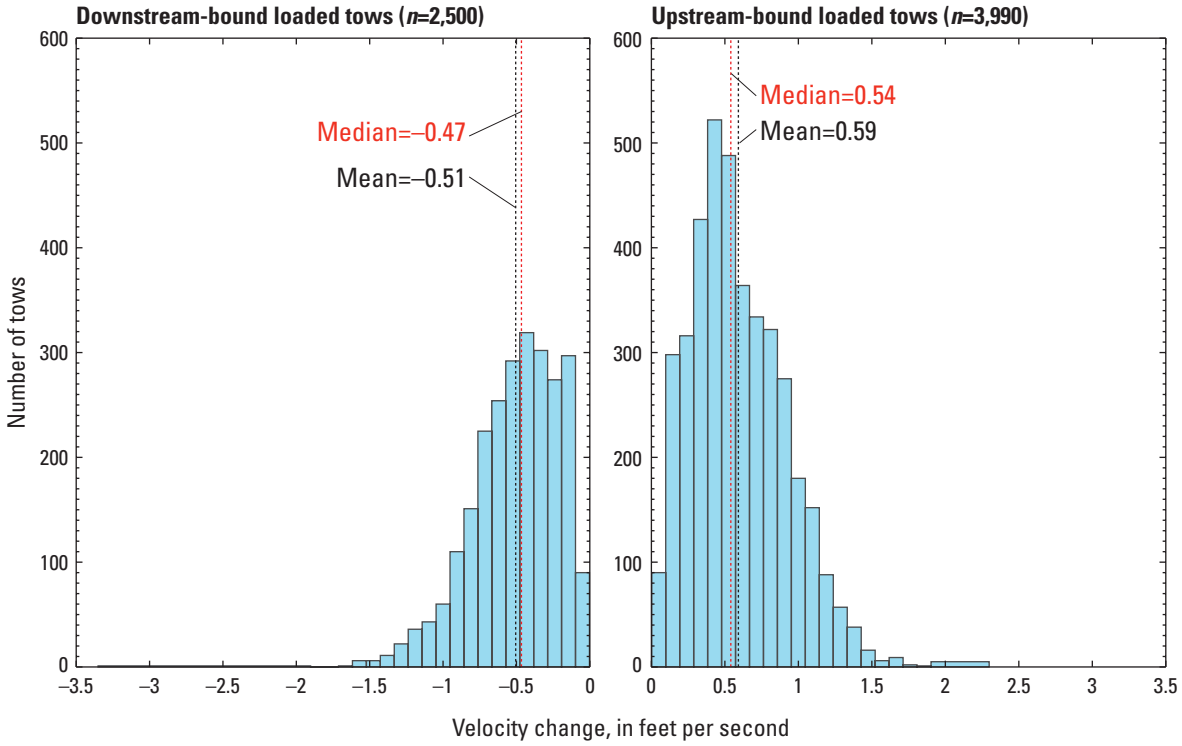

Figure 39. Distributions of the change in depth-averaged streamwise velocity in the water column below a loaded tow vessel relative to the depth-averaged streamwise velocity before the tow passage for downstream-bound and upstream-bound tows at the U.S. Geological Survey streamgage on the Chicago Sanitary and Ship Canal near Lemont, Illinois (05536890), January 14, 2014, to July 10, 2017. [*n*, number of tows]

sediment from the Calumet Sag Channel, loaded tows, tow vessels without barges, and even large recreational vessels can create broad peaks in RSSI.

An empty-tow detection algorithm based on a broad-peak RSSI data filter was developed and tested by Dr. Jessica LeRoy in 2016 (Dr. Jessica LeRoy, USGS, written commun., 2016). She tested the empty-tow algorithm for a small dataset containing 9 empty tows, 5 loaded tows, and 3 tows without barges that passed the site on June 17, 2016. The algorithm successfully identified passage of all 9 empty tows and all 3 tow vessels without barges. However, the algorithm also identified one loaded tow that was not detected by the loaded-tow algorithm and one unidentified event (no video record of a vessel passage). Although this algorithm successfully identifies empty tows and tow vessels passing the site, it also can misidentify loaded tows as empty tow passages and is prone to false detections. Use of this algorithm without ground-truth video data will likely result in a high bias in the empty tow passage counts. Because of the relatively limited flow disturbance created by empty tows compared to loaded tows, and the high potential for error in empty tow identification, using the up-looking ADCP broad RSSI peak algorithm to identify empty tow passage is not advised at this time.

Based on the analysis of more than 6,400 loaded-tow passages, the net effect on measured discharge in the Chicago Sanitary and Ship Canal near Lemont, Ill., is small. Assuming a mean channel velocity of 0.5 ft/s, a stage of 25 ft (Q=1940 ft^3/s), and a 1-min tow passage duration, a 10-min discharge measurement made during a tow passage would change by about 10 percent (higher for upstream-bound tows, lower for downstream-bound tows). Using a conservative estimate of 10 double-wide, loaded-tow passages per day (6 upstream-bound tows and 4 downstream-bound loaded tows), the net change in daily mean discharge would be about +4 ft^3/s (or less than a 0.2 percent). Therefore, the effect of navigational traffic on discharge measurement in the canal near Lemont, Ill., is negligible compared to other sources of error.

Summary and Conclusions

The U.S. Geological Survey (USGS) streamgage on the Chicago Sanitary and Ship Canal near Lemont, Illinois (05536890), is a critical component in monitoring the diversion of Great Lakes water from Lake Michigan into the canal by the State of Illinois. The diversion of Great Lakes water through the canal is limited by a Supreme Court decree and is overseen by the U.S. Army Corps of Engineers Chicago District through the Lake Michigan Diversion Accounting (LMDA) program. Every 5 years, the LMDA Technical Review Committee (TRC) is responsible for ensuring that the best engineering practices are being used at this streamgage, and the records for this gage are complete and accurate. The sixth (2008) and seventh (2013) LMDA TRCs questioned the overall effect of unsteady flows in the canal on the methods used to measure discharge at this site. Of particular interest was the evolution in time of the vertical distribution of streamwise velocity during high-flow events and transient surges in the system. The seventh LMDA TRC recommended the USGS continue to use the up-looking acoustic Doppler current profiler (ADCP) to evaluate the vertical velocity distribution at the site and its effect on the uncertainty of diversion accounting. Additionally, questions were raised about the potential effects of commercial navigation on the flows measured at the streamgage, and the sixth LMDA TRC recommended "quantification of the barge transit effect."

This study by the USGS, in cooperation with the U.S. Army Corps of Engineers Chicago District, addresses these recommendations through the long-term deployment of an up-looking ADCP in the Chicago Sanitary and Ship Canal near Lemont, Ill. Analysis of more than 3.5 years of data from this instrument provides a detailed understanding of the evolution of the vertical profile of streamwise velocity during highly unsteady flows in the canal and has revealed gravity-driven underflows at this site. The up-looking ADCP data were sufficient to develop two additional methods of discharge computation at this streamgage and to identify the passage of loaded tows.

Vertical profiles of streamwise velocity in the Chicago Sanitary and Ship Canal near Lemont, Ill., become less uniform, develop higher gradient profiles, and become more logarithmic in shape as discharge increases. The median velocity profiles for discharge ranging from 6,000 to 12,000 cubic feet per second (ft^3/s) indicate a velocity maximum well below the water surface at heights above the bed of about $0.8H$, which is inconsistent with the aspect ratio of the canal. Although an inverse stage-discharge relation is observed over the range 0 to 12,000 ft^3/s, a positive stage-discharge relation is observed above 12,000 ft^3/s. The inverse stage-discharge relation is associated with drawdown of the Chicago Area Water System (CAWS) at Lockport in anticipation of large storms. The positive stage-discharge relation is associated with high-precipitation storms that produce runoff to the CAWS at a rate that exceeds the conveyance capacity of the control structures at and near Lockport, Ill., at the minimum water level allowed for navigation (−10.0 ft Chicago City Datum at Lockport Controlling Works).

Negative surges induced by lockages at Lockport Lock propagate upstream and are evident in the USGS discharge record for the Chicago Sanitary and Ship Canal near Lemont, Ill. Negative surges produce a temporary decrease in stage and increase in discharge. For these highly unsteady flows, hysteresis in the stage-discharge relation can lead to a phase (time) shift between the peak discharge, peak velocity, and the peak stage as the surge passes a fixed site in the channel. Based on analysis of 8,545 lockage surges in the canal near Lemont, Ill., negative upstream surges generally produce a peak discharge 2 minutes (min) before the minimum water-surface elevation associated with the negative surge. Although acoustic Doppler velocity meter (ADVM) velocity and discharge are in phase (no time lag), the peak velocity from the up-looking ADCP lags the peak discharge by 2 min and is primarily due to the physical separation of the ADVM and up-looking ADCP (170 ft upstream from the ADVM). The time lag between discharge and stage can account for the slightly lower water-surface elevation computed for the falling limb compared to the rising limb for the lockage surges. Additionally, large differences between velocity profiles for the rising and falling limbs of a surge for the same discharge can be attributed to the spatial separation of the instrumentation and the associated lag time between discharge and up-looking ADCP velocity.

Seasonal analysis of velocity profiles from the up-looking ADCP revealed an increase in near-bed velocities for flows as high as 5,000 ft^3/s during the winter. The increase in near-bed velocity is temperature-dependent and is greatest when near-bed water temperature is just above freezing, and near-bed velocity decreases with increasing near-bed water temperature. The seasonal and temperature dependence of these features suggests that these near-bed velocity anomalies are real and driven by environmental factors. Examination of the density profiles in the Chicago Sanitary and Ship Canal near Lemont, Ill., revealed the formation of gravity currents that produce density-driven underflows at the site. Density-driven underflows are most prevalent when the air and water temperatures are coldest between October and May, can be present for extended periods of more than 1 month, and are temporarily disrupted by high-flow events. A correlation analysis determined underflows in the canal near Lemont have the strongest association with water temperature and density in the canal at Cicero Avenue, which is just upstream from the outfall from the Stickney Water Reclamation Plant (WRP). This correlation may suggest that the underflows at Lemont are due, in part, to formation of gravity currents farther upstream where canal water and water from the Stickney WRP outfall interact. However, underflows also were strongly associated with water temperature and density at sites throughout the CAWS as well as daily minimum air temperature. With the canal largely ice-free in the winter, formation of dense water and underflows because of surface cooling cannot be ruled out. Although road-salt runoff has been determined to drive gravity

currents in the CAWS, specific conductance exhibited weaker correlations than water temperature. This analysis suggests that winter underflows in the canal near Lemont, Ill., are likely triggered by a combination of factors including surface cooling, stratified flows created by the outfall from the Stickney WRP, and density difference between the canal and Calumet Sag Channel.

Index-velocity ratings for the up-looking ADCP were developed using multiple- and single-transect discharge measurements. The seventh LMDA TRC proposed that an index-velocity rating developed using single-transect discharge measurements may be more appropriate for the highly unsteady flows in the Chicago Sanitary and Ship Canal. The index-velocity rating curves developed by each of the methods were nearly identical, and no accuracy or advantage was gained by using single-transect discharge measurements. Discharge computed using the multiple-transect (M1) index-velocity rating for the up-looking ADCP for January 14, 2014, to July 10, 2017, compared well to the ADVM-derived discharge. Although the up-looking ADCP slightly underestimated the daily mean flow by about 41 ft^3/s compared to the ADVM (determined to be statistically significant at the 5-percent significance level), differences in the monthly and annual mean flows were statistically insignificant. Therefore, for the purposes of LMDA in which the diversion is assessed based on an annual mean discharge, the discharge computed from the up-looking ADCP M1 index-velocity rating curve is an acceptable backup to the primary ADVM-computed discharge. Furthermore, the M1 index-velocity rating from the up-looking ADCP includes the effect of underflows. The statistical equivalency of the discharge records from the up-looking ADCP and the ADVM at the monthly and annual time scales suggests that although underflows are common in the winter months, they do not substantially affect the discharge reported by the USGS for the Chicago Sanitary and Ship Canal near Lemont, Ill., under the LMDA program.

Discussions with the sixth LMDA TRC included the topic of directly computing discharge from vertical and transverse profiles of streamwise velocity produced by the up-looking ADCP and ADVM, respectively. The committee suggested this method might yield more accurate results than the index-velocity method because it includes information about the vertical and the horizontal distribution of the velocity in the cross section. The discharge was directly computed using a modified velocity profile method that used the vertical velocity profile from the up-looking ADCP to compute a shift applied to the transverse profile of streamwise velocity from the ADVM, ultimately yielding an estimate of the mean velocity for the cross section and discharge (using stage-area rating 3.1). For the period of record between January 14, 2014, and July 10, 2017, the direct computation of discharge using the up-looking ADCP and ADVM produces a discharge record that compares well to the official discharge record produced using the ADVM index-velocity method; adequately reproduces high, low, and reverse flows; and captures the highly variable flows related to passage of lockage surges. Although the computed daily mean discharges for the direct computation method are higher than the ADVM-derived discharges (median difference of 10.5 ft^3/s; 5-percent significant level), the monthly and annual mean discharges computed using the direct computation method are not statistically different from the ADVM index-velocity method at the 5-percent significance level (median differences of 13.0 ft^3/s and −2.2 ft^3/s for the monthly and annual mean discharges, respectively). For the purposes of LMDA in which the diversion is assessed based on an annual mean discharge, the use of the proposed direct computation method for computing discharge from the up-looking ADCP and ADVM is an acceptable method and would not result in a significantly different annual mean discharge record. However, the proposed method relies on two instruments being operational (compared to one for the index-velocity method), requires regression equations for the velocity ratio (which is more complicated than an index-velocity regression), and has not been proven to yield more accurate records. Therefore, use of this method in place of the index-velocity method is not justified at this time.

Of the three primary hydroacoustic instruments at the USGS streamgage on the Chicago Sanitary and Ship Canal near Lemont, Ill. (05536890), only the up-looking ADCP proved to reliably detect passage of loaded tows with respect to timing and direction of travel. Tows with mixed loading (loaded and empty barges) and tows that were 1-barge wide can be missed using the proposed detection algorithm for the up-looking ADCP. In addition, tows with empty barges proved to be difficult to reliably detect. Application of the loaded-tow detection algorithm to the 1-min up-looking ADCP data from January 14, 2014, to July 10, 2017, identified more than 6,400 loaded-tow passages, most likely primarily made up of double-wide, fully-loaded tows. Downstream-bound tows produce a median decrease in streamwise velocity of about 0.47 feet per second (n=2,500), whereas upstream-bound tows produce a median increase in streamwise velocity of about 0.54 feet per second (n=3,990). Despite producing a substantial change in the velocity field as a tow passes the gage, the short duration (typically less than 1 min) and relatively infrequent passages result in negligible changes in discharge when discharge is computed at the daily, monthly, and annual time scales. For this reason, data screening to remove data affected by tow passages is not deemed necessary at this time. Should it be necessary to do so in the future, an improved algorithm or alternate technology (such as use of magnetometers) should be developed to capture all tow passages regardless of loading and configuration.

The long-term application of an up-looking ADCP in the Chicago Sanitary and Ship Canal near Lemont, Ill., allowed the flows at this site to be examined from a new perspective: one that is not possible with the horizontally oriented instrument deployed at the site. This report presented results from more than 3.5 years of continuous monitoring data from an up-looking ADCP at the study site, which allowed the characterization of the variability in the vertical profile of streamwise velocity over a wide range of highly unsteady flows. These

data revealed seasonal, density-driven underflows triggered by a combination of environmental variables. Two new methods for computing discharge were developed using this instrument and were of sufficient quality for LMDA purposes. Finally, the up-looking ADCP and barge-detection camera allowed the effect of commercial tows on streamgaging at the site to be evaluated. The addition of an up-looking ADCP to the USGS streamgage on the canal near Lemont, Ill., has ensured the best current engineering practices and scientific knowledge are implemented in LMDA in accordance with the U.S. Supreme Court decree of 1967, as amended in 1980.

References Cited

Bagherimiyab, F., Parlange, M., Lemmin, U., 2012, Sediment suspension dynamics in turbulent unsteady, depth-varying open-channel flow over a gravel bed: Lausanne, Switzerland, Ecole Polytechnique Fédérale, Ph.D. thesis, 242 p., accessed January 31, 2018, at https://infoscience.epfl.ch/record/167918.

Bareš, V., Jirak, J., and Pollert, J., 2008, Spatial and temporal variation of turbulence characteristics in combined sewer flow: Flow Measurement and Instrumentation, v. 19, nos. 3–4, p. 145–154, accessed February 2018 at https://doi.org/10.1016/j.flowmeasinst.2007.06.002.

Bombar, G., 2016, Hysteresis and shear velocity in unsteady flows: Journal of Applied Fluid Mechanics, v. 9, no. 2, p. 839–853.

Bonakdari, H., Larrarte, F., Lassabatere, L., and Joannis, C., 2008, Turbulent velocity profile in fully-developed open channel flows: Environmental Fluid Mechanics, v. 8, no. 1, p. 1–17, accessed October 2017 at https://doi.org/10.1007/s10652-007-9051-6.

Clesceri, L.S., Greenberg, A.E., and Eaton, A.D., eds., 1999, Standard methods for examination of water and wastewater (20th ed.): Washington, D.C., American Public Health Association, 1,325 p.

Das, S.N., Das, S.K., and Kariya, J.N., 2012, Simulation of return flow in restricted navigation channel for barge-tow movements: The Open Ocean Engineering Journal, v. 5, p. 34–46.

Davis, J.J., LeRoy, J.Z., Shanks, M.R., Jackson, P.R., Engel, F.L., Murphy, E.A., Baxter, C.L., Trovillion, J.C., McInerney, M.K., and Barkowski, N.A., 2017, Effects of tow transit on the efficacy of the Chicago Sanitary and Ship Canal Electric Dispersal Barrier System: Journal of Great Lakes Research, v. 43, no. 6, p. 1119–1131, accessed November 2017 at https://doi.org/10.1016/j.jglr.2017.08.013.

Davis, J.J., Jackson, P.R., Engel, F.L., Leroy, J.Z., Neeley, R.N., Finney, S.T., and Murphy, E.A., 2016, Entrainment, retention, and transport of freely swimming fish in junction gaps between commercial barges operating on the Illinois Waterway: Journal of Great Lakes Research, v. 42, no. 4, p. 837–848, accessed September 2016 at https://doi.org/10.1016/j.jglr.2016.05.005.

Dorevitch, S., 2011, The Chicago health, environmental exposure, and recreation study (CHEERS) final report: Metropolitan Water Reclamation District of Greater Chicago Report 11–43, 29 p., accessed January 31, 2018, at https://www.mwrd.org/irj/go/km/docs/documents/MWRD/internet/reports/Monitoring_and_Research/pdf/2011/11-43_CHEERS_FINAL_Report_August_30_2011.pdf.

Duncker, J.J., and Johnson, K.K., 2015, Hydrology of and current monitoring issues for the Chicago Area Waterway System, northeastern Illinois: U.S. Geological Survey Scientific Investigations Report 2015–5115, 48 p., accessed December 2015 at https://doi.org/10.3133/sir20155115.

Espey, W.H., Clemmens, B., and Halverson, B., 2014, Lake Michigan Diversion Committee—Findings of the Seventh Technical Committee for Review of Diversion Flow Measurements and Accounting Procedures: United States Army Corps of Engineers Chicago District, 124 p., accessed January 31, 2018, at http://www.lrc.usace.army.mil/Portals/36/docs/divacct/technical/LK%20Michigan%20Seventh%20TC%20FINAL.pdf.

Espey, W.H., Melching, C., and Muste, M., 2009, Lake Michigan Diversion Committee—Findings of the Sixth Technical Committee for Review of Diversion Flow Measurements and Accounting Procedures: United States Army Corps of Engineers Chicago District, 198 p., accessed January 31, 2018, at http://www.lrc.usace.army.mil/Portals/36/docs/divacct/technical/Sixth_Technical_complete.pdf.

Fofonoff, N.P., and Millard, R.C., Jr., 1983, Algorithms for computation of fundamental properties of seawater: UNESCO Technical Papers in Marine Science, no. 44, 53 p.

Jackson, P.R., 2013, Circulation, mixing, and transport in nearshore Lake Erie in the vicinity of Villa Angela Beach and Euclid Creek, Cleveland, Ohio, September 11–12, 2012: U.S. Geological Survey Scientific Investigations Report 2013–5198, 34 p., accessed December 2013 at https://doi.org/10.3133/sir20135198.

Jackson, P.R., 2016, Acoustic Doppler current profiler velocity data collected in the Chicago Sanitary and Ship Canal in 2010 and 2011 in support of the interbasin transport study for invasive Asian carp: U.S. Geological Survey data release, accessed January 2017 at https://doi.org/10.5066/F7S180KR.

Jackson, P.R., García, C.M., Oberg, K.A., Johnson, K.K., and García, M.H., 2008, Density currents in the Chicago River—Characterization, effects on water quality, and potential sources: The Science of the Total Environment, v. 401, no. 1–3, p. 130–143.

Jackson, P.R., and Johnson, K.K., 2018, Continuous measurements of velocity from an up-looking acoustic Doppler current profiler deployed in the Chicago Sanitary and Ship Canal near Lemont, Illinois, January 2014 to July 2017: U.S. Geological Survey data release, https://doi.org/10.5066/F7G73D0G.

Jackson, P.R., Johnson, K.K., and Duncker, J.J., 2012, Comparison of index velocity measurements made with a horizontal acoustic Doppler current profiler and a three-path acoustic velocity meter for computation of discharge in the Chicago Sanitary and Ship Canal near Lemont, Illinois: U.S. Geological Survey Scientific Investigations Report 2011–5205, 42 p., accessed March 2012 at https://pubs.usgs.gov/sir/2011/5205/.

Jackson, P.R., Sinha, S., Dutta, S., Johnson, K.K., Duncker, J.J., and Garcia, M.H., 2013, Evaluation of the potential for hysteresis in index-velocity ratings for the Chicago Sanitary and Ship Canal near Lemont, Illinois: U.S. Geological Survey Scientific Investigations Report 2013–5095, 33 p., accessed May 2013 at http://pubs.usgs.gov/sir/2013/5095/.

Johnson, K.K., Duncker, J.J., and Jackson, P.R., 2012, The role of the U.S. Geological Survey in Lake Michigan Diversion Accounting in Illinois, 1984–2010: U.S. Geological Survey Open-File Report 2012–1243, 73 p., accessed March 2013 at https://pubs.usgs.gov/ofr/2012/1243/.

Langhi, M., Hosoda, T., and Dey, S., 2013, Velocity deformation model for unsteady open-channel flows over smooth and rough beds: Journal of Hydraulic Engineering, v. 139, no. 4, p. 433–443, accessed July 2014 at https://doi.org/10.1061/(ASCE)HY.1943-7900.0000677.

Levesque, V.A., and Oberg, K.A., 2012, Computing discharge using the index velocity method: U.S. Geological Survey Techniques and Methods 3–A23, 148 p., accessed November 2012 at http://pubs.usgs.gov/tm/3a23/.

Le Coz, J., Pierrefeu, G., and Paquier, A., 2008, Evaluation of river discharges monitored by a fixed side-looking Doppler profiler: Water Resources Research, v. 44, no. 4, 13 p., accessed January 2018 at https://doi.org/10.1029/2008WR006967.

Kay, R.T., Mills, P.C., and Jackson, P.R., 2016, Geology, hydrology, water quality, and potential for interbasin invasive-species spread by way of the groundwater pathway near Lemont, Illinois: U.S. Geological Survey Scientific Investigations Report 2016–5095, 91 p., accessed February 2018 at https://doi.org/10.3133/sir20165095.

Ma, A.X., Lu, Y.J., Cao, M.X., Wang, X.H., and Haung, T.J., 2015, Velocity distribution and charatcertistics in unsteady open-channel flow over a rough bed, *in* Liquan Xie, ed., Hydraulic Engineering III—Proceedings of the Third Technical Conference on Hydraulic Engineering (CHE2014), December 13–14, 2014: Hong Kong, p. 15–22.

Maeck, A., and Lorke, A., 2014, Ship-lock-induced surges in an impounded river and their impact on subdaily flow velocity variation: River Research and Applications, v. 30, no. 4, p. 494–507, accessed February 2018 at https://doi.org/10.1002/rra.2648.

MathWorks, Inc., 2015, MATLAB version R2015b (8.6.0.267246): Natick, Mass., MathWorks, Inc.

Metropolitan Water Reclamation District of Greater Chicago [MWRD], 2008, Description of the Chicago Waterway System for the use attainability analysis: Metropolitan Water Reclamation District of Greater Chicago Report 08–15R, 23 p., accessed January 31, 2018, at https://www.mwrd.org/irj/go/km/docs/documents/MWRD/internet/reports/Monitoring_and_Research/pdf/2008/08-15%20Description%20of%20CWS%20Report%20for%20UAA.pdf.

Metropolitan Water Reclamation District of Greater Chicago [MWRD], 2013, Systems dispatcher manual: Metropolitan Water Reclamation District of Greater Chicago, manual ver. 7, 90 p.

Metropolitan Water Reclamation District of Greater Chicago [MWRD], 2016, Continuous Dissolved Oxygen Monitoring Quality Assurance Project Plan: Metropolitan Water Reclamation District of Greater Chicago, report CDOM–QAPP rev. 2.1, 28 p., accessed January 31, 2018, at https://www.mwrd.org/irj/go/km/docs/documents/MWRD/internet/reports/Monitoring_and_Research/pdf/CDOM/CDOMQAPP.pdf.

Nezu, I., Kadota, A., and Nakagawa, H., 1997, Turbulent structure in unsteady depth-varying open-channel flows: Journal of Hydraulic Engineering, v. 123, no. 9, p. 752–763.

Nezu, I., and Sanjou, M., 2006, Numerical calculation of turbulence structure in depth-varying unsteady open-channel flows: Journal of Hydraulic Engineering, v. 132, no. 7, p. 681–695, accessed February 2018 at https://doi.org/10.1061/(ASCE)0733-9429(2006)132:7(681).

Seo, I.W., and Baek, K.O., 2004, Estimation of the longitudinal dispersion coefficient using the velocity profile in natural streams: Journal of Hydraulic Engineering, v. 130, no. 3, p. 227–236.

Song, T., and Graf, W.H., 1996, Velocity and turbulence distribution in unsteady open-channel flows: Journal of Hydraulic Engineering, v. 122, no. 3, p. 141–154, accessed July 2014 at https://doi.org/10.1061/(ASCE)0733-9429(1996)122:3(141).

Teledyne RD Instruments [Teledyne RDI], 2007, WorkHorse Rio Grande—Acoustic Doppler current profiler technical manual, P/N 957–6241–00 (November 2007), 254 p.

Turner, J.S., 1973, Buoyancy effects in fluids: Cambridge, U.K., Cambridge University Press, 367 p.

U.S. Army Corps of Engineering [USACE], 1949, Hydraulic Design—Surges in Canals—Change 1: Engineering and Design, p. 1–15, accessed February 1, 2018, at http://www.publications.usace.army.mil/LinkClick.aspx?fileticket=ESI8ER-AaOY%3d&tabid=16439&portalid=76&mid=43544.

Wang, D., Dutta, S., Garcia, M.H., and Jackson, P.R., 2016, Three-dimensional numerical modeling of mixing at the junction of the Calumet-Sag Channel and the Chicago Sanitary and Ship Canal—A comparison between density-driven and advection-driven mixing, *in* George Constantinescu, Marcelo Garcia, and Dan Hanes, ed., River Flow 2016—Proceedings of the International Conference on Fluvial Hydraulics (River Flow 2016), July 11–14, 2016: St. Louis, Missouri, p. 1587–1596.

Wang, X., Wang, Z.Y., Yu, M., and Li, D., 2001, Velocity profile of sediment suspensions and comparison of log law and wake law: Journal of Hydraulic Research, v. 39, no. 2, p. 211–217.

Wells, M.G., and Sherman, B., 2001, Stratification produced by surface cooling in lakes with significant shallow regions: Limnology and Oceanography, v. 46, no. 7, p. 1747–1759.

Yang, S.Q., Tan, S.K., and Lim, S.Y., 2004, Velocity distribution and dip phenomenon in smooth uniform open channel flow: Journal of Hydraulic Engineering, v. 130, no. 12, p. 1179–1186.

Appendix 1. Data Tables Used in Index-Velocity Rating Development

This section contains two tables used for index-velocity rating development for the up-looking acoustic Doppler current profiler deployed in the Chicago Sanitary and Ship Canal near Lemont, Illinois (U.S. Geological Survey streamgage 05536890). The mean channel velocity and index velocity for multiple-transect discharge measurements made at the site between January 2014 and August 2017 are provided in table 1.1. The mean channel velocity and index velocity for single-transect discharge measurements made at the site for the same period are provided in table 1.2. Note that measurement 122 was excluded from the analysis because there are no 1-minute up-looking acoustic Doppler current profiler data for this measurement.

Table 1.1. Multiple-transect discharge measurements and associated mean channel velocity and index velocity at the U.S. Geological Survey streamgage on the Chicago Sanitary and Ship Canal near Lemont, Illinois (05536890), January 2014 to August 2017.

[CST, central standard time; V_{indx}, index velocity for the up-looking acoustic Doppler current profiler; V_{mean}, mean channel velocity]

Measurement number	Date	Start time (CST)	End time (CST)	Discharge, in cubic feet per second	V_{indx}, in feet per second	V_{mean}, in feet per second
133	7/10/2017	15:44:44	16:24:45	3,848	1.069	0.984
132	4/25/2017	10:32:52	11:10:26	3,136	0.879	0.768
131	3/31/2017	9:14:39	9:42:01	8,604	2.356	2.114
130	3/14/2017	14:39:39	15:16:17	2,408	0.681	0.586
129	1/3/2017	15:32:18	16:21:04	1,375	0.378	0.339
128	11/8/2016	9:56:52	10:46:32	966	0.310	0.241
127	8/31/2016	11:05:17	11:48:47	2,672	0.703	0.667
126	6/16/2016	15:07:45	15:38:35	3,036	0.862	0.740
125	5/12/2016	8:19:12	8:54:27	11,062	3.407	2.872
124	4/4/2016	13:33:22	14:18:03	347	0.187	0.084
123	2/2/2016	13:59:02	14:33:15	4,876	1.387	1.228
121	10/7/2015	8:23:11	9:06:49	1,352	0.366	0.331
120	7/7/2015	10:52:59	12:14:05	3,279	0.885	0.818
119	5/6/2015	13:07:48	14:05:22	4,946	1.334	1.235
118	3/11/2015	11:29:05	12:41:53	3,325	0.986	0.824
117	12/18/2014	13:39:04	14:15:36	1,298	0.418	0.330
116	10/7/2014	13:46:17	14:19:37	1,259	0.554	0.326
115	9/10/2014	11:51:03	12:16:45	11,138	3.361	2.930
114	9/10/2014	9:02:55	9:34:28	8,516	2.490	2.230
113	9/10/2014	8:11:33	8:43:55	7,096	2.013	1.854
112	8/19/2014	9:33:09	10:22:00	2,068	0.610	0.515
111	7/8/2014	7:58:40	8:38:25	5,637	1.653	1.417
110	6/26/2014	14:34:36	16:01:02	3,825	1.162	0.957
109	6/10/2014	14:17:57	14:54:50	1,116	0.327	0.273
108	4/9/2014	7:46:21	8:23:52	2,345	0.668	0.571
107	2/11/2014	10:53:28	11:28:30	1,178	0.430	0.290

Table 1.2. Single-transect discharge measurements and associated mean channel velocity and index velocity at the U.S. Geological Survey streamgage on the Chicago Sanitary and Ship Canal near Lemont, Illinois (05536890), January 2014 to August 2017.

[CST, central standard time; V_{indx}, index velocity for the up-looking acoustic Doppler current profile; V_{mean}, mean channel velocity]

Measurement number	Date	Start time (CST)	End time (CST)	Discharge, in cubic feet per second	V_{indx}, in feet per second	V_{mean}, in feet per second
133	7/10/2017	15:44:44	15:47:47	2,987	0.861	0.760
133	7/10/2017	15:47:58	15:50:19	3,042	0.891	0.774
133	7/10/2017	15:50:33	15:53:54	3,209	0.846	0.817
133	7/10/2017	15:54:01	15:56:48	3,395	0.959	0.865
133	7/10/2017	15:56:54	16:00:10	4,043	1.096	1.032
133	7/10/2017	16:00:21	16:03:02	4,399	1.204	1.124
133	7/10/2017	16:03:09	16:05:57	4,435	1.259	1.135
133	7/10/2017	16:06:01	16:08:33	4,533	1.280	1.161
133	7/10/2017	16:08:38	16:11:20	4,161	1.216	1.067
133	7/10/2017	16:11:29	16:14:02	4,272	1.078	1.095
133	7/10/2017	16:14:10	16:16:44	3,920	1.088	1.004
133	7/10/2017	16:16:51	16:19:31	3,966	1.057	1.015
133	7/10/2017	16:19:35	16:22:11	3,664	1.056	0.937
133	7/10/2017	16:22:16	16:24:45	3,587	1.049	0.916
132	4/25/2017	10:32:52	10:36:05	2,404	0.629	0.585
132	4/25/2017	10:36:11	10:39:32	2,836	0.734	0.691
132	4/25/2017	10:39:40	10:43:27	3,675	0.907	0.896
132	4/25/2017	10:43:30	10:46:11	3,842	1.168	0.938
132	4/25/2017	10:46:17	10:48:53	4,046	1.210	0.990
132	4/25/2017	10:50:07	10:53:09	3,306	1.018	0.809
132	4/25/2017	10:53:13	10:55:27	3,462	1.022	0.846
132	4/25/2017	10:55:31	10:58:18	2,945	0.913	0.719
132	4/25/2017	10:58:21	11:00:51	3,035	0.885	0.741
132	4/25/2017	11:00:55	11:04:08	2,967	0.752	0.724
132	4/25/2017	11:04:16	11:07:12	2,781	0.705	0.678
132	4/25/2017	11:07:15	11:10:26	2,336	0.675	0.569
131	3/31/2017	9:14:39	9:16:48	8,504	2.298	2.090
131	3/31/2017	9:16:51	9:19:13	8,792	2.312	2.160
131	3/31/2017	9:19:17	9:21:13	8,226	2.304	2.021
131	3/31/2017	9:21:17	9:23:33	8,691	2.258	2.135
131	3/31/2017	9:23:37	9:25:30	8,465	2.333	2.080
131	3/31/2017	9:25:34	9:27:50	8,535	2.320	2.097
131	3/31/2017	9:27:54	9:30:15	8,672	2.322	2.131
131	3/31/2017	9:30:18	9:32:46	8,851	2.438	2.175
131	3/31/2017	9:32:52	9:35:00	8,757	2.500	2.153
131	3/31/2017	9:35:04	9:37:17	8,578	2.428	2.109
131	3/31/2017	9:37:22	9:39:42	8,641	2.301	2.124
131	3/31/2017	9:39:48	9:42:01	8,539	2.406	2.099
130	3/14/2017	14:39:39	14:42:30	2,836	0.741	0.693

Table 1.2. Single-transect discharge measurements and associated mean channel velocity and index velocity at the U.S. Geological Survey streamgage on the Chicago Sanitary and Ship Canal near Lemont, Illinois (05536890), January 2014 to August 2017.—Continued

[CST, central standard time; V_{indx}, index velocity for the up-looking acoustic Doppler current profile; V_{mean}, mean channel velocity]

Measurement number	Date	Start time (CST)	End time (CST)	Discharge, in cubic feet per second	V_{indx}, in feet per second	V_{mean}, in feet per second
130	3/14/2017	14:42:39	14:45:30	2,599	0.708	0.634
130	3/14/2017	14:45:35	14:48:31	2,560	0.677	0.625
130	3/14/2017	14:48:37	14:51:26	2,326	0.678	0.567
130	3/14/2017	14:51:33	14:54:27	2,247	0.679	0.548
130	3/14/2017	14:54:33	14:57:31	2,039	0.625	0.497
130	3/14/2017	14:57:38	15:00:53	2,316	0.614	0.564
130	3/14/2017	15:00:59	15:04:11	2,622	0.690	0.638
130	3/14/2017	15:04:17	15:07:32	2,631	0.735	0.641
130	3/14/2017	15:07:36	15:10:28	2,446	0.718	0.596
130	3/14/2017	15:10:33	15:13:29	2,202	0.663	0.536
130	3/14/2017	15:13:37	15:16:17	2,068	0.634	0.504
129	1/3/2017	15:32:18	15:36:32	1,433	0.384	0.354
129	1/3/2017	15:36:40	15:40:28	1,345	0.388	0.332
129	1/3/2017	15:41:29	15:44:35	1,532	0.368	0.378
129	1/3/2017	15:44:41	15:48:27	1,491	0.387	0.368
129	1/3/2017	15:48:56	15:52:43	1,392	0.420	0.344
129	1/3/2017	15:52:48	15:56:57	1,523	0.396	0.376
129	1/3/2017	15:57:22	16:01:22	1,317	0.381	0.325
129	1/3/2017	16:01:25	16:05:55	1322	0.408	0.326
129	1/3/2017	16:05:57	16:09:31	1374	0.368	0.339
129	1/3/2017	16:09:39	16:13:32	1,271	0.344	0.314
129	1/3/2017	16:13:41	16:17:40	1,208	0.349	0.298
129	1/3/2017	16:17:47	16:21:04	1,288	0.339	0.318
128	11/8/2016	9:56:52	10:00:28	948	0.315	0.237
128	11/8/2016	10:00:36	10:04:02	846	0.335	0.211
128	11/8/2016	10:04:10	10:07:41	637	0.294	0.159
128	11/8/2016	10:07:49	10:11:53	721	0.244	0.180
128	11/8/2016	10:12:00	10:16:12	904	0.256	0.226
128	11/8/2016	10:16:20	10:19:47	1,006	0.321	0.251
128	11/8/2016	10:19:54	10:23:42	1,045	0.330	0.261
128	11/8/2016	10:23:46	10:27:15	1,075	0.321	0.268
128	11/8/2016	10:27:22	10:30:40	964	0.284	0.240
128	11/8/2016	10:30:48	10:33:42	1,141	0.307	0.285
128	11/8/2016	10:33:51	10:36:55	1,140	0.355	0.284
128	11/8/2016	10:37:04	10:39:53	1,018	0.324	0.254
128	11/8/2016	10:40:03	10:43:23	895	0.308	0.223
128	11/8/2016	10:43:31	10:46:32	1,186	0.359	0.296
127	8/31/2016	11:05:17	11:07:38	2,219	0.608	0.554
127	8/31/2016	11:07:43	11:10:09	2,378	0.639	0.594

Table 1.2. Single-transect discharge measurements and associated mean channel velocity and index velocity at the U.S. Geological Survey streamgage on the Chicago Sanitary and Ship Canal near Lemont, Illinois (05536890), January 2014 to August 2017.—Continued

[CST, central standard time; V_{indx}, index velocity for the up-looking acoustic Doppler current profile; V_{mean}, mean channel velocity]

Measurement number	Date	Start time (CST)	End time (CST)	Discharge, in cubic feet per second	V_{indx}, in feet per second	V_{mean}, in feet per second
127	8/31/2016	11:15:49	11:20:11	2,399	0.696	0.599
127	8/31/2016	11:20:18	11:22:57	2,190	0.620	0.547
127	8/31/2016	11:23:02	11:25:42	2,073	0.632	0.517
127	8/31/2016	11:25:46	11:28:11	2,437	0.598	0.608
127	8/31/2016	11:28:17	11:31:04	2,259	0.619	0.563
127	8/31/2016	11:31:08	11:33:37	2,583	0.686	0.645
127	8/31/2016	11:33:44	11:36:20	2,600	0.668	0.649
127	8/31/2016	11:36:27	11:38:46	2,666	0.717	0.666
127	8/31/2016	11:38:52	11:41:19	3,123	0.758	0.780
127	8/31/2016	11:41:25	11:43:40	3,418	0.855	0.855
127	8/31/2016	11:43:46	11:46:20	3,392	0.971	0.850
127	8/31/2016	11:46:28	11:48:47	3,672	0.956	0.921
126	6/16/2016	15:07:45	15:10:30	3,689	1.041	0.904
126	6/16/2016	15:11:16	15:14:01	3,391	0.942	0.830
126	6/16/2016	15:14:04	15:16:41	3,213	0.899	0.786
126	6/16/2016	15:16:44	15:19:11	3,187	0.899	0.779
126	6/16/2016	15:19:15	15:21:33	3,107	0.920	0.758
126	6/16/2016	15:21:38	15:23:52	3,019	0.914	0.736
126	6/16/2016	15:23:56	15:26:30	2,818	0.801	0.687
126	6/16/2016	15:26:32	15:29:02	2,658	0.778	0.647
126	6/16/2016	15:29:04	15:31:31	2,646	0.750	0.644
126	6/16/2016	15:31:36	15:33:54	2,782	0.736	0.677
126	6/16/2016	15:33:56	15:36:16	2,911	0.761	0.709
126	6/16/2016	15:36:20	15:38:35	3,009	0.837	0.733
125	5/12/2016	8:19:12	8:22:47	11,129	3.329	2.885
125	5/12/2016	8:22:56	8:25:09	10,943	3.495	2.838
125	5/12/2016	8:25:15	8:28:17	11,282	3.505	2.927
125	5/12/2016	8:28:23	8:31:56	11,033	3.456	2.863
125	5/12/2016	8:32:05	8:35:16	10,636	3.420	2.761
125	5/12/2016	8:35:23	8:37:44	11,354	3.324	2.948
125	5/12/2016	8:37:49	8:40:41	10,990	3.374	2.854
125	5/12/2016	8:40:45	8:44:05	11,088	3.463	2.881
125	5/12/2016	8:44:11	8:47:06	11,020	3.330	2.864
125	5/12/2016	8:47:13	8:49:24	10,925	3.281	2.840
125	5/12/2016	8:49:33	8:52:19	11,084	3.425	2.882
125	5/12/2016	8:52:26	8:54:27	11,262	3.345	2.929
124	4/4/2016	13:33:22	13:36:27	441	0.240	0.106
124	4/4/2016	13:36:34	13:40:01	400	0.208	0.096
124	4/4/2016	13:40:08	13:43:51	326	0.200	0.079

Table 1.2. Single-transect discharge measurements and associated mean channel velocity and index velocity at the U.S. Geological Survey streamgage on the Chicago Sanitary and Ship Canal near Lemont, Illinois (05536890), January 2014 to August 2017.—Continued

[CST, central standard time; V_{indx}, index velocity for the up-looking acoustic Doppler current profile; V_{mean}, mean channel velocity]

Measurement number	Date	Start time (CST)	End time (CST)	Discharge, in cubic feet per second	V_{indx}, in feet per second	V_{mean}, in feet per second
124	4/4/2016	13:43:56	13:47:34	225	0.204	0.054
124	4/4/2016	13:47:39	13:51:24	-17	0.106	-0.004
124	4/4/2016	13:51:32	13:55:10	125	0.136	0.030
124	4/4/2016	13:55:15	13:59:01	330	0.175	0.080
124	4/4/2016	13:59:07	14:02:52	238	0.167	0.057
124	4/4/2016	14:02:59	14:07:05	410	0.142	0.099
124	4/4/2016	14:07:09	14:10:55	638	0.183	0.154
124	4/4/2016	14:11:00	14:14:16	672	0.275	0.162
124	4/4/2016	14:14:21	14:18:03	375	0.226	0.091
123	2/2/2016	13:59:02	14:01:56	5,014	1.307	1.259
123	2/2/2016	14:02:06	14:05:00	5,380	1.470	1.353
123	2/2/2016	14:05:06	14:07:50	5,467	1.560	1.378
123	2/2/2016	14:07:56	14:10:45	5,438	1.553	1.373
123	2/2/2016	14:10:50	14:13:30	5,103	1.453	1.288
123	2/2/2016	14:13:37	14:16:30	4,937	1.423	1.245
123	2/2/2016	14:17:05	14:19:48	4,661	1.396	1.173
123	2/2/2016	14:19:57	14:22:43	4,670	1.357	1.174
123	2/2/2016	14:22:51	14:25:29	4,584	1.335	1.153
123	2/2/2016	14:25:35	14:28:21	4,434	1.310	1.115
123	2/2/2016	14:28:27	14:30:49	4,433	1.276	1.114
123	2/2/2016	14:30:56	14:33:15	4,387	1.181	1.103
121	10/7/2015	8:23:11	8:27:14	1,403	0.370	0.343
121	10/7/2015	8:27:19	8:30:52	1,352	0.371	0.331
121	10/7/2015	8:30:57	8:35:02	1,321	0.361	0.323
121	10/7/2015	8:35:07	8:38:25	1,346	0.364	0.330
121	10/7/2015	8:38:30	8:42:05	1,326	0.350	0.325
121	10/7/2015	8:42:10	8:45:28	1,386	0.346	0.340
121	10/7/2015	8:45:34	8:49:18	1,366	0.388	0.335
121	10/7/2015	8:49:23	8:52:23	1,371	0.385	0.336
121	10/7/2015	8:52:28	8:56:08	1,358	0.368	0.333
121	10/7/2015	8:56:11	8:59:27	1,289	0.364	0.316
121	10/7/2015	8:59:35	9:03:40	1,355	0.360	0.332
121	10/7/2015	9:03:45	9:06:49	1,354	0.367	0.332
120	7/7/2015	10:52:59	10:56:09	2,622	0.702	0.653
120	7/7/2015	11:07:38	11:10:27	2,875	0.803	0.716
120	7/7/2015	11:10:35	11:13:05	2,691	0.727	0.670
120	7/7/2015	11:13:12	11:15:50	2,595	0.686	0.646
120	7/7/2015	11:15:54	11:18:03	2,636	0.731	0.656
120	7/7/2015	11:18:09	11:20:51	2,498	0.752	0.622

Table 1.2. Single-transect discharge measurements and associated mean channel velocity and index velocity at the U.S. Geological Survey streamgage on the Chicago Sanitary and Ship Canal near Lemont, Illinois (05536890), January 2014 to August 2017.—Continued

[CST, central standard time; V_{indx}, index velocity for the up-looking acoustic Doppler current profile; V_{mean}, mean channel velocity]

Measurement number	Date	Start time (CST)	End time (CST)	Discharge, in cubic feet per second	V_{indx}, in feet per second	V_{mean}, in feet per second
120	7/7/2015	11:20:55	11:23:13	2,651	0.782	0.659
120	7/7/2015	11:42:15	11:45:02	4,228	1.056	1.058
120	7/7/2015	11:45:06	11:47:46	4,190	0.997	1.047
120	7/7/2015	11:47:53	11:50:34	3,953	1.053	0.987
120	7/7/2015	11:50:40	11:52:57	3,981	1.046	0.994
120	7/7/2015	11:53:03	11:55:40	3,575	1.057	0.891
120	7/7/2015	11:55:44	11:58:15	3,522	0.997	0.877
120	7/7/2015	11:58:22	12:01:01	3,561	0.952	0.886
120	7/7/2015	12:01:05	12:03:41	3,522	0.969	0.875
120	7/7/2015	12:03:44	12:06:17	3,390	0.903	0.842
120	7/7/2015	12:06:20	12:08:54	3,337	0.847	0.828
120	7/7/2015	12:09:02	12:11:37	3,243	0.878	0.804
120	7/7/2015	12:11:41	12:14:05	3,223	0.951	0.799
119	5/6/2015	13:07:48	13:11:38	4,673	1.325	1.166
119	5/6/2015	13:11:46	13:15:46	4,702	1.184	1.173
119	5/6/2015	13:15:51	13:19:41	4,937	1.186	1.233
119	5/6/2015	13:19:45	13:23:24	4,959	1.236	1.239
119	5/6/2015	13:23:29	13:27:24	5,050	1.408	1.261
119	5/6/2015	13:27:33	13:31:35	5,073	1.377	1.266
119	5/6/2015	13:31:41	13:35:37	5,116	1.377	1.277
119	5/6/2015	13:35:42	13:39:49	5,000	1.364	1.248
119	5/6/2015	13:39:54	13:44:00	5,013	1.419	1.252
119	5/6/2015	13:44:07	13:48:05	5,099	1.352	1.273
119	5/6/2015	13:57:27	14:00:33	4,852	1.406	1.210
119	5/6/2015	14:01:03	14:05:22	4,876	1.286	1.216
118	3/11/2015	11:29:05	11:32:46	3,253	1.023	0.806
118	3/11/2015	11:32:57	11:37:00	3,260	1.033	0.808
118	3/11/2015	11:37:04	11:41:55	3,324	1.057	0.824
118	3/11/2015	11:41:58	11:46:21	3,324	1.054	0.824
118	3/11/2015	11:46:26	11:51:03	3,220	1.003	0.798
118	3/11/2015	11:51:08	11:55:11	3,384	1.044	0.839
118	3/11/2015	11:55:18	11:59:54	3,311	1.125	0.821
118	3/11/2015	12:21:30	12:26:07	3,340	0.885	0.828
118	3/11/2015	12:26:11	12:29:58	3,316	0.861	0.822
118	3/11/2015	12:30:03	12:33:23	3,366	0.988	0.834
118	3/11/2015	12:33:27	12:36:27	3,381	0.940	0.838
118	3/11/2015	12:36:31	12:39:23	3,402	0.898	0.843
118	3/11/2015	12:39:27	12:41:53	3,347	0.871	0.829
117	12/18/2014	13:39:04	13:42:19	1,571	0.497	0.400

Table 1.2. Single-transect discharge measurements and associated mean channel velocity and index velocity at the U.S. Geological Survey streamgage on the Chicago Sanitary and Ship Canal near Lemont, Illinois (05536890), January 2014 to August 2017.—Continued

[CST, central standard time; V_{indx}, index velocity for the up-looking acoustic Doppler current profile; V_{mean}, mean channel velocity]

Measurement number	Date	Start time (CST)	End time (CST)	Discharge, in cubic feet per second	V_{indx}, in feet per second	V_{mean}, in feet per second
117	12/18/2014	13:42:29	13:45:31	1,731	0.521	0.441
117	12/18/2014	13:45:38	13:48:45	1,581	0.487	0.403
117	12/18/2014	13:48:49	13:51:27	1,587	0.506	0.404
117	12/18/2014	13:51:30	13:54:11	1,554	0.513	0.396
117	12/18/2014	13:54:14	13:56:55	1,534	0.533	0.390
117	12/18/2014	13:57:00	13:59:48	1,423	0.470	0.362
117	12/18/2014	13:59:52	14:02:49	1,350	0.423	0.343
117	12/18/2014	14:02:54	14:06:34	1,209	0.391	0.307
117	12/18/2014	14:06:40	14:09:23	798	0.272	0.202
117	12/18/2014	14:09:27	14:12:26	600	0.232	0.152
117	12/18/2014	14:12:30	14:15:36	636	0.218	0.161
116	10/7/2014	13:46:17	13:49:24	657	0.475	0.170
116	10/7/2014	13:49:27	13:51:43	1,127	0.453	0.292
116	10/7/2014	13:51:46	13:54:05	681	0.408	0.176
116	10/7/2014	13:54:08	13:56:36	876	0.431	0.226
116	10/7/2014	13:56:39	13:58:56	800	0.363	0.207
116	10/7/2014	13:59:00	14:01:41	1,234	0.396	0.319
116	10/7/2014	14:01:45	14:04:09	1,103	0.465	0.285
116	10/7/2014	14:04:13	14:06:58	1,055	0.585	0.273
116	10/7/2014	14:07:09	14:09:44	1,404	0.616	0.363
116	10/7/2014	14:09:54	14:13:02	2,223	0.694	0.576
116	10/7/2014	14:13:08	14:15:55	1,685	0.772	0.437
116	10/7/2014	14:16:02	14:19:37	2,265	0.821	0.588
115	9/10/2014	11:51:03	11:53:20	11,161	3.432	2.934
115	9/10/2014	11:53:25	11:55:27	11,153	3.203	2.933
115	9/10/2014	11:55:32	11:57:27	11,123	3.417	2.925
115	9/10/2014	11:57:32	11:59:33	11,235	3.338	2.955
115	9/10/2014	11:59:36	12:01:31	11,084	3.367	2.915
115	9/10/2014	12:01:35	12:03:30	11,058	3.374	2.909
115	9/10/2014	12:03:35	12:05:44	11,210	3.436	2.949
115	9/10/2014	12:05:49	12:07:52	11,145	3.252	2.932
115	9/10/2014	12:08:01	12:10:15	11,106	3.415	2.922
115	9/10/2014	12:10:20	12:12:27	11,216	3.353	2.951
115	9/10/2014	12:12:31	12:14:29	11,010	3.205	2.897
115	9/10/2014	12:14:34	12:16:45	11,160	3.306	2.937
114	9/10/2014	9:02:55	9:05:33	8,384	2.489	2.197
114	9/10/2014	9:05:38	9:08:02	8,570	2.534	2.246
114	9/10/2014	9:08:05	9:10:33	8,582	2.457	2.249
114	9/10/2014	9:10:38	9:13:05	8,652	2.516	2.267

Table 1.2. Single-transect discharge measurements and associated mean channel velocity and index velocity at the U.S. Geological Survey streamgage on the Chicago Sanitary and Ship Canal near Lemont, Illinois (05536890), January 2014 to August 2017.—Continued

[CST, central standard time; V_{indx}, index velocity for the up-looking acoustic Doppler current profile; V_{mean}, mean channel velocity]

Measurement number	Date	Start time (CST)	End time (CST)	Discharge, in cubic feet per second	V_{indx}, in feet per second	V_{mean}, in feet per second
114	9/10/2014	9:13:09	9:15:43	8,325	2.456	2.181
114	9/10/2014	9:15:49	9:18:08	8,639	2.445	2.263
114	9/10/2014	9:18:14	9:20:41	8,498	2.535	2.226
114	9/10/2014	9:20:44	9:23:10	8,522	2.506	2.230
114	9/10/2014	9:23:13	9:26:00	8,542	2.544	2.234
114	9/10/2014	9:26:05	9:28:49	8,467	2.317	2.213
114	9/10/2014	9:28:52	9:31:49	8,390	2.496	2.191
114	9/10/2014	9:31:52	9:34:28	8,621	2.520	2.252
113	9/10/2014	8:11:33	8:14:16	6,931	2.169	1.817
113	9/10/2014	8:14:23	8:17:02	7,038	2.059	1.844
113	9/10/2014	8:17:07	8:19:34	7,175	2.017	1.879
113	9/10/2014	8:19:40	8:22:14	7,009	2.059	1.834
113	9/10/2014	8:22:19	8:24:46	7,051	1.888	1.844
113	9/10/2014	8:24:50	8:27:26	6,939	1.973	1.814
113	9/10/2014	8:27:30	8:30:06	7,036	1.924	1.838
113	9/10/2014	8:30:10	8:32:51	7,065	2.069	1.844
113	9/10/2014	8:32:55	8:35:32	6,935	1.928	1.810
113	9/10/2014	8:35:36	8:38:19	7,072	1.975	1.846
113	9/10/2014	8:38:23	8:40:57	7,280	2.037	1.900
113	9/10/2014	8:41:01	8:43:55	7,615	2.067	1.988
112	8/19/2014	9:33:09	9:37:08	1,964	0.608	0.489
112	8/19/2014	9:37:13	9:40:57	1,897	0.597	0.472
112	8/19/2014	9:41:02	9:45:04	1,930	0.614	0.480
112	8/19/2014	9:45:09	9:49:04	1,952	0.596	0.486
112	8/19/2014	9:49:09	9:53:04	1,931	0.602	0.481
112	8/19/2014	9:53:07	9:57:22	2,122	0.585	0.528
112	8/19/2014	9:57:26	10:01:17	2,031	0.569	0.506
112	8/19/2014	10:01:20	10:05:28	2,252	0.618	0.561
112	8/19/2014	10:05:32	10:09:22	2,253	0.623	0.561
112	8/19/2014	10:09:25	10:13:43	2,180	0.643	0.543
112	8/19/2014	10:13:47	10:17:38	2,126	0.649	0.530
112	8/19/2014	10:17:42	10:22:00	2,183	0.626	0.544
111	7/8/2014	7:58:40	8:02:01	6,139	1.786	1.548
111	7/8/2014	8:02:09	8:05:03	5,828	1.734	1.469
111	7/8/2014	8:05:09	8:08:07	6,026	1.703	1.518
111	7/8/2014	8:08:10	8:11:09	5,655	1.672	1.423
111	7/8/2014	8:11:12	8:14:20	5,754	1.699	1.448
111	7/8/2014	8:14:23	8:17:26	5,620	1.650	1.413
111	7/8/2014	8:17:29	8:21:21	5,613	1.626	1.411

Table 1.2. Single-transect discharge measurements and associated mean channel velocity and index velocity at the U.S. Geological Survey streamgage on the Chicago Sanitary and Ship Canal near Lemont, Illinois (05536890), January 2014 to August 2017.—Continued

[CST, central standard time; V_{indx}, index velocity for the up-looking acoustic Doppler current profile; V_{mean}, mean channel velocity]

Measurement number	Date	Start time (CST)	End time (CST)	Discharge, in cubic feet per second	V_{indx}, in feet per second	V_{mean}, in feet per second
111	7/8/2014	8:21:23	8:24:48	5,455	1.648	1.371
111	7/8/2014	8:24:50	8:28:27	5,428	1.614	1.363
111	7/8/2014	8:28:28	8:31:36	5,328	1.560	1.338
111	7/8/2014	8:31:38	8:35:13	5,388	1.596	1.353
111	7/8/2014	8:35:15	8:38:25	5,415	1.547	1.359
110	6/26/2014	14:34:36	14:37:35	3,850	1.173	0.965
110	6/26/2014	14:37:48	14:40:47	3,976	1.152	0.997
110	6/26/2014	14:50:27	14:53:52	3,825	1.218	0.958
110	6/26/2014	14:54:05	14:56:59	3,741	1.233	0.936
110	6/26/2014	14:57:13	15:00:28	3,718	1.241	0.930
110	6/26/2014	15:00:41	15:04:14	3,735	1.213	0.934
110	6/26/2014	15:04:39	15:07:49	3,740	1.200	0.936
110	6/26/2014	15:08:01	15:11:22	3,670	1.201	0.918
110	6/26/2014	15:11:35	15:15:01	3,723	1.163	0.932
110	6/26/2014	15:15:13	15:18:09	3,731	1.180	0.934
110	6/26/2014	15:37:19	15:40:30	3,692	1.096	0.924
110	6/26/2014	15:40:42	15:43:25	3,924	1.106	0.982
110	6/26/2014	15:43:35	15:46:35	3,927	1.143	0.983
110	6/26/2014	15:46:45	15:49:24	3,933	1.125	0.985
110	6/26/2014	15:49:36	15:52:42	3,998	1.132	1.001
110	6/26/2014	15:52:51	15:55:31	3,950	1.148	0.988
110	6/26/2014	15:55:40	15:58:20	3,822	1.096	0.956
110	6/26/2014	15:58:31	16:01:02	3,889	1.113	0.972
109	6/10/2014	14:17:57	14:19:59	970	0.370	0.237
109	6/10/2014	14:20:04	14:22:23	1,106	0.294	0.271
109	6/10/2014	14:22:40	14:24:36	789	0.285	0.193
109	6/10/2014	14:24:40	14:26:48	1,083	0.263	0.265
109	6/10/2014	14:26:51	14:28:35	846	0.352	0.207
109	6/10/2014	14:28:41	14:30:40	1,137	0.261	0.278
109	6/10/2014	14:40:11	14:42:32	1,379	0.348	0.337
109	6/10/2014	14:42:36	14:45:12	1,192	0.375	0.291
109	6/10/2014	14:45:16	14:47:13	1,358	0.370	0.332
109	6/10/2014	14:47:18	14:49:46	1,168	0.369	0.285
109	6/10/2014	14:49:50	14:52:06	1,191	0.310	0.291
109	6/10/2014	14:52:11	14:54:50	1,177	0.314	0.287
108	4/9/2014	7:46:21	7:49:42	2,255	0.697	0.549
108	4/9/2014	7:49:50	7:53:01	2,128	0.660	0.518
108	4/9/2014	7:53:07	7:55:58	2,214	0.654	0.539
108	4/9/2014	7:56:02	7:58:43	2,211	0.637	0.538

Table 1.2. Single-transect discharge measurements and associated mean channel velocity and index velocity at the U.S. Geological Survey streamgage on the Chicago Sanitary and Ship Canal near Lemont, Illinois (05536890), January 2014 to August 2017.—Continued

[CST, central standard time; V_{indx}, index velocity for the up-looking acoustic Doppler current profile; V_{mean}, mean channel velocity]

Measurement number	Date	Start time (CST)	End time (CST)	Discharge, in cubic feet per second	V_{indx}, in feet per second	V_{mean}, in feet per second
108	4/9/2014	7:58:47	8:01:42	2,322	0.652	0.565
108	4/9/2014	8:01:49	8:04:46	2,304	0.619	0.561
108	4/9/2014	8:04:52	8:07:45	2,411	0.636	0.588
108	4/9/2014	8:07:51	8:10:58	2,436	0.675	0.594
108	4/9/2014	8:11:13	8:14:29	2,481	0.684	0.605
108	4/9/2014	8:14:34	8:17:49	2,514	0.700	0.613
108	4/9/2014	8:17:56	8:20:47	2,452	0.681	0.597
108	4/9/2014	8:20:53	8:23:52	2,409	0.688	0.587
107	2/11/2014	10:53:28	10:55:44	1,788	0.497	0.441
107	2/11/2014	10:55:50	10:58:09	1,621	0.543	0.400
107	2/11/2014	10:58:14	11:00:40	1,539	0.531	0.379
107	2/11/2014	11:00:54	11:04:14	1,349	0.469	0.332
107	2/11/2014	11:05:12	11:07:54	849	0.422	0.209
107	2/11/2014	11:08:43	11:11:29	1,203	0.363	0.296
107	2/11/2014	11:11:38	11:14:09	691	0.378	0.170
107	2/11/2014	11:14:16	11:17:12	1,159	0.401	0.285
107	2/11/2014	11:17:19	11:19:48	789	0.429	0.194
107	2/11/2014	11:19:54	11:22:32	1,262	0.391	0.311
107	2/11/2014	11:22:40	11:25:23	783	0.384	0.193
107	2/11/2014	11:25:30	11:28:30	1,103	0.395	0.272

For more information about this publication, contact
Director, USGS Central Midwest Water Science Center
405 N Goodwin Ave
Urbana, IL 61801
(217) 328–8747

For additional information visit https://www.usgs.gov/centers/cm-water

Publishing support provided by the
Rolla Publishing Service Center

ISSN 2328-0328 (online)
https://doi.org/10.3133/sir20185128